Department of Organic Chemistry
Faculty of Science
University of Ghent
Belgium

ANALYSIS OF SACCHARIDES BY CAPILLARY ELECTRODRIVEN SEPARATION METHODS

Jiayu Peng

Thesis submitted to the Faculty of Science
in fulfilment of the requirements
for the Degree of Doctor in Science (Chemistry)

Promoter

Prof. Dr. Pat SANDRA

February 2002

Acknowledgements

I express my deepest thanks to my promoter Prof. Dr. Pat Sandra for giving me the opportunity to work and study in his laboratory and particularly for his great guidance, constant inspiration and unforgetable generosity. These priceless experiences will be deeply remembered and will definitely influence my further life.

My most sincere thanks go to my colleagues Frédéric Lynen and Gerd Vanhoenacker for the many discussions during my research work, as well as for their help in the preparation of this thesis. Many thanks also go to Koen Desmet, Tine Van den Bosch, Joeri Vercammen, Bart Tienpont, Christophe Devos, Yining Zhao, An Dermaux … I will always cherish the precious moments I shared with them.

Special thanks go to Dr. Jan Demyttenære for his help with correcting the thesis, to Jan Verstraete, Marc Schelfaut and André D'Oosterlinck for their support with my practical work.

I would like to thank Imperial Chemical Industries PLC (ICI) for supporting this research project (ICI Strategic Research Fund Ref. R3AB2352) and Dr. Francis Scanlan, the project coordinator and, the Univerity of Ghent for study grant GOA 12051898.

Last but not least, I do appreciate very much my family. I would not have been able to finalise this work without their encouragement and support.

Analysis of Saccharides
by Capillary Electrodriven Separation Methods

Contents

Introduction

Carbohydrates or saccharides affect almost every aspect of human live. They can have a monomeric, oligomeric or polymeric structure with an amazing variety of chemical and physical characteristics. Best known is that they are an essential part of our nutrition. The soluble mono- and disaccharides like glucose, fructose, saccharose and lactose, serve as sweeteners, while insoluble high molecular weight polysaccharides are fibers. Polysaccharides are also used as gelling and thickening agents in food, as stabilisers for emulsions, as modifiers for textures, as flavour inducing compounds by reaction with amino acids (Maillard reaction), etc. In the last decades, the roles carbohydrates play in biological pathways and processes have been intensively studied resulting in the development of a new research discipline namely glycobiology. Saccharides anchored to proteins and lipids named glycoproteins and glycolipds, respectively, exert an important effect on the characteristics of these molecules. The nature of the saccharide can, for example, influence the activity, the solubility, the stability, etc., of the glycoproteins. Attached to cell surface proteins or as part of membrane lipids, the saccharides allow cells to communicate with each other through specific intercellular recognition and adhesion mechanisms which are yet not fully understood [1]. Changes in glycosilation of biomolecules often are associated with severe diseases like cancer, I-cell disease, etc. Also the pharmaceutical industry is highly interested in these molecules and recombinant glycosilated proteins are evaluated as therapeutic agents.

A better understanding of carbohydrate chemistry is running in parallel with the development of new methods for measuring and characterising this class of molecules. Because of the diversity of structural and functional properties encountered in carbohydrates, their proper separation has been an analytical challenge for many years.

Capillary gas chromatography (GC) and high performance liquid chromatography (HPLC) are today the two most common separation techniques used for saccharide analysis. GC combined with hydrolysis and derivatisation, remains a very important technique especially to characterise monosaccharides although DP (degree of polymerisation) numbers as high as 10 can be eluted from a capillary GC column. As an example, plant gums were fingerprinted using GC coupled with mass spectroscopy (MS) [2]. Among the HPLC techniques used for the separation of carbohydrates such as reversed phase liquid chromatography (RPLC), size exclusion chromatography (SEC) and high performance anion exchange chromatography (HPAEC) [3], the latter in combination with pulsed amperometric detection (PAD) provides the best resolution for polysaccharides. The separation of glucosyl polysaccharides with DPs higher than 50 was reported [4]. However, one of the inherent shortcomings of HPAEC-PAD is the strong alkaline medium needed for elution that could possibly induce epimerisation and degradation of reducing carbohydrates [5]. Size exclusion chromatography (SEC) in the gel filtration format is widely used to generate information on molecular weight distribution of polysaccharides. SEC is also used for fractionation of gelling polysaccharides such as pectin and carrageenan [3]. Because of the effect of pH and ionic strength on inter- and intramolecular association and, in many

cases, on molecular conformation, the separation of polysaccharides by SEC is highly dependent on the composition of the mobile phase. This is the major difficulty encountered when using this form of chromatography. The lack of standard polysaccharides is another problem in the elucidation of the molecular weight distribution.

For bio-related polysaccharides, electrophoresis on cellulose acetate membranes, polyacrylamide gels or agarose gels followed by staining with dyes such as toluidine blue and fuchsin [6] is often used. The application of polyacrylamide gels instead of cellulose acetate membranes greatly enhanced resolution, especially in combination with small sample sizes and fluorescent tags. Separation by this type of technique, however, is mainly based on size filtering, and species having the same molecular weight cannot be differentiated.

The miniature form of electrophoresis, namely capillary electrophoresis (CE) has attracted much attention for the analysis of polysaccharides in the last decade. The intrinsic high resolving power of CE is particularly suitable for the separation of polysaccharides that possess a wide distribution of molecular weights with subtle differences in charge to mass ratio between adjacent polymer chains. The ultra sensitive laser induced fluorescence (LIF) detector coupled with CE allows to monitor high DP polysaccharides after derivatisation. Several derivatisation methods have been developed to introduce ionisable functions and chromophores in the saccharide molecules [7]. Precolumn derivatisation is the most important mode used to label saccharides based on the reductive amination mechanism. Selection of the derivatisation reagents play a crucial role in both detection and separation since the tags generally improve the electrophoretic properties of

sugars. El Rassi *et al.* [7-9] and Waterval *et al.* [10] published extensive reviews on the derivatisation reagents and the reaction schemes applicable to carbohydrate analysis. Several papers have demonstrated the potential of CE for the analysis of saccharides and we refer to the references [1,10,11,12].

The aim of this work, in first instance, was to explore the possibilities of CE in combination with LIF detection by means of the analysis of some model saccharides. During this work we were also confronted with some real samples e.g. inulin and its hydrolysates, gums, and chemical and enzymatic hydrolysis of hemicellulose. Secondly, CE-LIFD analysis is until now not documented with quantitative data. It was therefore also the aim to study this quantitative aspect.

References

[1] A. Klockow-Beck, Chromatographia CE Series, Analysis of carbohydrates by capillary electrophoresis, Edited by K. D. Altria, Vieweg publishing, Braunschweig/Wiesbaden, **1999**

[2] J. Bleton, P. Mejanelle, J. Sanaoulet, S. Goursaud and A. Tchapla, *J. Chromatogr. A*, 720, **1996**, 27

[3] Z. El. Rassi, *Journal of Chromatography Library*, Vol. 58, Carbohydrate analysis, Elsevier, Amsterdam, **1995**

[4] Y. C. Lee, *J. Chromatogr. A*, 720, **1996**, 137

[5] I. H. Grant and W. Steuer, *J. Microcolumn Sep.* 2, **1990**, 74

[6] J. Haines and P. D. Patel, *Trends in food science & technology* Vol. 8, **1997**, 395

[7] Z. El Rassi, High performance capillary electrophoresis of carbohydrates, Volume VIII, Beckman Instruments, Inc. publishing, Fullerton, CA, USA, **1996**

[8] Z. El Rassi, *Electrophoresis* 17, **1996**, 275

[9] Z. El. Rassi, *Electrophoresis* 18, **1997**, 2400

[10] J. C. M. Waterval, H. Lingeman, A. Bult and W. J. M. Underberg, *Electrophoresis* 21, **2000**, 4029

[11] A. Paulus and A. Klockow, *J. Chromatogr. A*, 720, **1996**, 353

[12] S. Suzuki and S. Honda, *Electrophoresis* 19, **1998**, 2539

Chapter 1

Principles of Capillary Electrodriven Separation Methods

Abstract

A brief overview of the basic principles and instrumentation of capillary electrodriven separation methods is presented. Emphasis is on capillary zone electrophoresis (CZE) and laser induced fluorescence detection (LIFD) since these are the main separation and detection modes, respectively, used in this work for the analysis of saccharides.

1.1 Introduction

Electrophoresis is defined as the differential movement of charged species (ions) by attraction or repulsion in an electric field and was introduced as a separation technique by Tiselius in 1937 [1]. For his pioneering work, Tiselius was awarded the Nobel Prize in 1948. The separation efficiency in free solution, as initially performed by Tiselius, was limited by thermal diffusion and convection. For this reason, electrophoresis has traditionally been performed in anti-convective media, such as polyacrylamide or agarose gels. Gels in the slab or tube format have been used primarily for the size-dependent separation of biomacromolecules like nucleic acids and proteins. Slab gel electrophoresis is a powerful analytical

technique but suffers from some disadvantages including long analysis times, low efficiencies, necessity for staining after the separation and difficulty to automate.

An early attempt to improve conventional electrophoresis was made by Hjertén [2]. A millimeter-bore capillary was rotated along its longitudinal axis to minimise the effects of convection. Later, glass capillaries with 200 to 500 µm internal diameter (i.d.) were applied for electrophoresis by Virtanen and Kivalo [3] and high voltage was applied in narrow-bore teflon tubes by Everaerts *et al.* [4].

In the early 1980s, Jorgenson and Lukacs [5, 6] advanced the technique by using 75 µm i.d. fused silica capillaries. This was a milestone in the development of capillary electrophoresis (CE). Nowadays, capillaries with internal diameters ranging from 10 to 100 µm are available and applied in capillary electrophoresis.

In many ways, the improvements in performance resulting from the use of capillaries instead of slab gels are similar to those attained by performing chromatography in a column rather than on a flat-bed. By applying high fields (100 to 500 V/m) in narrow bore columns, extremely high efficiencies in short analysis time are reached because the problem of Joule heating is circumvented. Moreover, only very small sample amounts (nL) are needed.

On-line UV or fluorescence detection as well as the combination with mass spectroscopy (MS) is feasible. Fully automated systems have been developed opening new possibilities for high throughput screening of DNA and RNA (genomics) and proteins (proteomics). Moreover, the availability of different separation mechanisms in CE has broadened the applicability of electrodriven

separations drastically. Small to large, charged and uncharged analytes can be separated with the same technique.

Recently, the miniature format of CE, *i.e.* lab-on-a chip, has been introduced for genomics and proteomics.

Electrodriven separation in fused silica capillaries is realised by two phenomena that occur simultaneously, namely electrophoresis and electroosmosis. An understanding of the fundamental principles behind these two phenomena is essential in order to effectively perform analyses by capillary electrophoresis.

1.2 Electrophoresis

1.2.1 Electrophoretic mobility (μ_{ep})

In an electric field (E), an ion with charge q is subjected to an electrostatic force F:

$$F = q\,E = q\,\frac{V}{L} \qquad \text{(eq. 1.1)}$$

with E = electric field (V/m)

V = applied voltage (V)

L = distance between the two electrodes (m)

q = charge of analyte (C) = z e

$e = 1.602 \times 10^{-19}$ (C)

z = valence of the ions

Cations will move towards the cathode (negative electrode) and anions will move towards the anode (positive electrode). During this movement, ions will be subjected to frictional forces (F') described by Stokes' law. The particle is hereby assumed to be spherical.

$$F' = - 6 \pi \eta r \nu_{ep} \qquad \text{(eq. 1.2)}$$

with η = viscosity of the medium (Pa s = Kg/m s)

ν_{ep} = ion velocity (m/s)

r = ion radius (m)

During electrophoresis, a steady state defined by the balance of these forces is attained. At this point the forces are equal but opposite and

$$q E = 6 \pi \eta r \nu_{ep} \qquad \text{(eq. 1.3)}$$

The electrophoretic mobility (μ_{ep}) of an ion is defined as its linear velocity (ν_{ep}) per unit of applied electric field (E), expressed in m^2/Vs

$$\mu_{ep} = \frac{n_{ep}}{E} = \frac{q}{6phr} \qquad \text{(eq. 1.4)}$$

Eq. 1.4 is only valid for rigid spherical ions having a homogenously distributed charge and can thus not be used for more complex ions. A more general approach therefore, is to express the electrophoretic mobility as a function of the zeta potential (ζ),

$$\mu_{ep} = \frac{ez}{6ph} = \frac{2e_0 e_r z}{3h} \qquad \text{(eq. 1.5)}$$

with ζ = zeta potential of the ion (V)

ε = dielectric constant of the medium (C^2/Jm)

ε_0 = permittivity of vacuum (C^2/Jm)

ε_r = relative permittivity of the buffer

The zeta potential is a quantity derived from the double layer models of Helmholtz, Goüy-Chapman and Stern [7-9].

1.2.2 Factors influencing the electrophoretic mobility (μ_{ep})

As can be seen in eq. 1.4, the migration of a species in an electric field depends on its charge, size and shape, as well as on the viscosity of the medium. When the temperature is increased, viscosity decreases, resulting in an increase of the ion mobility.

It is evident that small and highly charged species have high mobilities. The pH of the separation medium plays an important role in the electrophoresis of weak electrolytes because the ion concentration is determined by the pH of the electrolyte solution and the pK_a-value of a weak acid or the pK_b-value of a weak base. Besides, as can be deduced from eq. 1.5, the ionic strength of the background electrolyte is controlling the zeta potential (ζ). When the ionic strength increases, the zeta potential decreases, resulting in a decreased ion mobility.

1.3 Electroosmosis

1.3.1 Electroosmotic flow (EOF)

The electroosmotic flow (EOF) is the bulk flow of the liquid in the capillary arising as a consequence of surface charges on the capillary wall. The EOF originates from the silica nature of the capillary. Chemically, the internal surface of an uncoated fused silica capillary contains silanol groups. At pH>3, the silanol groups dissociate and generate negative charges on the capillary surface and H^+ ions in the electrolyte. The surface charge density on a fused silica capillary will strongly depend on the pH. With an estimated pK of the silanol groups between 3 and 5, the surface charge density is low at acidic pH and increases at higher pH. Above pH 9, all silanol groups are dissociated and the EOF reaches a maximum.

As shown in Figure 1.1, in a high pH medium, the cations and H^+ are attracted towards the negatively charged silanol groups, forming an ionic layer next to the capillary wall. The charge density of this layer decreases exponentially with increasing distance from the capillary wall. Upon application of an electric field, the cations in the double layer next to the wall start moving towards the cathode, entailing by solvation the whole liquid plug.

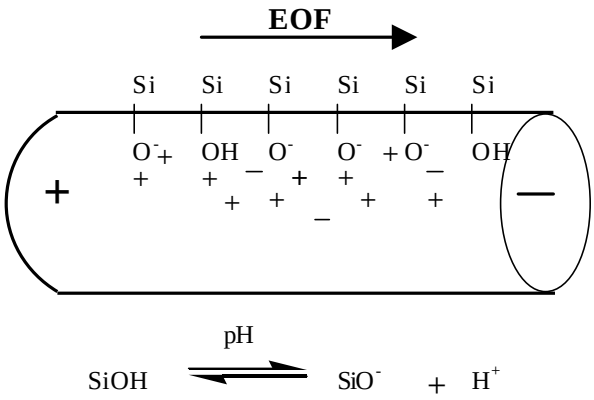

Figure 1.1 ***Schematic representation of the EOF***

The electroosmotic velocity ν_{eo} (m/s) is defined as

$$\nu_{eo} = \mu_{eo} E \qquad \text{(eq. 1.6)}$$

and the electroosmotic mobility, μ_{eo} (m^2/Vs)as,

$$\mu_{eo} = \frac{ez}{4ph} \qquad \text{(eq. 1.7)}$$

Thus, the EOF is a function of the dielectric constant ε, the zeta-potential ? and the viscosity h of the medium in the capillary.

The zeta potential is a function of the surface charge density on the capillary wall, and is proportional to the double layer thickness and inversely proportional to the ionic strength of the buffer medium.

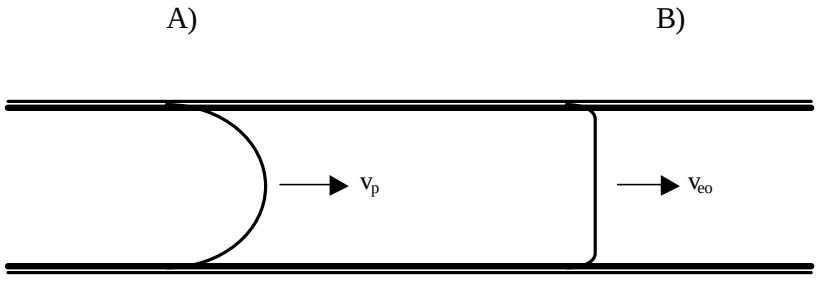

Figure 1.2 ***Flow profile and corresponding solute dispersion: A) pressure-driven profile, B) electrodriven profile***

The electroosmotic flow profile differs from a pressure-driven flow profile. The latter generates a parabolic (laminar) profile (Figure 1.2 A), resulting in severe solute zone broadening or dispersion, whereas the electroosmotic flow profile (Figure 1.2 B) is flat except close to the capillary wall (10% of the diameter). Hence, an electrodriven flow provides much higher efficiencies.

In a pressure-driven separation, reproducible flow conditions of the mobile phase and thus reproducible retention times are easily achieved through precise pressure control. This is in contrast to CE, where the electroosmotic velocity depends on a number of parameters, e.g. applied electric field, buffer medium, wall conditions, etc. Unfortunately, those parameters are not as easily and independently manipulated as pressure. EOF control is thus of utmost importance in electrodriven separation methods.

1.3.2 Factors influencing the electroosmotic flow (EOF)

While the EOF can be beneficial, it often needs to be suppressed. The charged capillary wall can cause adsorption of cationic solutes through Coulombic interactions. This phenomenon occurs especially in the separation of basic proteins. The electrophoretic separation modes isoelectric focusing, isotachophoresis, and capillary gel electrophoresis often require reduction of the EOF. The most important factor to manipulate the EOF is the pH. By changing the pH of the buffer solution, the dissociation of the silanol groups is influenced. The nature of the buffer and the buffer concentration influence the EOF by modifying the thickness of the double layer. Table 1.1 contains some acidic and basic electrolyte compositions and their corresponding EOF [10]. The EOF can also be affected by adjusting the concentration and ionic strength of the buffer. The zeta potential, and thus also the EOF, are reduced when the concentration of the buffer is increased. By increasing the temperature, the viscosity is reduced and the EOF is increased. In addition, organic modifiers such as methanol change the viscosity and usually decrease the EOF. The effect of organic modifiers on the

zeta potential is very complex and should be determined experimentally. Another way to manipulate the surface charge density and thus the magnitude of the EOF is modification of the capillary surface. Both neutral and positively charged coatings have been developed. Table 1.2 lists a selection of commercially available coated columns with, if available, the chemical nature of the coating and the recommended pH range [10].

Table 1.1 ***EOF in different electrolyte systems***

Electrolyte	Concentration (mM)	pH	EOF (10^{-5} cm^2/ Vs)
phosphate	10	2.5	4.2
phosphate	50	2.5	1.7
phosphate	100	2.5	<0.7
citrate	50	2.5	2.6
phosphate	50	9.0	49
borate	50	9.0	58
borate	150	9.5	46

Table 1.2 ***Commercially available coated CE capillaries***

Source	Brand name/pH range	Chemical nature of the coating
Beckman	eCAP Amine	polyamine
(Fullerton, CA, USA)	eCAP neutral/pH 4-8	polyacrylamide
Hewlett Packard	PVA/pH 2.5-9	poly(vinyl alcohol)
(Waldbronn Germany)	(no borate buffers)	
Supelco, Inc.	CElect-P	neutral hydrophilic
(Bellafonte, PA, USA)	CELet-H	weakly hydrophobic C_1 coating
	CElect-N	neutral hydrophilic
Scientific Resources	PEG-100	polyethylene glycol
(Eatontown, NJ, USA)		

1.4 CE modes

A schematic presentation of a basic CE instrument is shown in Figure 1.3. With the same instrumental set-up different electrodriven separation techniques can be realised.

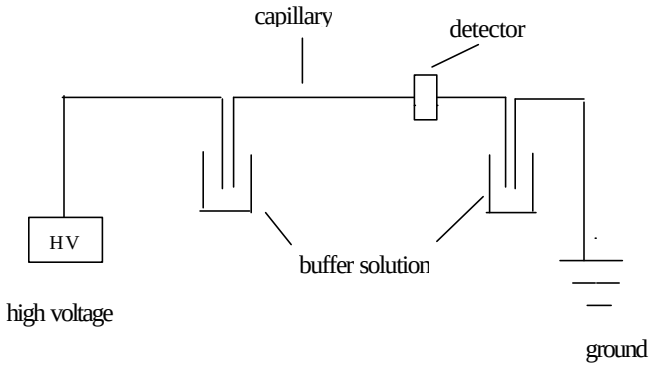

Figure 1.3 ***Capillary electrophoresis system***

1.4.1 Capillary zone electrophoresis (CZE)

CZE is the most popular and most widely applied electrodriven separation mode. A carrier or background electrolyte (BGE) is used to maintain a constant electric field along the separation axis. In the constant electric field, sample ions will migrate with a linear velocity proportional to their mobility (eq. 1.4). When mobilities differ, separation zones are formed. All zones move at a constant and characteristic speed.

1.4.2 Micellar electrokinetic chromatography (MEKC)

MEKC, introduced by Terabe in 1984 [11], is one of the most widely used CE modes. Its main strength is the ability to separate neutral solutes as well as

charged ones. Compared to CZE an additional selectivity principle is involved [12]. A charged surfactant is added to the run buffer and the formed micelles act as a pseudo-stationary phase. In this way, neutral molecules interacting with the micelles can be separated in an electric field.

1.4.3 Isotachophoresis (ITP)

ITP is the oldest CE mode. Everaerts' group particularly improved the technique in 1979 [13].

ITP is comparable to chromatographic focusing: the solutes are separated in discrete zones according to their electrophoretic velocity, between a leading (LE) and a terminating (TE) electrolyte. This train of solute bands moves at constant velocity passing the stationary detector. Every solute has a specific electrophoretic mobility, but field strength changes along the solute train. If zone mixing due to diffusion occurs at the front or the end of a band, these solutes leaving "their" zone will experience a different electric field, causing a slow-down or acceleration. The resulting effect of self-focusing, which is the most important advantage of ITP, is most often applied to ion analysis and charged small organic molecules. Although ITP failed to gain widespread acceptance, isotachophoretic effects may be useful for sample concentration during CZE analysis.

1.4.4 Capillary isoelectric focusing (CIEF)

The use of CIEF [14] is limited to the separation of amphoteric molecules such as proteins. An ampholyte mixture is used as the background electrolyte. It consists of amphoteric molecules with a range of pI values, covering the desired pH-

interval. Along the separation axis, a pH gradient is formed. Sample constituents will migrate, constantly adapting their charge to the local pH. When the local pH is equal to the isoelectric point, the protein will no longer migrate and remain focused in a narrow band. An additional step is necessary to force the zones to pass through the detector. This can be accomplished by inducing a hydrodynamic flow or electrophoretically, by changing the buffer, resulting in a breakdown of the pH gradient.

1.4.5 Capillary gel electrophoresis (CGE)

Capillary gel electrophoresis (CGE) is directly comparable to the traditional slab gel electrophoresis since the separation mechanisms are identical. CGE offers a number of advantages over traditional slab gel electrophoresis, including the use of a 10 to 100 times higher electric field without the deleterious effects of Joule heating, on-line detection and instrumental automation. In addition, due to the anticonvective nature of the capillary, it is not necessary to use a gel that is anticonvective by itself.

CGE is mainly employed in biological sciences for the size-based separation of macromolecules such as proteins and nucleic acids [15]. Cross-linked gels or entangled polymer solutions are used to suppress the EOF and to keep band diffusion small. Sieving occurs as the solutes move through the pore network of the gels or entangled polymer solution. By choosing appropriate separation conditions (buffer pH, buffer additives, polymer composition, coated capillary) the electrophoretic mobility depends only on molecular size. Therefore, CGE can be used for size separation. CGE represents an automated miniature format of slab

gel electrophoresis and has presently great impact on routine analytical procedures in biotechnology.

1.4.6 Capillary electrochromatography (CEC)

CEC, pioneered by the group of Knox [16], is basically a chromatographic separation technique. A stationary phase, typically silica or chemically modified silica, is used as chromatographic support, with particle diameters of 1-3 μm and filled into a capillary of 50-200 μm inner diameter. The mobile phase, which has to contain some electrically conductive components, is moved by the EOF when an electric field is applied. As in chromatography, the separation mechanism depends on the nature of the stationary phase. For charged solutes the chromatographic process is super-imposed by an electrophoretic process. Because of the plug-shaped flow profile of the EOF, the plate height is smaller and the separation power of CEC is superior to that of conventional LC systems. Moreover, longer columns and smaller particles can be applied compared to LC because of the lack of pressure drop.

1.5 Analytical parameters in capillary zone electrophoresis

1.5.1 Apparent mobility (μ_{app})

In CZE, the migration of solutes along the capillary is determined by the apparent mobility μ_{app} (m^2/Vs), which equals the vectorial sum of the electroosmotic mobility μ_{eo} and the electrophoretic mobility μ_{ep} as expressed by eq. 1.8:

$$\mu_{app} = \mu_{ep} + \mu_{eo} \qquad \text{(eq.1.8)}$$

Accordingly, the migration velocity ν_{app} (m/s) is

$$\nu_{app} = \mu_{app} E = (\mu_{ep} + \mu_{eo}) E = \nu_{ep} + \nu_{eo} \qquad \text{(eq.1.9)}$$

At low pH (pH 2-3), the EOF is negligible compared to the electrophoretic mobility. In this case, the magnitude and direction of the electrophoretic mobility of the analytes of interest determine the apparent mobility. Positive and negative analytes can no longer be separated together in one run. In order to detect negatively charged analytes, the polarity of the electrical field should be reversed. In contrast to the condition with a large EOF, injection occurs at the cathodic side and detection at the anodic side.

1.5.2 Migration time (t)

The time required for a solute to migrate to the detector is called migration time, and is given by the ratio of the migration distance to the velocity. The migration time t (s) can be calculated according to the equation:

$$t = \frac{l}{n_{app}} = \frac{l}{m_{app} E} = \frac{l}{m_{app}} \frac{L}{V} \qquad \text{(eq. 1.10)}$$

where $\mu_{app} = \mu_{ep} + \mu_{eo}$ (m^2/Vs)

E = electric field (V/m)

V = applied voltage (V)

L = total length of the capillary (m)

l = capillary length from inlet to the detector (m)

This equation shows that the use of short capillaries in combination with high voltages will result in short migration times.

A similar equation can be used to express the EOF in time units:

$$t_{eo} = \frac{l}{m_{eo}} \frac{L}{V} \qquad \text{(eq. 1.11)}$$

From eq. 1.10 and eq. 1.11, the electrophoretic mobility μ_{ep} (m^2/Vs) can be calculated by

$$\mu_{ep} = \frac{lL}{V} \frac{t_{eo} - t}{t_{eo} t} \qquad \text{(eq. 1. 12)}$$

1.5.3 Separation efficiency (N)

Separation in electrophoresis is based on differences in solute mobility. The difference necessary to resolve two zones is dependent on the length of the zones. Zone length is strongly determined by dispersive processes. Dispersion should be controlled because it increases zone length and the mobility difference necessary to achieve separation.

Under ideal conditions (i.e. small injection plug length, no solute-wall interactions, etc.), the only contribution to solute-zone broadening in CE is considered to be longitudinal diffusion along the capillary. Radial diffusion (across the capillary) is unimportant due to the plug flow profile. Similarly, convective broadening is unimportant due to the anticonvective properties of the capillary. Thus, zone broadening in CE by diffusion, after a time t (s), is given by Einstein's equation:

$$\sigma^2 = 2Dt \qquad \text{(eq. 1.13)}$$

where D = molecular diffusion coefficient (m^2/s)

σ^2 = spatial variance (m^2)

The plate height H (m), which is equal to $\frac{s^2}{x}$, can be expressed as

$$H = \frac{2Dt}{x} = \frac{2D}{v} \text{ (cm)} \qquad \text{(eq. 1.14)}$$

where x (m) is the migration distance at a migration time t (s), and $x = \nu t$, with ν = velocity of the charged species (m/s). Because $\nu_{ep} = \mu_{ep} E$, this gives

$$H = \frac{2D}{m\ E} \qquad \text{(eq. 1.15)}$$

Since the theoretical plate number is related to H by $N = \frac{x}{H}$,

$$N = \frac{xm\,E}{2D} \qquad \text{(eq. 1.16)}$$

If we assure that the migration takes place across the whole length of the capillary, the field strength can be replaced by $\frac{V}{x}$ and we obtain

$$N = \frac{m\,V}{2D} \qquad \text{(eq. 1.17)}$$

or taking the electroosmotic mobility into account

$$N = \frac{(m + m_{eo})V}{2D} \qquad \text{(eq. 1.18)}$$

From eq. 1.18, it can derived that increasing the voltage will result in higher efficiency as long as Joule heating does not contribute to band broadening. In addition to the longitudinal diffusion, there are many other factors contributing to dispersion, namely injection plug length, solute interactions with the capillary wall (usually causing serious peak tailing), conductivity mismatch of sample and buffer (resulting in electro-dispersion: peak tailing or peak fronting) and zone broadening related to the detection system.

Experimentally, the theoretical plate number (N) can be determined directly from an electropherogram using equation [17]:

$$N = 5.54 \left(\frac{t}{w_{1/2}}\right)^2 \qquad \text{(eq. 1.19)}$$

where t = migration time (s)

$w_{1/2}$ = peak width at half height (s)

1.5.4 Resolution (R_s)

The resolution R_s of two peaks is defined as the quotient of the distance between the peak centres Δx and $w_b = 4\sigma$, the mean of the two standard deviations for a Gaussian peak

$$R_s = \frac{\Delta x}{4s} \qquad \text{(eq. 1.20)}$$

in which w_b = peak width at the base line.

The resolution between two peaks in CE can be deduced to give equation [17]:

$$R = 0.177 \, (\mu_{ep1} - \mu_{ep2}) \sqrt{\frac{V}{D(\overline{m}_{ep} + m_{eo})}} \qquad \text{(eq. 1.21)}$$

where $\overline{m}_{ep}$ is the mean of the electrophoretic mobility of components 1 and 2.

From eq. 1.21, it can be deduced that to increase the resolution, an increase of voltage is not very efficient because of the square root relation. Theoretically, the best resolution is obtained when $\mu_{eo} = -\overline{m}_{ep}$. In practice, a resolution of 1.25 is sufficient even for quantitative analysis and resolution higher than 1.5 is considered a waste of time.

The resolution can be directly calculated from the electropherogram by

$$R_s = \frac{t_2 - t_1}{\frac{1}{2}(w_{b_1} + w_{b_2})} = \frac{t_2 - t_1}{\overline{w}} = \frac{t_2 - t_1}{4s} \qquad \text{(eq. 1.22)}$$

where t = migration time (s)

w_b = baseline peak width (s)

$\overline{w}$ = mean of the baseline peak width (s)

σ = standard deviation,

subscripts 1 and 2 refer to the two solutes.

1.6 Instrumental aspects

1.6.1 Injection

To introduce the sample into the capillary, hydrodynamic or electrokinetic injection approaches are used. Hydrodynamic injection is driven by pressure, whereas electrokinetic injection is done by applying a voltage.

The main advantage of hydrodynamic injection is that the quantity of sample loaded is nearly independent on the sample matrix and that "electrophoretic discrimination" is absent. The volume (m^3) injected can be calculated using the Hagen-Poiseuille equation:

$$\text{volume} = \frac{\Delta P d^4 p \ t}{128 h L} \qquad \text{(eq. 1.23)}$$

where Δ P = pressure difference across the capillary (Pa)

d = internal diameter of the capillary (m)

t = injection time (s)

η = viscosity of sample (Pa s = Kg/ms)

L = total capillary length (m).

In the electrokinetic injection mode, the analytes enter the capillary by both electrophoretic and electroosmotic migration. The disadvantage of this method is

that the quantity of sample loaded is dependent on the electrophoretic mobility of the individual solutes. Discrimination occurs for ionic species since more mobile ions are loaded to a greater extent than the less mobile ones. Due to this phenomenon, electrokinetic injection is generally not as reproducible as its hydrodynamic counterpart. The quantity injected, Q (moles) is

$$Q = \frac{(m_{ep} + m_{eo})Vr^2p \quad Ct}{L} \qquad \text{(eq. 1.24)}$$

where μ_{ep} = electrophoretic mobility of the analyte (m^2/ Vs)

μ_{eo} = electroosmotic mobility (m^2/ Vs)

V = voltage (V)

r = capillary radius (m)

C = analyte concentration (moles/m^3)

L = total capillary length (m)

t = injection time (s)

1.6.2 Capillaries

The capillaries in CE are made almost exclusively from fused silica. Only in few reports teflon capillaries are applied.

Fused silica capillaries are available in almost any inner diameter varying from 1 to 530 μm. For protection, the fused silica capillaries are coated on their outside with a 10-20 μm thick film of polyimide making them flexible and easier to handle. Today, polyimide coated fused silica capillaries with inner diameters (i.d.) of 50 to 100 μm and outer diameters of 360 μm are most commonly used in commercial instrumentation. The volume of capillaries ranges from 39.2 nL for a

10 μm i.d. capillary to 15.7 μL for a 200 μm i.d. capillary with 50 cm in length which is commonly applied in CE. Since only about 1% of the column volume should be used for injection and detection, these volumes are in the order of 0.4 to 160 nL. Consequently this puts a heavy burden on sensitive detection in CE.

1.6.3 Detection

Fused silica is optically similar to pure quartz glass and by burning off a small section of the polyimide coating, a perfect window for the detection is obtained. The most important detection methods used in CE and the limits of detection (LOD) are summarised in Table 1.3.

Table 1.3 ***Detection methods and detection limits (LOD) in CE***

Detection	LOD (M)	Detection	LOD (M)
UV	$10^{-5} - 10^{-6}$	indirect UV	10^{-5}
LIF	$10^{-12} - 10^{-13}$	indirect LIF	10^{-7}
conductivity	10^{-6}	thermo optical absorbance	10^{-8}
amperometry	10^{-8}	mass spectrometry	10^{-7}-10^{-8}

1.6.3.1 UV detection

UV detection is a popular detection method for separation techniques performed in a condensed phase because of its almost universal applicability. For its use in CE, commercial UV detectors for HPLC with deuterium lamps were modified for on-column detection. The drawback of on-column UV detection in CE is the sensitivity since only the capillary cross-section of 10 to 100 μm is available as path length. Several approaches have been developed to improve the sensitivity, e.g. Z-shaped cell [18], multi-reflection flow cell [19], bubble cell [20], etc.

For high sensitivity, sample preconcentration steps such as stacking [21], isotachophoresis [13] or derivatisation prior to analysis are necessary.

Spectral information can be obtained using a diode array detector or a fast scanning multiple wavelength detector.

Even with techniques that utilise increased path-length cell or/and chemical derivatisation, absorbance detectors are ultimately limited according to Beer's law. As a result, UV-absorption techniques have modest detection limits that generally do not exceed the 10^{-6} M range.

1.6.3.2 Indirect UV detection

Optical CE detection methods suffer not only from a short optical path length but also from the fact that solutes of interest do not always absorb radiation. Although many solutes show some absorption at wavelengths from 195 nm to 200 nm, the majority of carbohydrates do not have any UV absorbance or fluorescence. To detect nonabsorbing and nonfluorescent solutes with UV and LIF, respectively, indirect optical detection can be used [22-27]. Figure 1.4 shows the principle of indirect detection methods. Using strong UV-absorbing or fluorescent solutes in the buffer, the detector is nearly saturated, rising the baseline at elevated level. If a non-absorbing or non-fluorescent solute moves through the detection window, it displaces molecules from the background and generates a negative peak. It was shown that the concentration limit of detection (C_{lim}) depends on three key factors: concentration of the active mobile phase additive (background concentration, C_{bg}), transfer ratio (TR) and dynamic reserve (DR) [28, 29] as

described in eq. 1.25. This transfer ratio is defined as the number of molecules of active mobile phase displaced by an analyte molecule.

$$C_{lim} = \frac{C_{bg}}{TR \times DR} \qquad \text{(eq. 1. 25)}$$

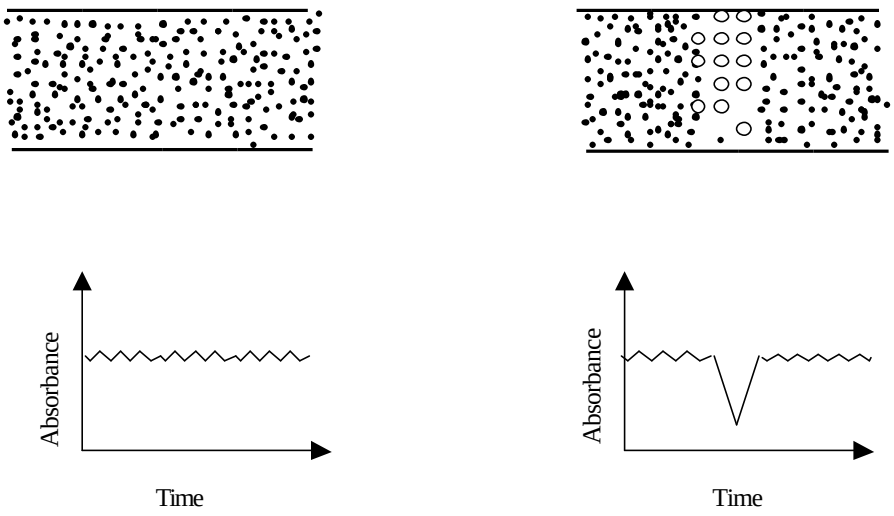

Figure 1.4 ***Principle of the indirect detection method***

A detection limit of 2×10^{-4} M was reported by using sorbic acid as UV-absorbing additive for the analysis of mono-, di- and trisaccharides [23]. Although the detection sensitivity is not sufficient for the analysis of glycoproteins which are proteins with carbohydrate side-chains, indirect UV detection works well for sugar analysis in food, e.g. the determination of glucose, fructose and saccharose in fruit juices [30].

Indirect LIF has been demonstrated by using coumarin 343 as fluorophore additive for the analysis of monosaccharides [31]. The detection limits were in the low micromolar range for saccharose, glucose and fructose and only slightly better than those obtained with indirect UV detection.

1.6.3.3 Laser induced fluorescence detection (LIFD)

Since the sensitivity of UV detection was generally regarded as insufficient for biological samples, considerable efforts were put into developing and improving alternative detection systems. There are several advantages of fluorescence detection including excellent sensitivity and a large linear dynamic range. Six or seven orders of magnitude in linearity are observed with fluorescence spectroscopy whereas only three or four orders of magnitude with other spectrophotometric procedures.

In a few reports, a deuterium or xenon arc lamp or a mercury line source was used for fluorescence excitation in CE [32, 33]. The small size of the detection window and the required high photon density for efficient excitation make lasers an ideal source for fluorescence detection in capillaries [34]. One drawback of fluorescence detection is that most analytes do not possess fluorophores, and this is especially true when working with carbohydrates. Laser induced fluorescence detection (LIFD) has become the most preferred detection method in CE for the anaysis of carbohydrates by tagging the later with fluorescence reagents [35, 36].

In LIFD, the sensitivity depends on the light source, its intensity, stability and the optical match of the excitation source with the fluorophore absorption maximum. Laser-based fluorescence is particularly well suited for CE because of the high

power available, the good focusing capability and the monochromaticity of the laser light.

Fluorescence emission in molecules occurs through the absorption of a quantum of radiation and involves changes in the electronic structure. Fluorescence is referred to as the emitted light when the excited electron returns to the ground level. The energy transmission of electrons is depicted in Figure 1.5.

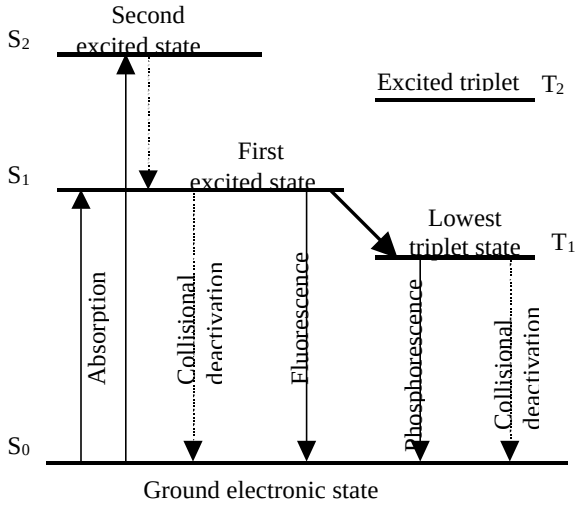

Figure 1.5 ***Schematic diagram of energy level transitions involved in photoluminescence***

When light strikes a molecule, it is absorbed, and a transition to a higher electronic state occurs. This absorption of radiation is highly specific with the result that radiation of a particular energy is absorbed only by a characteristic molecular structure. The electron is raised to an upper excited singlet (S_1, S_2, etc.) through a ground-to-singlet state transition that is responsible for the visible and UV absorption spectra observed for molecules. During the time the molecule spends in the excited state, some energy is not further dissipated by collisions with other molecules, and the electron returns to the ground electronic state, with the

emission of a photon. This phenomenon is called fluorescence. The emission of light is usually in the UV to visible region of the spectrum. Because some energy is lost during that period before emission can occur, the emitted energy (fluorescence) is lower than the energy that was absorbed, and the resulting wavelength (λ) of the emitted light is longer.

The efficiency with which fluorescence occurs in molecules is given by [37]:

$$\Phi = \frac{No_{em}}{No_{ab}} = \text{quantum efficiency} \qquad \text{(eq. 1.26)}$$

with No_{em} = number of photons emitted

No_{ab} = number of photons absorbed

The basic equation defining the relationship of fluorescence to the concentration is:

$$F = \Phi I_o (1-e^{-\varepsilon bc}) \qquad \text{(eq. 1.27)}$$

where I_o = incident radiant power (W)

ε = molar extinction coefficient ($M^{-1}cm^{-1}$)

b = path length (cm)

c = molar concentration (M)

According to eq. 1.27, the fluorescence intensity is enhanced by increasing (i) the quantum efficiency, (ii) the intensity of incident radiation I_o, (iii) the molar extinction coefficient of the analyte e and (iv) the concentration of the analyte.

LIFD systems are comprised of two basic parts, namely a laser excitation source and an optical detection system. In most systems, excitation is performed on-column and the emitted fluorescence is collected orthogonally to the direction of

the laser beam. The limits of detection (LOD) of this detector ranges from 10^{-6} M to 10^{-10} M.

An arrangement with a post-column LIF detection system based upon a quartz sheath-flow cuvette utilises both a 488 nm argon ion laser [38] and a 543 nm helium-neon laser [39] for different applications. This LIF detection minimises laser scattering, thus reducing the most important source of background noise. Hernandez and co-workers [40, 41] used a different arrangement whereby the laser beam and the emitted light are collinear. The collinear set-up reduces laser scattering onto the walls of the capillary and enhances the collection of fluorescence. The advantages of the collinear arrangement as an alternative to the orthogonal design for the on-column detection in capillary electrophoresis were discussed by Hernandez *et al.* [41]. With the collinear arrangement the authors claimed a LOD of 10^{-13} M for fluorescein isothiocyanate (FITC) derivatised arginine.

The Beckman PACE laser module used in this work also employs a collinear arrangement and is schematically shown in Figure 1.6. A fiber optical cable transmits laser light from a 3 mW argon-ion laser to the detector and illuminates the capillary window. The ellipsoidal mirror collects and focuses the fluorescent light back onto the photo-multiplier tube (PMT). To reduce unwanted laser light, a centred hole in the ellipsoidal mirror allows most of the beam to pass. In addition, a beam block is used to attenuate scattered laser light. A notch 488 nm "rejection" filter is used to prevent stray laser light from entering the PMT while a band pass filter allows only emitted fluorescence light at the 520 nm band to pass into the PMT.

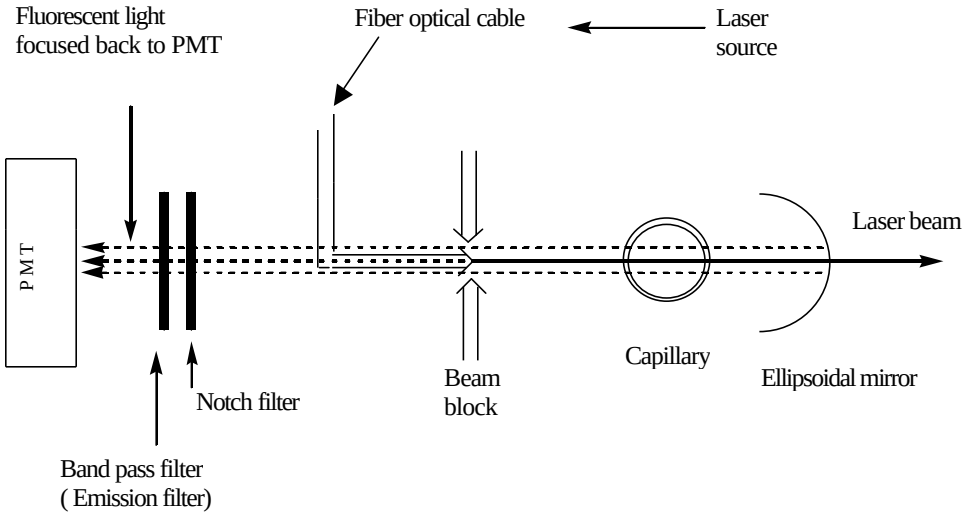

Figure 1.6 ***The laser module with collinear arrangement (Beckman)***

1.6.3.4 Electrochemical detection (ECD)

Electrochemical detection for CE was first introduced by Wallingford and Ewing [42] using a porous glass joint to decouple the amperometric detector from the high electric field of the separation capillary. With a high EOF, the solute is pushed past the intersection towards the detector. Amperometric detection with a carbon electrode lends itself to the separation and sensitive detection of easily oxidised species such as catecholamines, achieving LODs in the range of 10^{-8} M. Using different electrode materials such as copper [43-46] or gold [45, 47], the detection of carbohydrates with ECD is feasible. Currently no commercial ECD instrumentation is on the market, inhibiting its widespread use.

1.6.3.5 Mass spectrometric detection (MS)

The advantages of coupling information rich mass spectrometric (MS) [48, 49] methods with the highly efficient CE have long been recognised. In addition, dimensions of CE perfectly fit with state-of-the art MS instrumentation. In order to harvest the benefits of CE-MS, an interface design for the sample transfer from the liquid phase to the MS vacuum must minimise band dispersion. Direct coupling of CE with MS has been described using fast atom bombardment (FAB) and atmospheric pressure ionisation (API) as ionisation methods. Off-line coupling has been reported for plasma desorption (PD) and matrix assisted laser desorption ionisation (MALDI). Von Brocke *et al.* recently published a review on CE coupling with electrospray ionisation-mass spectrometry (CE/ESI-MS) [50].

References

[1] A. Tiselius, *Trans. Faraday Soc.* 33, **1937**, 524

[2] S. Hjertén, *Chromatogr. Rev.* 9, **1969**, 122

[3] R. Virtanen and P. Kivalo, *Suomen Kemistilehti B,* **1969**, 182

[4] F. E. P. Mikkers, F. M. Everaerts and Th. P. E. M. Verheggen, *J. Chromatogr.* 169, **1979**, 11

[5] J. W. Jorgenson and K.D. Lukacs, *Anal. Chem*. 53, **1981,** 1289

[6] J. W. Jorgenson and K. D. Lukacs, *Science* 222, **1983**, 266

[7] R. Audubert and S. De Mende, The principles of electrophoresis, Hotchinson & Co., London, **1959**

[8] S. Hjertén, *Topics Bioelectrochem. Bioenerg.* 2, **1978**, 89

[9] B. Michov, *Electrophoresis* 9, **1988**, 201

[10] A. Paulus and A. Klochow-Beck, Analysis of carbohydrates by capillary electrophoresis, Chromatographia, CE series, K. D. Altria Ed., Vieweg publishing, Wiesbaden, **1999**

[11] S. Terabe, *Trends Anal. Chem*. 8, **1989**, 129

[12] J. Vindevogel and P. Sandra, Introduction to micellar electrokinetic chromatography, Hüthig Buch Verlag, Heidelberg, **1992**

[13] E. E. P. Mikkers, F. M. Everaerts and T. E. P. M. Verheggen,

J. Chromatogr. 169, **1979**, 11

[14] P. Righetti, E. Gianazza, E., C. Gelfi, M. Chiari and P. Sinha, *Anal. Chem*. 61, **1989**, 160

[15] C. Heller, Analysis of nucleic acids by capillary electrophoresis, Vieweg Publishing, Wiesbaden, **1997**

[16] J. H. Knox and I. H. Grant, *Chromatographia* 24, **1987**, 135

[17] R. Kuhn and S. Hoffstetter-Kuhn, Capillary electrophoresis: principles and practice, Springer-Verlag, Heidelberg, **1993**

[18] J. Chervet, R. Van Soest and M. Ursem, *J. Chromatogr.* 543, **1991**, 439

[19] T. Wang, J. Aiken, C. Huie and J. Hartwick, *Anal. Chem.*14, **1991**, 1372

[20] D. Heiger, "High performance capillary electrophoresis", Hewlett-Packard, Walbronn, **1992**

[21] R. L. Chien and D. S. Burgi, *Anal. Chem.* 64, **1992**, 1046

[22] F. Foret, S. Fnanli, L. Ossicini and P. Bocek, *J. Chromatogr.* 470, **1986**, 299

[23] P. J. Oefner, A. E. Vorndran, E. Grill, C. Huber and G. K. Bonn, *Chromatographia* 34, **1992**, 308

[24] G. J. M. Bruin, A. C. van Asten, X. Xu and H. Poppe, *J. Chromatogr.* 608, **1992**, 97

[25] W. Kuhr and E. S. Yeung, *Anal. Chem*. 60, **1998**, 2642

[26] L. Gross and E. S. Yeung, *Anal. Chem.* 62, **1990**, 427

[27] T. W. Garner and E. S. Yeung, *J. Chromatogr.* 515, **1990**, 639

[28] E. Yenug, *Acc. Chem. Res.* 22, **1989**, 125

[29] E. Yenug and W. Kuhr, *Anal. Chem*. 63, **1991**, 275

[30] A. Klockow, A. Paulus, V. Figueiredo, R. Amado and H. M. Widmer, *J. Chromatogr. A* 680, **1994**, 187

[31] T. W. Garner and E. S. Yeung, *J. Chromatogr.* 515, **1990**, 639

[32] J. W. Jorgenson and K. D. Lukacs, *Science,* 222, **1983**, 266

[33] M. Albin, R. Weinberger, E. Sapp and S. Moing, *Anal. Chem.* 63, **1991**, 417

[34] E. Gassman J. E. Kuo and R. N. Zare, *Science* 230, **1985**, 813

[35] M. Hong and M. V. Novotny, *Anal. Chem.* 70, **1998**, 568

[36] R. A. Evangelista, M.-S. Liu and F.-T. A. Chen, *Anal. Chem.* 67, **1995**, 2239

[37] Journal of Chromatography Library – Volume 58, Carbohydrate analysis, high performance liquid chromatography and capillary electrophoresis, Ed. Z. El Rassi, Elseviers, Amsterdam, **1995**

[38] Y. F. Cheng, S. Wu, D. Y. Chen and N. J. Dovichi, *Anal. Chem.* 62, **1990**, 496

[39] S. Wu and N. J. Dovichi, *J. Chromatogr.* 480, **1989**, 141

[40] C. Toulas and L. Hermandez, *LC.GC Intl.* 5, **1988**, 27

[41] L. Hernandez, J. Escalona, N. Joshi and N. Guzman, *J. Chromatogr.* 559, **1991**, 183

[42] R. A. Wallingford and A.G. Ewing, *Anal. Chem.* 59, **1987**, 1762

[43] L. A. Colon, R. Dadoo and R. N. Zare, *Anal. Chem.* 65, **1993**, 476

[44] J. Ye and R. P. Baldwin, *J. Chromatogr. A* 687, **1994**, 141

[45] X. Huang and W. T. Kok, *J. Chromatogr. A* 707, **1995**, 335

[46] J. Ye and R. P. Baldwin, *Anal. Chem.* 65, **1993**, 3525

[47] T. J. O'Shea, S. M. Lunte and W. R. Lacourse, *Anal. Chem.* 65, **1993**, 948

[48] J. Cai and J. Henion, *J. Chromatogr. A* 703, **1995**, 667

[49] R. D. Smith, D. R. Goodlett, and J. H. Wahl, "Capillary electrophoresis – mass spectrometry", in "Handbook of capillary electrophoresis", Ed. J. P. Landers, CRC Press, Boca Raton, **1994**

[50] A. von Brocke, G. Nicholson and E. Bayer, *Electrophoresis* 22, **2001**, 1251

Chapter 2

Structures and Properties of Saccharides

Abstract

A brief description of the structures and properties of saccharides including monosaccharides, oligosaccharides and polysaccharides is presented. Polysaccharides of interest like amylose and gums are described in more detail.

2.1 Introduction

Saccharides, also called sugars or carbohydrates, can be divided into monosaccharides, oligosaccharides and polysaccharides depending on the number of sugar units that are linked together. Monosaccharides are the monomer units and cannot be hydrolysed into smaller molecules whereas oligosaccharides contain 2 to 10 monosaccharide residues joined by glycosidic linkages. The polysaccharides are polymers of high molecular weight consisting of more than 10 monosaccharide units. Due to their size, polysaccharides are less water-soluble than the mono- and oligosaccharides. They do not taste sweet and are chemically less reactive.

Monosaccharides can be joined together *via* all equivalent hydroxyl groups and the variety obtained is even increased by the complicated stereochemistry. Two identical monosaccharides can form up to 11 different disaccharides. Four

different hexoses (e.g. glucose, galactose, mannose and allose) can produce more than 36,000 tetrasaccharides [1]. The consequence is an enormous diversity and complexity in saccharide structure and chemistry. Such a structural diversity creates many difficulties in the analysis of saccharides.

.

2.2 Monosaccharides

Monosaccharides are principally polyhydroxyaldehydes (aldoses) or polyhydroxyketones (ketoses) derived from glyceraldehyde or dihydroxyacetone, respectively, through insertion of CHOH-units. They follow the general molecular formula $C_n(H_2O)_n$. The aldoses are classified according to the number of carbon atoms starting with the triose glyceraldehyde (3 C-atoms), into tetroses (4 C-atoms), pentoses (5 C-atoms, e.g. ribose, xylose) and hexoses (6 C-atoms, e.g. glucose, mannose, galactose). The ketoses, starting with the triulose dihydroxyacetone, are called tetruloses (4 C-atoms), pentuloses (5 C-atoms, e.g. ribulose, xylulose) and hexulose (6-atoms, e.g. fructose, sorbose).

Glyceraldehyde has one asymmetric carbon atom resulting in an enantiomeric pair, D- and L-glyceraldehyde. The prefixes D and L designate the absolute configuration. The compounds derived from D-glyceraldehyde by inserting CHOH groups are called D-aldoses and those derived from L-glyceraldehyde are called L-aldoses. Figure 2.1 shows the stereoisomeric family of monosaccharides derived from D-glyceraldehyde (for aldose). The L-series and D-series of monosaccharides only differ from each other as object and mirror image. A molecule with n asymmetric centres has 2^n stereoisomers.

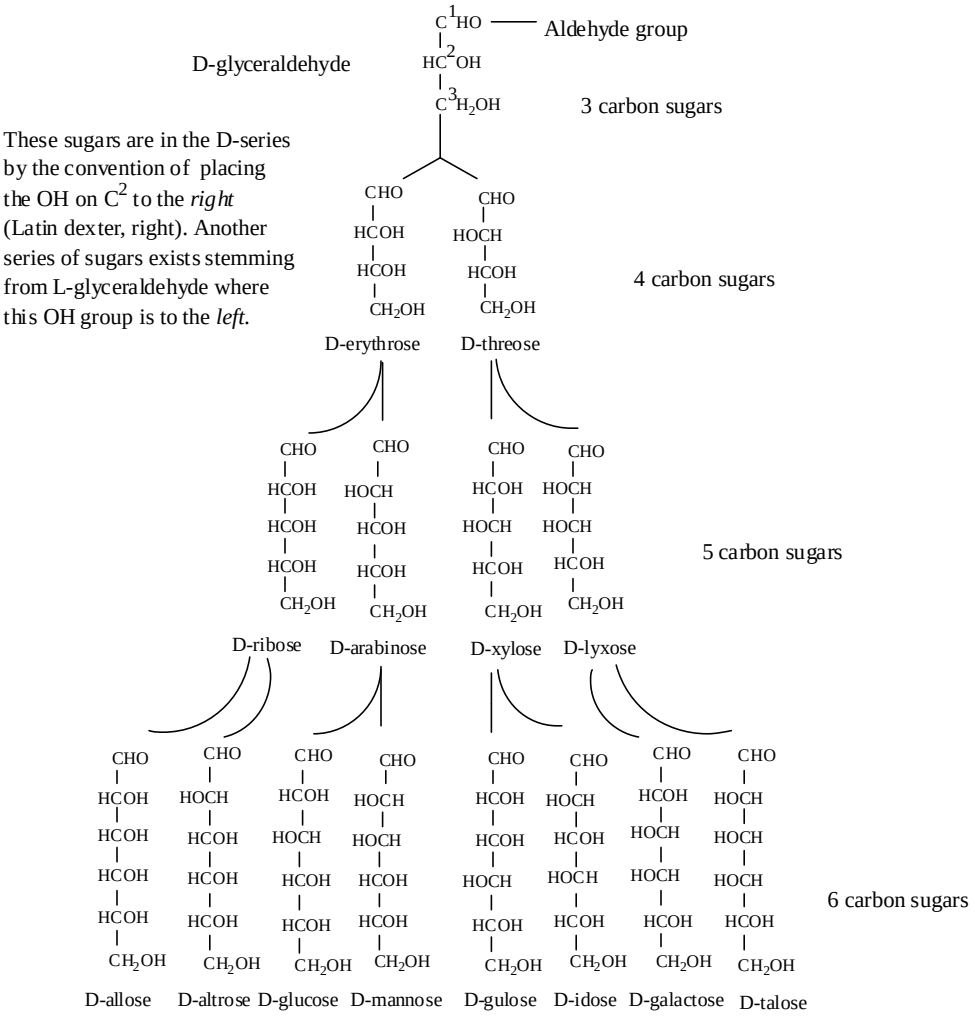

Figure 2.1 ***The family of D-aldoses***

All monosaccharides can principally form stable 5-membered (furanose) and 6-membered (pyranose) rings through formation of an intramolecular hemiacetal. The lactol formation leads to an additional chiral centre and therefore to formation of anomers that are designated with α and β. α means that the hydroxyl group at C_1 is below the plane of the ring and β means that it is above the plane of the ring. The tendency for ring formation is so high that most monosaccharides exist in an equilibrium of cyclic hemiacetals in solution and only a small amount of the open-

chain form is present. The cyclic forms turn out to be much more stable than the open-chain forms. Consequently, in solution each monosaccharide occurs in five different forms as depicted for D-glucose in Figure 2.2.

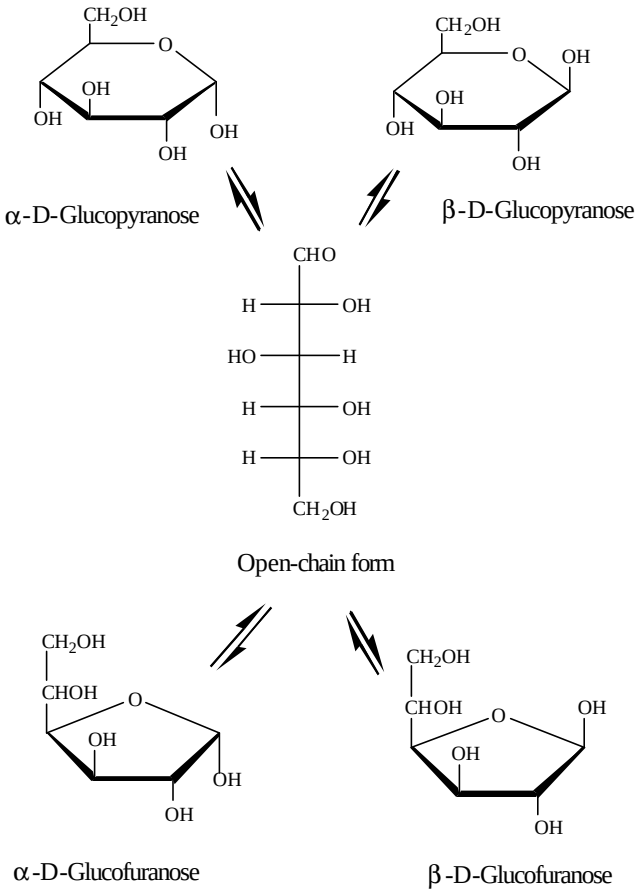

Figure 2.2 ***Structures of the five different forms of D-glucose in water***

In equilibrium glucose is present almost exclusively in its pyranose forms with 36% α and 64% β [1]. For other monosaccharides the equilibrium mixture can be very different. The different ring forms always interconvert through the open chain form of the sugars. This is called mutarotation. For a comprehensive

discussion of the structural and stereochemical features of monosaccharides, we refer to organic chemistry and biochemistry textbooks [2, 3].

Deoxysugars and monosaccharides containing functional groups such as acidic sugars and amino sugars are important components in oligo- and polysaccharides.

Deoxysugars: Deoxysugars, in which one or more of the hydroxyl groups of an aldose or ketose has been replaced by hydrogen, are widely distributed in nature. 6-Deoxyhexoses such as 6-deoxy-L-mannose (L-rhamnose) and 6-deoxy-L-galactose (L-fucose) are present in many polysaccharides and glycoproteins.

Acidic sugars: There are three different types of acidic sugars. They are classified according to the terminal group that has been oxidised. *Aldonic acids* are formed by oxidation of the carbonyl group, *uronic acid* by oxidation of the terminal alcohol group and *aldaric acids* by oxidation of both the carbonyl and the terminal alcohol group. The most important type of acidic sugars are uronic acids, which occur almost exclusively as hexuronic acids. They are intermediates in the conversion of hexoses and pentoses in biosynthetic pathways. D-glucuronic acid and D-galacturonic acid are found in plant gums and bacterial cell walls whereas D-glucuronic acid and L-iduronic acid are components of proteoglycans.

Aminosugars: The anomeric carbon atom of a monosaccharide can be linked to the nitrogen of an amine by an *N*-glycosidic bond. Most aminosugars occur as constituents in oligo- and polysaccharides. The most abundant aminosugar is 2-amino-2-deoxy-D-glucose that occurs widely in polysaccharides and in glycoproteins as its *N*-acetylated derivative (*N*-acetylglucosamine).

2.3 Oligosaccharides

The linkage of two monosaccharides through an *O*-glycosidic bond results in the formation of a disaccharide. Glycosidic linkage between the hydroxyl group at the anomeric carbon of two monosaccharides results in a non reducing disaccharide such as sucrose, while condensation of one hydroxyl group at the anomeric carbon and one free hydroxyl group results in a reducing disaccharide, e.g. maltose and lactose.

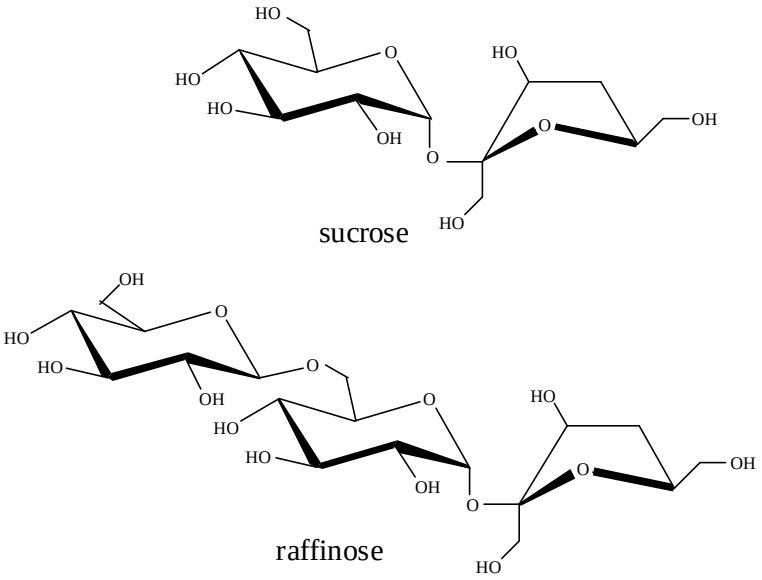

Figure 2.3 ***Structures of sucrose and raffinose***

The most common naturally occurring oligosaccharide is saccharose (sucrose) that is widely distributed in the plant world. It is the main component in the carbohydrate reserve and an important energy source. The principle sources for commercial production of this disaccharide are sugar cane, sugar beet and the sap of maple trees. It is composed of one D-glucose and one D-fructose unit, joined by an acetal linkage between two anomeric carbons. The glucose unit is in the

pyranose form while fructose is in the furanose form. The structure is shown in Figure 2.3.

Raffinose (Figure 2.3) is an example of a trisaccharide. This naturally occurring saccharide is as widely distributed as sucrose but in much lower concentration (e.g. 0.05% in sugar beet, 1.9% in soybean) [1].

Other important oligosaccharides are cyclodextrin (cyclomalto-oligosaccharides) including α-cyclodextrin (cyclohexaose), β-cyclodextrin (cycloheptaose) and γ-cyclodextrin (cyclo-octaose). Due to their cyclic structure, cyclodextrins can form inclusion complexes with small molecules. Cyclodextrins are used in the formulation of pharmaceuticals, pesticides, foodstuffs and toiletries as protecting agents, emulsion stabilisers or as slow releasing agents. Besides, charged cyclodextrin derivatives are used as chiral selectors in the separation of enantiomers by CE [4].

2.4 Polysaccharides

Polysaccharides differ from the oligosaccharides only by the number of monosaccharides that make up the molecules. Polysaccharides are built from either one (homopolysaccharides) or several monosaccharide types (heteropolysaccharides). They can have a linear structure in which the individual monosaccharides are joined one to the other by glycosidic bonds, or they can be branched. A branched polysaccharide has a linear backbone, but additional hydoxyl groups on some of the monosaccharide units are involved in glycosidic bonding to another chain of sugars. Table 2.1 and Table 2.2 show a selection of common homo- and heteropolysaccharides, respectively [1, 5].

Table 2.1 ***Structure and source of homopolysaccharides***

Name	*Linkage*	*Source*
D-Fructans		
Inulin	(2,1)-β-D- linear	dahlias, Jerusalem artichokes
Levan	(2,6)-β-D-, (2,1)-β-D- branched	plants and bacteria
D-Galactans		
Carrageenan	(1,3)-β-D-, (1,4)-α-D- linear	red seaweeds
	(1,4)-β-D- linear	plant pectic substance
D-Galacturonans		
Pectic acid	(1,4)-α-D- linear	plant pectic substance
D-Glucans		
Laminaran	(1,3)-β-D- linear	brown seaweeds, plants
Scleroglucan	(1,3)-β-D-, (1,6)-)-β-D- branched	fungi
Lichenan	(1,3)-β-D-, (1,4)-β-D- linear	iceland moss, cereal grains
Amylose	(1,4)-α-D- linear	plants
Amylopectin	(1,4)-α-D-, (1,6)-α-D- linear,	plants
Glycogen	(1,4)-α-D-, (1,6)-α-D- linear	animals
Cellulose	(1,4)-β-D- linear	plant cell-walls
Pullulan	(1,4)-α-D-, (1,6)-α-D- linear	fungi
Dextran	(1,6)-β-D- linear	bacteria
2-Amino-2-deoxy-D-Glucans		
Chitin	(1,4)-β-D- linear	crab and lobster shell, fungi
D-Mannans		
	(1,4)-β-D- linear	seaweed, plants
	(1,2)-α-D-, (1,6)-α-D- branched	yeasts
D-xylans		
	(1,4)-β-D- linear	plant cell walls
Rhodymenan	(1,3)-β-D- linear	green seaweed

Table 2.2 ***Structure and source of heteropolysaccharides***

Name	*Constituent monosaccharides and chain type*	*Source*
Agarose	D-, L-galactose, linear	red seaweeds
Alginic acid	L-guluronic acid,	bacteria
	D-mannuronic acid, linear	brown seaweeds
Gum arabic	L-arabinose, L-rhamnose, D-galactose	acacia trees
	D-glucuronic acid, branched	
Gum tragacanth	D-galacturonic, D-xylose, L-fucose	plant gum from
	D-galactose, branched	*Astragalus spp.*
Guaran	D-mannose, L-galactose, branched	seeds from
		Cyanopsis
		tetragonolaba
Locust bean	D-mannose, D-galactose, branched	tree *Ceratonia*
		siliqua L.
Karaya	L-rhamnose, D-galactose,	tree *Sterculia*
	D-galacturonic acid, branched	*urens* Roxb,
		Sterculiaceae
Ghatti	L-arabinose, D-galactose, D-mannose,	stems of
	D-xylose, D-glucuronic acid, branched	*Anogeissus*
		Latifolia
Pectin	D-galacturonic acid, L-rhamnose, D-galactose	plants
	L-arabinose, D-xylose, branched	
Xanthan	D-glucose, D-mannose, branched	bacteria

2.4.1 Cellulose

Cellulose is probably the most abundant organic compound on earth. It is the main structural component of plant cells. Structurally, cellulose is a polymer of D-glucose in which the individual units are linked by β-1,4-glycosidic bonds as shown in Figure 2.4.

The β-conformation allows cellulose to form very long straight linear chains corresponding to a molecular weight of 1.6-2.4 million. The cellulose chains show

the tendency to build microfibrils through inter- and intramolecular hydrogen bonding resulting in the formation of highly ordered structures with a high tensile strength. The strength of wood is derived principally from hydrogen bonds of the hydrogen groups of one chain to hydroxyl groups of neighbouring chains. These ordered structures also cause the insolubility of cellulose in most solvents.

2.4.2 Starch

Starch is the second most abundant polysaccharide and occurs in both the vegetable and animal kingdoms. It is the major polysaccharide serving as a nutrient for humans rather than as a structural element. Natural starch can be separated into two gross fractions, called amylose and amylopectin, which vary in their relative amounts among the different starches. The majority of starches contain 15-35% amylose.

Amylose, the structurally linear type of starch consists of α-1,4-linked glucose residues. Amylopectin which represents the branched type of starch, contains about one α-1,6-glycosidic linkage per 15-30 α-1,4-glycosidic linkages distributed irregularly throughout the molecules. The structures are shown in Figure 2.4. Amylose exists as a random coil in neutral aqueous solution. The presence of complexating agents in the solution induces the formation of a helical structure [3]. This helical conformation gives rise to the characteristic blue colour of amylose-iodine complexes and is responsible for the complex formation with fats and polar organic solvents.

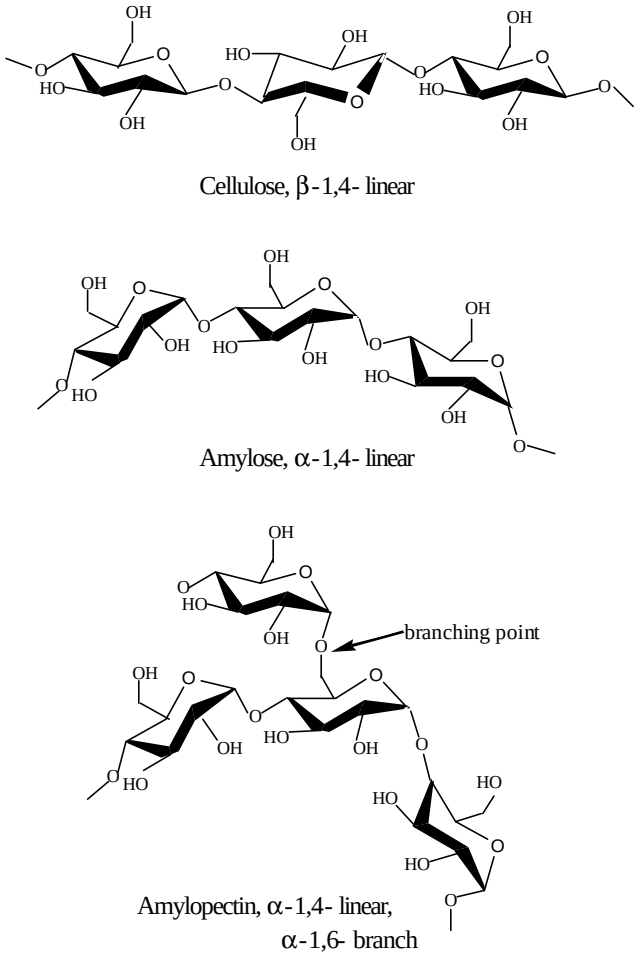

Figure 2.4 ***Structure of cellulose, amylose, and amylopectin***

2.4.3 Hemicellulose

Hemicellulose is defined as a large group of polysaccharides found in association with lignin, besides cellulose and pectin, in the primary and secondary cell wall of all plants and of some seaweed [5]. There are variations in the hemicellulose composition of plants and even between the organs of the same plants. The principal sugar residues present in hemicellulose are D-xylose, D-glucose, D-galactose, D-mannose, L-arabinose, L-fucose, L-rhamnose, D-glucuronic acid, D-

galacturonic acid and 4-*O*-methyl-D-glucuronic acid. The most ubiquitous and abundant hemicellulose is xylan that is composed of linear and/or branched chains of β-1,4 linked D-xylopyranosyl units. Isolated hemicellulose has many potential useful properties including its application as food additive, thickener, emulsifier, gelling agent, adhesive and adsorbant [6].

2.4.4 Gums

Gums are polysaccharides that are widely used in food as stabilising, gelling and thickening agents because they provide excellent water binding capacity. Some gums possess a natural biological activity related to the glycoproteins they contain, which results in a particular role of gums in the pharmaceutical industry. Gums may be harvested in nature from trees, seeds and marine weeds or they may be synthesised biologically and chemically. A selection of gums is documented in Table 2.1 (carrageenan) and Table 2.2. Most gums are heterogeneous polysaccharides (Table 2.2) with complicated structures and extremely high masses. A broadly functional classification is given in Table 2.3, in which the rows represent similar properties and the columns represent similar origins or sources [7]. A brief description of each group of gums, listed in Table 2.3, is given in this section. For a more detailed chemical, physical and functional property review of gums, we refer to the references [5, 6, 8].

Table 2.3 ***Gums commonly used in foods***

Exudate	Extract	Flour	Synthetic	Chemical
Arabic	Agar	Guar	Xanthan	Carboxymethyl cellulose
Tragacanth	Alginate	Locust bean		
Karaya	Carrageenan			
Ghatti				

2.4.4.1Exudate gums

The gums exudated from plants (Table 2.3) are polysaccharides containing hexuronic acids in salt forms and a number of neutral monosaccharides which are often esterified in highly branched structures [9]. These hexuronic acids or salts favour their water solubility. The contents of uronic acids in these gums vary, e.g. karaya contains 37% of uronic acid residues while ghatti consists of 10% of D-glucuronic acids [5]. The molecular weight (MW) of these gums generally ranges from one hundred to one thousand kilodalton (KDa). In addition, the exudate gums exhibit compositional heterogeneity combined with branched linkages (Table 2.2).

2.4.4.2 Gums extracted from seaweeds

The most common gums extracted from seaweeds are carrageenan, agar and alginic acid. They are highly negatively charged polysaccharides consisting mainly of the sulfate esters (carrageenan, agar) and D-mannosyluronic acid and gulosyluronic acid (alginic acid). Compositionally and structurally, the gums in this group are simpler than exudate gums because carrageenan and agar are only made up from galactose with linear chain linkages while alginic acid contains two uronic acids (Table 2.1 and Table 2.2).

Both agar and carrageenan have alternating β-(1,4) and α-(1,3) linked galactose residues with 3,6-anhydride. The basic repeating units are disaccharides as shown in Figure 2.5.

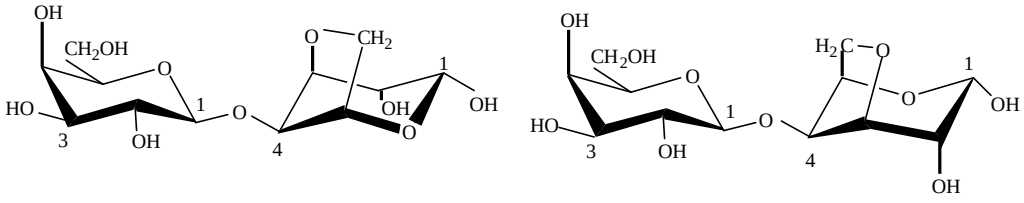

Figure 2.5 ***Basic repeating units of agars (agarobiose) and carrageenans (carrabiose)***

Agars differ from carrageenans in that the (1,4)-linked residue in agar is the L-enantiomer, whereas in carrageenans it is the D-enantiomer. The (1,3)-linked residues are D-galactose in both agars and carrageenans.

Agars can be separated into a neutral gelling fraction, agarose, and a sulfated non-gelling fraction, agaropectin, varying in total charge content. There are three extremes of the structure noted, namely neutral agarose, pyruvated agarose having little sulfation, and a sulfated galactan [5]. Gelling property is function of the agarose fraction of the agar.

Several members in the carrageenan family are known and they differ in the amount of the sulfate esters and/or other substituted groups they carry. The structures of the repeating units of the three principle carrageenan types, kappa (κ), iota (ι) and lambda (λ), are depicted in Figure 2.6.

As can been seen, these three differ discretely in their charge content per residues.

Kappa is sulfated only at C_4 in the 1,3-linked galactose ring, while iota has an

additional sulfate at C_2 in the 1,4-linked 3,6-anhydro-D-galactose ring. These structures allow the formation of double-helical segments that can form gel structures [9].

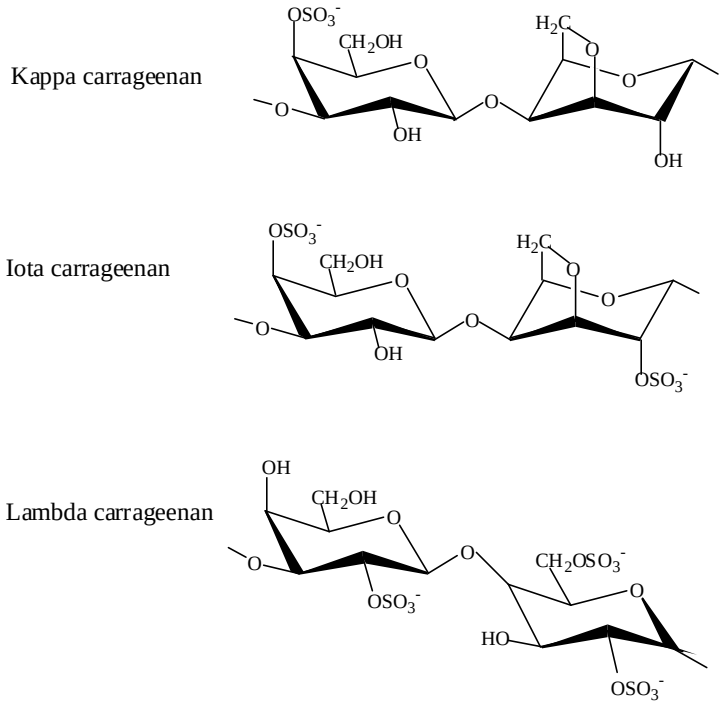

Figure 2.6 ***Three types of basic repeating disaccharides of carrageenan (kappa, iota and lambda carrageenan)***

Lambda carrageenan differs from iota and kappa carrageenan in several respects. Firstly, the level of sulfation is higher, with three charges per disaccharide residue. Secondly, the β-(1,4)-D-galactose ring is not conformationally locked in the 3,6-anhydro form. Finally, it carries sulfate groups at C_2 and C_6 in the α-(1,3)-D-galactose residues. Removal of the anhydro-bridge confers a kinking effect that

inhibits double helix conformational ordering, and hence blocking the gel formation [9].

Alginic acid is a linear polymer of β-(1,4)-D-mannosyluronic acid and α-(1,4)-L-gulosyluronic acid, the relative proportions of which vary depending on the organism and the tissue from which it is isolated. The most important food related property of this gum is its ability to interact with calcium ions. This interaction produces a useful increase in viscosity at low levels of added calcium and, ultimately, as the calcium level is increased, gel formation.

2.4.4.3 Gums from seed flour (guar and locust bean)

Guar gum and locust bean gum (LBG) are structurally similar since they both consist of linear chains of β-(1,4)-D-mannopyranosyl units with α-D-galactopyranosyl units attached by (1,6) linkages, but they have different contents of D-galactose and D-mannose. For guar gum, the ratio of D-galactose to mannose is 1:2 while it is 1:4 or 1:5 for LBG. [5]. Therefore, the structure of LBG differs from that of guar gum in terms of the frequency and distribution of the galactose side chains, which is not regular [7].

After starch, guar gum is the most widely used food thickener, primarily because of its relatively low cost. Guar has a higher degree of substitution than locust bean gum and hence, is cold water-soluble while LBG requires heat [10].

2.4.4.4 Xanthan gum

The primary structure of xanthan consists of a cellulose backbone with trisaccharide side chains, the repeating units being a pentasaccharide [5]. It is

composed of D-glucosyl, D-mannosyl and D-glucosyluronic acid residues and differing proportions of *O*-acetyl and pyruvic acid acetal.

Xanthan gum was the first bacterial polysaccharide to be widely used as thickener and stabiliser in foods. Because of a particular helical-architecture, the molecule exists in solution as a "rigid rod" stabilised by interactions between the main cellulose backbone and the trisaccharide side chains [10]. In the presence of salt or acid and at elevated temperatures, the stable molecular structure persists, resulting in constant viscosity under various conditions frequently encountered in foods.

2.4.4.5 Carboxymethyl cellulose (CMC)

CMC is made directly from cellulose recovered from wood pulp or cotton wool. It is the most important cellulose derivative applied in foods. The negatively charged carboxyl groups (Figure 2.7) confer solubility on the cellulose molecule. CMC is a thickener giving an extremely clear solution - a distinct advantage over other gums [10].

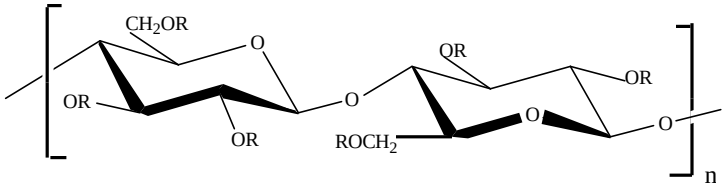

R = -H or -CH_2COOH

Figure 2.7 ***Structure of the repeating unit of CMC***

2.4.5 Pectin

Pectin is a polysaccharide with a molecular weight of 20,000-400,000 present in the cell wall of all plant tissues and functions as an intercellular cementing material [5]. One of the richest sources of pectin is lemon or orange rind, which contains about 30% of the polysaccharide. Pectin occurs naturally as the partial methyl ester of α-(1,4) linked D-polygalacturonate sequences interrupted with (1,2)-L-rhamnose residues. Neutral sugars such as D-galactose, L-arabinose, D-xylose and L-fucose form side chains on the pectin molecules. The secondary and tertiary structures exist in solution and gels. In terms of gelling properties, pectin can be divided into two broad categories, the high DE (degree of esterification) and the low DE. The widely accepted model for the gelation mechanism is that low DE pectin starts formation of a rigid three-dimensional network by coordination of available carboxyl groups to divalent cations, the presence of which is essential. The low DE pectin would usually be gelled with a milli-molar concentration of calcium. For high DE pectin, gellation is achieved in systems of high solid content (typically containing 60% sucrose) and is thought to involve hydrophobic interaction and hydrogen bonding. The DE of a pectin sample is thus of great importance in understanding and controlling the nature of its gel [11].

2.4.6 Glycosaminoglycan (GAG)

Glycosaminoglycan is a polysaccharide containing amino sugars with the alternating disaccharide units. These disaccharide units comprise acidic monosaccharides such as glucuronic acid (GlcA), iduronic acid (IdoA) and basic monosaccharides such as *N*-acetylglucosamine (GlcNAc) and *N*-acetyl-

galactosamine (GalNAc). These polysaccharides are covalently attached to protein backbones to form proteoglycans that play an important biological role and are, for example, related to some human diseases. They are of interest to medical science and for details we refer to reference [12]. In recent years, intensive analytical research has been carried out to characterise hyaluronic acid, chondroitin sulfate and heparin. An overview was presented by Novotny and Sudor [13] and later by Honda and Suzuki [14].

2.4.6.1 Hyaluronic acid (HA)

The molecular weight of hyaluronic acid is in the range of 50,000 to 8,000,000 depending on the source and method of preparation [5]. In the past, hyaluronic acid was extracted from bovine vitreous humour, roster combs, or umbilical cords explaining the very high price. Nowadays, the polysaccharide produced by the bacteria *Streptococcus zooepidemicus* is recovered in a large scale with good yields and high purity.

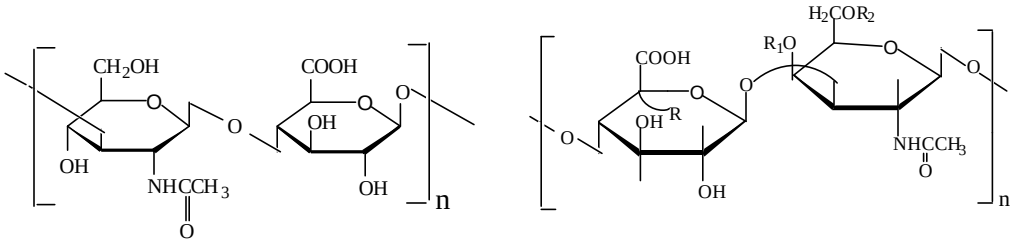

Repeating unit of HA
(a)

Chondroitin sulfate
(b)

Figure 2.8 ***Structure of the repeating units of HA (a) and chondroitin sulfate (b)***

The main uses of HA are in ophthalmic surgery, arthritic treatment and cosmetic formulations. The structure of HA is shown in Figure 2.8 (a).

2.4.6.2 Chondroitin sulfate

This polysaccharide is the ubiquitous component of connective tissues. The molecular weight is estimated at 50,000. These biological polymers act as the flexible connecting matrix between the tough protein filaments in cartilage to form a polymeric system similar to reinforced rubber. The structures of three patterns of chondroitin sulfate are depicted in Figure 2.8 (b).

In cartilage, chondroitin sulfate (in the form of a proteoglycan) comprises up to 10% of the total tissue dry weight. With ageing and in various pathological states, particularly osteoarthritis, the ratio of the 4- (type A) and 6-sulfated (type C) isomers varies greatly. It has been reported [13] that changes in the native structure of chondroitin sulfate chains may be the diagnosis for osteoarthritis. These changes may be related to altered sulfation patterns (type A and type C) of the chondroitin chains. Dermatan sulfate, formerly called chondroitin sulfate B, as shown in Figure 2.8 (b), is present in soft connective tissue and is abundant in skin, arterial walls and heart valves.

2.4.6.3 Heparin

Heparin is a heterogenous mixture of different sulfated polysaccharides. The molecular weight range is from 6,000 to 30,000 [5]. Heparin occurs as a proteoglycan consisting of a small protein core to which multiple large glycosaminoglycan side chains are attached. The glycosaminoglycan chains vary

in length and consist of repeating uronic acid glucosamine disaccharide sequences in which the uronic acid may be either L-iduronic or D-glucuronic acids, and the glucosamine residue may be either *N*-acetylated or *N*-sulfated [15]. Various heterogeneous polymers, both in molecular mass and structure, are thus formed. A final cause of heterogeneity is the occurrence of a unique natural pentasaccharide, shown in Figure 2.9, which is responsible for the anticoagulant activity of heparin through a high-affinity binding to antithrombin [16].

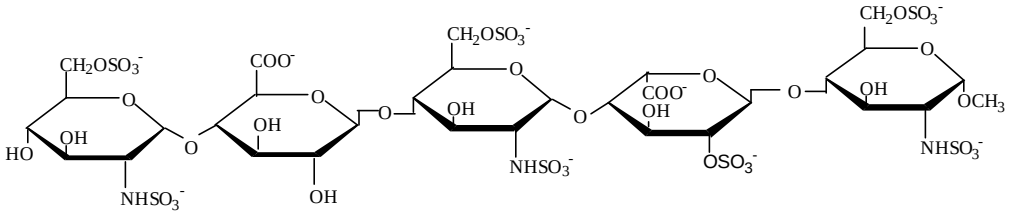

Figure 2.9 ***Structure of pentasaccharide present in heparin***

References

[1] A. Paulus and A. Klockow-Bech, Chromatographia CE series, "Analysis of carbohydrates by capillary electrophoresis", K. D. Altria, Ed., Vieweg publishing, Wiesbaden, **1999**

[2] A. Streitwieser, C. H. Heathcock and E. M. Kosower, "Introduction to organic chemistry", Fourth edition, Macmillan Publishing, New York, **1992**

[3] J. Lehmann, Translated by A. H. Haines, "Carbohydrates structure and biology", Organic chemistry monograph series, Thieme, Stuttgart, New York, **1998**

[4] K. Verleysen, "Chiral capillary electrophresis", Ph. D thesis, Department of Organic Chemistry, Ghent University, Belgium, **1999**

[5] S. Budavari, Ed. Merck Index, Eleventh edition, Merck & Co. Inc. publishing, **1989**

[6] A. M. Stephen, "Food polysaccharides and their applications", XIII, Marcel Dekker, Inc. publishing, New York, **1995**

[7] D. M. W. Anderson and S. A. Andon, *American Association of Cereal Chemists, Inc.* Vol.33, No.10, **1988**, 844

[8] S. Dumitriu, "Polysaccharides, structural diversity and functional versatility", Marcel Dekker, Inc. publishing, New York, **1998**

[9] M. A. Roberts, H.-J. Zhong, J. Prodolliet and D. M. Goodall, *J. Chromatogr. A* 817, **1998**, 353

[10] G. R. Sanderson, *Food technology*, Mar. **1996**, 81

[11] H.-J. Zhong, M. A. K. Williams, R. D. Keenan, D. M. Goodall and C. Rolin, *Carbohydr. Polym.* 32, **1997**, 27

[12] S. Dumitriu, "Polysaccharides in medicinal applications**",** Marcel Dekker, Inc. publishing, New York, **1996**

[13] M. Novotny and J. Sudor, *Electrophoresis* 14, **1993**, 373

[14] S. Suzuki and S. Honda, *Electrophoresis* 19, **1998**, 2539

[15] J. B. L. Damm, G. T. Overklift, B. W. M. Vermeulen, C. F. Fluitsma and G. W. K. Van Dedem, *J. Chromatogr.* 608, **1992**, 297

[16] J. B. L. Damm and G. T. Overklift, *J. Chromatogr. A* 678, **1994**, 151

Chapter 3

Derivatisation Strategies in the Analysis of Saccharides by CE

Abstract

Successful CE analysis and detection in most cases requires pre-column transformation of the saccharides. On the one hand, by derivatisation, charges are introduced to enhance electrophoretic mobility and, on the other hand, chromophores or fluorophores are attached allowing sensitive detection. The derivatising reagents and derivatisation reactions applied are discussed.

3.1 Introduction

Two major problems arise when capillary electrophoresis (CE) is applied to the analysis of sugars. Firstly, with the exception of some sulfonated, acetylated and phosphorylated sugars, carbohydrates in general are neutral compounds and consequently exhibit no mobility in an electric field. Secondly, most carbohydrate species neither absorb nor fluoresce, hindering their sensitive detection. The molar extinction coefficient in the low UV region at 195 nm of monosaccharides is only 2-5 $M^{-1}cm^{-1}$ for aldoses and 12 $M^{-1}cm^{-1}$ for fructose [1]. This is in contrast to an extinction coefficient of several hundreds to thousands for multi-ring compounds with conjugated functional groups. The UV concentration

detection limits of 10^{-5}-10^{-6} M quoted in Chapter 1 (Table 1.3) are based on extinction coefficients of 1,000-10,000 $M^{-1}cm^{-1}$.

Derivatisation is a modification intended to give the analytes of interest more suitable characteristics for analysis. In most cases, derivatisation is detection-oriented and involves the incorporation of UV-absorbing or fluorescent groups into the analytes to obtain high sensitivity and selectivity. Apart from these two reasons, derivatisation is also used to give the analyte a more suitable mass to charge ratio, to increase the hydrophobicity necessary for MEKC separation, etc.

3.2 Derivatisation modes

3.2.1 Pre-column derivatisation

Pre-column derivatisation is most widely used for saccharides because of (1) the large flexibility in optimising the reaction conditions, (2) the fact that the conditions for derivatisation do not have to be compatible with the electrophoretic buffer, (3) the availability of a wide variety of labelling reagents and (4) the fact that no complex instrumentation or tools are needed. The disadvantages of this approach are that in a number of cases excess reagent should be removed from the reaction mixture before the actual separation and that the derivatives are not always sufficiently hydrolytically or thermally stable.

The essential criteria for successful pre-column derivatisation include (1) high yield, (2) the formation of a single product for each species, (3) no detectable side products, (4) minimum sample work-out and clean-up, and (5) no cleavage of an essential sugar residue, e.g. sialic acid.

3.2.2 On-column derivatisation

Till now, on-column derivatisation of saccharides has not been reported. According to a recent review of Underberg *et al.* [2], the main reasons are that the reaction kinetics involved are generally slow (reaction time > 1 hour), that a multi-step procedure is often required and that rather high temperatures are usually needed. These conditions are difficult to realise in CE.

3.2.3 Dynamic labelling

Dynamic labelling is based on the introduction of a suitable chromophore or fluorophore in the electrolyte to form a complex with the analyte of interest. This detection approach is simple, does not require any sample handling, and can result in sensitive detection.

In the case of saccharides, chelation with Cu (II) provides *in situ* charged species that can be separated according to their different mobilities [3]. In addition, this complexation results in a substantial increase in UV absorption between 230 nm and 320 nm. If the background noise of the electrolyte is sufficiently low, the detection of micromolar concentrations of saccharides becomes possible. This was demonstrated by the separation and detection of a mixture of α-, β- and γ-cyclodextrins (CDs) with CE-LIF by forming an inclusion complex with 2-anilinonaphthalene-6-sulfonic acid (2, 6-ANS) as background electrolyte [4].

3.2.4 Post-column derivatisation

The derivatisation performed after the separation, but before detection, is called post-column derivatisation. This derivatisation mode has attracted attention of

carbohydrate analysts using liquid chromatography (LC) since LC meets the demands of post-column derivatisation such as appropriate reaction time at desired temperature and compatible with the extra volume of reaction devices [5]. In contrast, electrophoresis does not afford sufficient time for post-separation derivatisation, and hence is not easily compatible with postcolumn derivatisation.

Inevitable disadvantages of post-electrophoretic reactions are that (1) the choice of the reaction conditions are rather critical and should be compatible with the separation conditions, (2) the reaction times are relatively short, which means that detectability is normally lower compared to the separation after pre-column derivatisation, (3) special equipment is necessary, and (4) the detection properties of the derivatives should be different from those of the reagent. Good separation efficiencies and detectabilities using post-column derivatisation were obtained with a sheath-flow cell reactor [6].

3.3 Derivatisation of saccharides

3.3.1 Derivatisation schemes

The best sites for tagging saccharides include (1) the carbonyl group in reducing sugars, (2) the amino group in amino sugars, and (3) the carboxylic function in acidic sugars. The polyhydroxy nature of sugars is attractive as far as the attachment of a tag to the molecule is concerned. This route of derivatisation has been used extensively in gas chromatography in order to increase the volatility of carbohydrates and consequently to allow their GC analysis [7]. However, derivatising the hydroxyl groups ŀad to multiple tagging and consequently multi-derivatives. Using the reactivity of hydroxyl groups of sugars, the profiling of

inulin and hydrolysates derivatised with fluorescein isothiocyanate (FITC) and CE analysis was reported by our laboratory [8]. Although multiple tagging occurred, the inulin molecular weight distribution was obtained. Five different pre-column derivatisation schemes commonly used for labelling saccharides are:

(1) reductive amination (Scheme i);

(2) condensation of carboxylated carbohydrates with aminated tags in the presence of carbodiimide (Scheme ii);

(3) base-catalysed condensation between the carbonyl group of reducing carbohydrates and the active hydrogen of 1-phenyl-3-methyl-5-pyrazolone (PMP), forming the bis-PMP derivative (Scheme iii);

(4) reductive amination of reducing carbohydrates with amines to yield 1-amino-1-deoxyalditols followed by reaction with 3-(4-carboxybenzoyl)-2 quinolinecarboxyaldehyde (CBQCA) in the presence of potassium cyanide (Scheme iv);

(5) reductive amination of reducing carbohydrates with amines to yield 1-amino-1-deoxyalditols followed by reaction with 5-carboxytetramethylrhodamine succinimidyl ester (TRSE) (Scheme v).

Reductive amination is the most widely used pre-column derivatisation method for labelling reducing saccharides and is also the main derivatisation scheme used in this work.

Reductive amination (Scheme i) involves ring opening catalysed by an acid to form the aldehyde or ketone, followed by a nucleophilic addition of the amino group of the reagent to form an imine (Schiff base), which is further reduced with sodium cyanoborohydride to form a stable secondary amine. Ring opening and

the Schiff base formation are commonly catalysed by acetic acid or stronger organic acids such as citric acid that were found to produce high yields of sugar derivatives with 9-aminopyrene-1,4,6-trisulfonate [9]. The stronger acids also help overcome steric hindrance effects in the ring opening or in the Schiff base formation, and have, as an example, a pronounced effect in the yields of the adducts of *N*-acetylamino sugars.

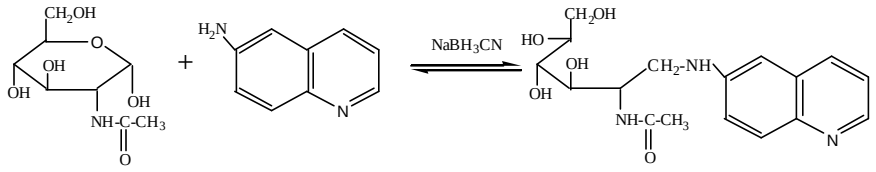

GlcNAc 6-AQ 6-AQ-GlcNAc

Scheme i ***Reductive amination for the reducing sugar N-acetylglucosamine (GlcNAc) and the tag 6-aminoquinoline (6-AQ)***

The use of a stronger acid catalyst, however, may increase the risk of removal of sialic acid residues at the non-reducing ends of oligosaccharides derived from glycoproteins.

A large peak from unreacted reagent is a frequently observed problem for many derivatisations. A solution to this problem was proposed by Mort *et al.* [10]. Excess reagent is reacted with "scavenger beads", carrying an appropriate functional group to remove the reagent from the sample solution. Examples were presented for removal of aminonaphthalene mono-, di- and trisulfonic acid from mixtures in which they were used to label mono- or oligosaccharides by reductive amination. Aldehyde-containing scavenger beads were made by oxidising Sephadex G-50 beads with sodium periodate. They were added to the labelling

reaction mixtures after reductive amination of the sugars was terminated. Almost complete elimination of the peak from the labelling agent could be achieved.

The other four reaction schemes are briefly illustrated. For a detailed description, we refer to the references [11, 12].

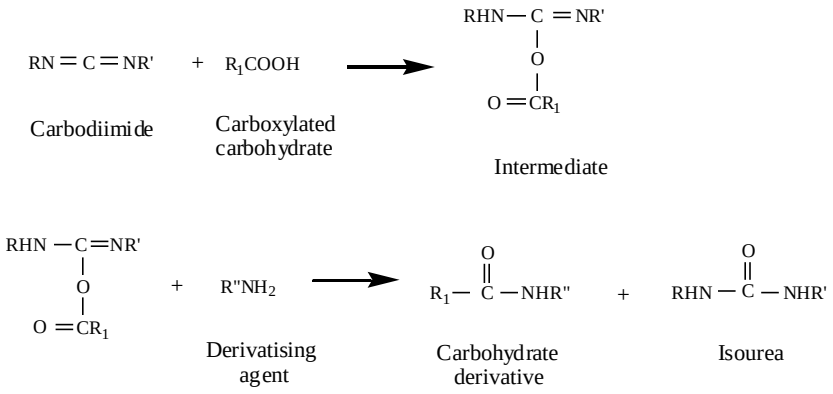

Scheme ii ***Precolumn derivatisation of carboxylated carbohydrates via a condensation reaction between the carboxylic group of the saccharide and the amino group of the derivatising agent in the presence of carbodiimide***

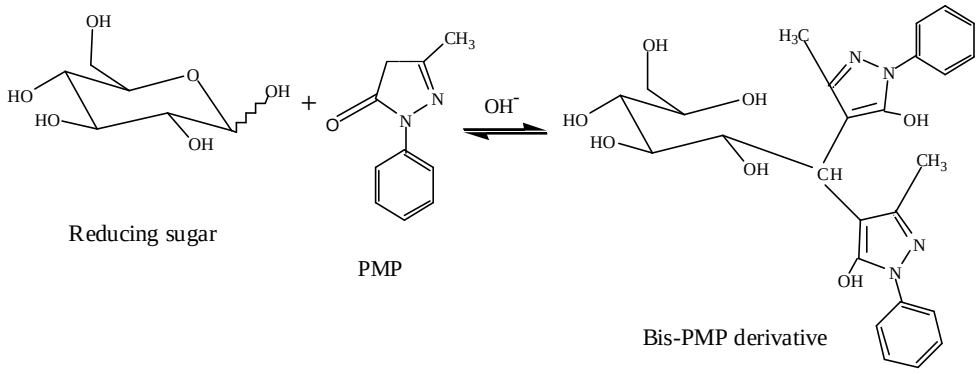

Scheme iii ***Illustration of the condensation reaction with 1-phenyl-3-methyl-5-pyrazolone (PMP)***

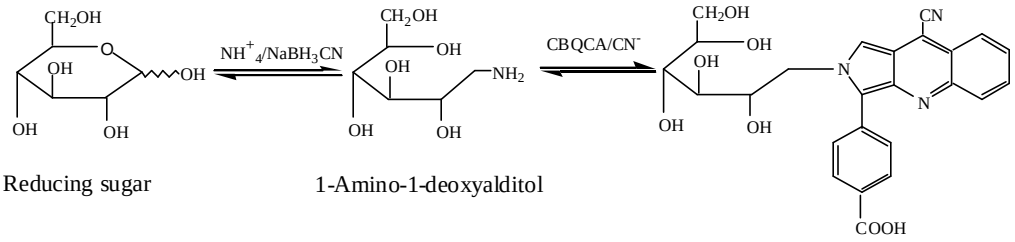

Scheme iv ***Illustration of precolumn derivatisation with 3-(4-carboxybenzoyl)-2-quinolinecarboxyaldehyde (CBQCA)***

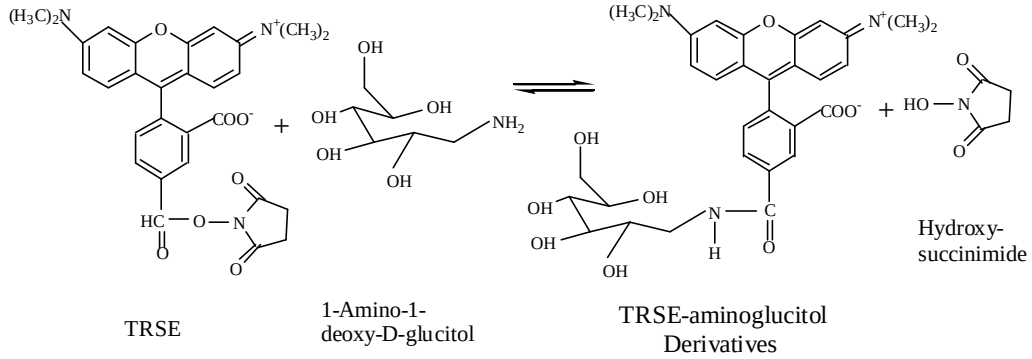

Scheme v ***Illustration of the derivatisation of aminated sugar with 5-carboxytetramethylrhodamine succinimidyl ester (TRSE)***

3.3.2 Derivatisation reagents

For UV detection, the tagging agent should exhibit a high molar extinction coefficient at a given wavelength with minimal interference from the running electrolyte to ensure sensitive detection of the derivatised carbohydrates. A fluorescence tag should exhibit high quantum efficiencies at a given excitation wavelength. These requirements become crucial when dealing with extremely small sample volumes encountered in nano-scale separation techniques like CE.

Sugars tagged with a suitable chromophore or fluorophore allow detection at low levels. The tagging process often brings drastic changes in the structure and thus in the electrophoretic properties of the analytes. For example, Stefansson and Novotny [13] demonstrated the pronounced effect of the charges of tags on the apparent electrophoretic mobility by labelling dextran with three derivatising reagents (see Table 3.1 and Table 3.2), i.e. 2-aminopyridine (2-AP, tag v), 5-aminonaphthalene-2-sulfonic acid (5-ANSA, tag xii) and 8-aminonaphthalene-1,3,6-trisulfonate (ANTS, tag xvii), which possess no charge, one and three negative charges, respectively. ANTS provides not only a strong chromophore but also multiple negative charges even at low pH allowing fast electrophoretic analysis.

Hence, it is preferred that the tags also supply charges necessary for electrophoretic separation over a relatively wide pH range or eventually that the tags impart a hydrophobic character to the derivatives so that the principles of MEKC can be applied to the separation of derivatised carbohydrates.

The most important derivatising reagents for carbohydrates can be classified into two types, namely (1) those yielding neutral or ionisable sugar derivatives and (2) those yielding permanently charged sugar derivatives. Table 3.1 lists the first type reagents and Table 3.2 the second type [11, 12].

Table 3.1 ***Structures, names and abbreviations of tags yielding neutral and ionisable sugar derivatives.*** (The spectral values listed correspond to the sugar derivatives of the indicated tags)

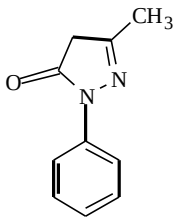	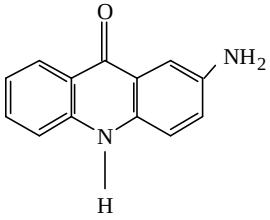	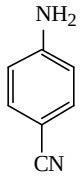
(i) 1-Phenyl-3-methyl-5-pyrazolone (PMP) λ_{max}= 245 nm	(ii) 2-Aminoacridone (2-AA) λ_{max}= 425 nm, λ_{em}= 520 nm, Argon ion laser 488 nm	(iii) *p*-Aminobenzonitrile (*p*-ABN) λ_{max} = 285 nm
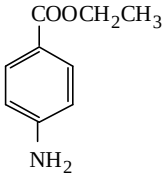	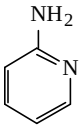	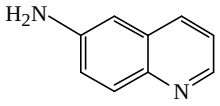
(iv) *p*-Aminobenzoic acid ethyl ester (*p*-ABEE) λ_{max} = 306 nm	(v) 2-Aminopyridine (2-AP) λ_{max} =240 nm, λ_{em} = 375 nm, He-Cd laser 325 nm	(vi) 6-Aminoquinoline (6-AQ) λ_{max} = 270 nm, λ_{em} = 495 nm, He-Cd laser 325
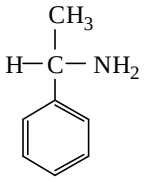	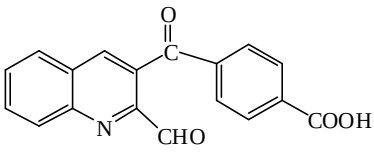	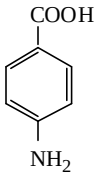
(vii) S-(−)-1-Phenethylamine λ_{max} = 200 nm	(viii) 3-(-4-Carboxybenzoyl)-2-quinolinecarboxaldehyde (CBQCA), λ_{em} = 552 nm, Argon ion laser 457 nm or 488 nm, He-Cd laser 442 nm	(ix) *p*-Aminobenzoic acid (*p*-ABA) λ_{max} = 285 nm

Table 3.2 ***Structures, names and abbreviations of tags yielding permanently charged sugar derivatives.*** (The spectral values listed correspond to the sugar derivatives of the indicated tags)

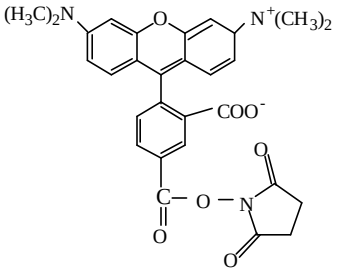

(x)
5-Carboxytetramethylrhodamine succinimidyl ester (TRSE)
λ_{max} = 235 nm, ?$_{em}$= 475 nm
He-Cd laser 543 nm

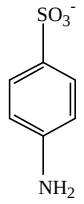

(xi)
Sulfanilic acid (SA)
λ_{max} = 247 nm

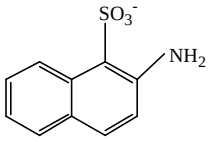

(xii)
2-Aminonaphthalene-1-sulfonic acid (2-ANSA)
λ_{max} = 235 nm

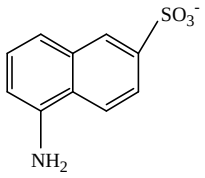

(xiii)
5-Aminonaphthalene-2-sulfonic acid (5-ANSA)
λ_{max} = 235 nm,
λ_{em} = 475 nm
He-Cd laser 325

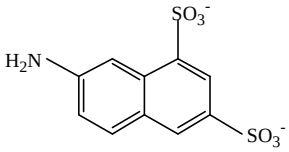

(xiv)
7-Aminonaphthalene-1,3-disulfonic acid (ANDSA),
λ_{max} = 247 nm, λ_{exc} =315 nm, λ_{em} = 420 nm
Xenon-Mercury Lamp

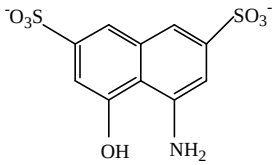

(xv)
4-Amino-5-hydroxynaphthalene-2,7-disulfonic acid (AHNS)
λ_{em} = 475 nm
He-Cd laser 325 nm

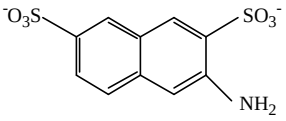

(xvi)
3-Aminonaphthalene-2,7-disulfonic acid (3-ANDA)
λ_{max} = 235 nm

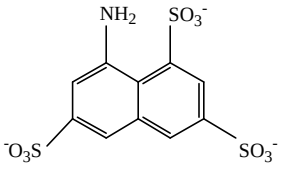

(xvii)
8-Aminonaphthalene-1,3,6-trisulfonic acid (ANTS),
λ_{exc} =370 nm, λ_{em} = 520 nm
He-Cd laser 325 nm

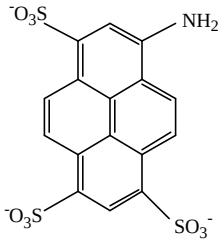

(xviii)
9-Aminopyrene-1,4,6-trisulfonic acid (APTS),
λ_{max} = 455 nm, λ_{em} = 512 nm, λ_{exc} = 488 nm
Argon ion laser

Besides the different spectral characteristics in terms of molar absorptivities, quantum efficiency and, whether they are UV absorbing and/or fluorescing tags, the different reagents listed yield sugar derivatives of varying electrophoretic mobilities. In this way the efficiency and selectivity of the separation can be controlled. The electrophoretic properties of the carbohydrates labelled with the different tags are related to the derivatising reagents as follows.

PMP (tag i), which labels carbohydrates according to Scheme iii, yields neutral sugar derivatives that become negatively charged in aqueous basic solution because of the partial dissociation of the enolic hydroxyl group of the PMP tag. Usually, weakly ionised derivatives do not separate well. Sugar-PMP derivatives will therefore require borate-based electrolytes and/or micellar phases such as sodium dodecyl sulfate (SDS) to introduce differential electromigration and thus separation.

2-AA (tag ii), *p*-ABN (tag iii) and *p*-ABEE (tag iv) will lead to neutral sugar derivatives *via* Scheme i, thus also requiring the borate-based electrolytes and/or micellar phases for separation.

Using Scheme i, the neutral sugar derivatives of 2-AP (tag v), 6-AQ (tag vi) and S-(–)-1-phenethylamine (tag vii) can acquire a positive charge at acidic pH or are able to form negatively charged borate complexes at alkaline pH. In addition, tag vi is an enantiomeric reagent that allows the separation of sugar enantiomers.

CBQCA (tag viii), which is used in pre-column derivatisation according to Scheme iv, will yield derivatives that can be negatively charged via ionisation of the carboxylic group.

p-ABA (tag ix) is an amphoteric reagent and leads to derivatives that are positively charged at pH < 3.0 and negatively charged at pH ≥ 3.8.

TRSE (tag x) is used for labelling carbohydrates according to Scheme v, and produces sugar derivatives that can acquire a net positive charge at acidic pH and become a zwitterion at neutral and basic pH.

By reductive amination (Scheme i), all the other tags (tag xi to xviii) in Table 3.2 yield sugar derivatives that are negatively charged over a wide pH range due to their strong sulfonic acid groups (pK_a values ≤ 3) while only a weak ability is present to protonate their amino groups.

Under a given set of conditions and for a given set of saccharides, the different tagging agents lead to sugar derivatives with different electrophoretic behaviour and thus separation selectivity.

Generally, sugar derivatives with the tags displayed in Table 3.1 require an alkaline borate buffer to form borate complexes in order to obtain the selectivity needed for the separation. The negative charges from the complexation contribute to the apparent mobility as well. On the other hand, the sugar derivatives with the tags displayed in Table 3.2 still need alkaline borate electrolytes to generate good selectivity although they do not require borate complexation to undergo differential electromigration since these derivatives carry sulfonic acid groups that are permanently ionised over a wide pH range. More applications of the labelling reagents in Table 3.1 and Table 3.2 can be found in references [2, 11, 12, 14, 15].

In conclusion, by using the derivatisation strategy in the CE analysis of saccharides, both the lack of UV-absorption and fluorescence and the poor electrophoretic properties can be circumvented.

References

[1] A. Paulus and A. Klockow-Beck, Chromatographia CE Series, Analysis of carbohydrates by capillary electrophoresis, K. D. Altria Ed. Friedr. wieweg publishing, Braunschweig/Wiesbaden, **1999**

[2] J. C. M. Waterval, H. Lingeman, A. Bult and W. J. M. Underberg, *Electrophoresis* 21, **2000,** 4029

[3] H. Lochmann, A. Bazzanella and K. Bachmann, *J. Chromatogr. A* 817, **1998**, 337

[4] S. G. Penn, R. W. Chiu and C.A. Monnig, *J. Chromatogr. A* 680, **1994**, 233

[5] S. Honda, *J. Chromatogr. A*, 720, **1996**, 183

[6] P. G. Coble and A. T. Timpermane, *J. Chromatogr. A* 829, **1998**, 309

[7] J. Bleton, P. Mejanelle, J. Sansoulet, S. Goursaud and A. Tchapla, *J. Chromatogr. A* 720, **1996**, 27

[8] J. Peng, F. Lynen and P. Sandra, *J. High Resolut. Chromatogr.* 23, **2000**, 656

[9] R. A. Evangelista, A. Guttman and F. –A Chen, *Electrophoresis* 17, **1996**, 347

[10] A. J. Mort, D. F. Zhan and V. Rodriguez, *Electrophoresis* 19, **1998**, 2129

[11] Z. El Rassi, High performance capillary electrophoresis of carbohydrates, Volume VIII, Beckman Instruments, Inc. publishing, Fullerton, California, USA, **1996**

[12] Z. El Rassi and Y. Mechref, *Electrophoresis* 17, **1996**, 275

[13] M. Stefansson and M. Novotny, *Anal. Chem.* 66, **1994**, 1134

[14] A. Paulus and A. Klockow, *J. Chromatogr. A* 720, **1996**, 353

[15] S. Suzuki and S. Honda, *Electrophoresis* 19, **1998**, 2359

Chapter 4

CE Analysis of Monosaccharides

Abstract

The CE separation of derivatised monosaccharides with both LIF and UV detection is presented. The electrophoretic properties influenced by the borate complexation and derivatisation are discussed.

4.1 Introduction

Capillary electrophoresis (CE) is a method for the separation of charged compounds. In principal, only a few of the native saccharides having charged functional groups such as uronic acids, sialic acid, amino sugars and the compositional sulfated sugars of chondroitin and heparin, can be separated directly by capillary zone electrophoresis (CZE) [1].

The saccharide hydroxyl groups only can be ionised at extremely high pH due to their weakly acidic properties ($pK_a \approx$ 12-13, Table 4.1). Hence, the separation of native neutral monosaccharides as their anions can be performed by CE with a high pH buffer. Electrolyte systems consisting of an alkali-metal hydroxide solution with pH 12-13 have been used in the separation of underivatised saccharides [2]. Electrochemical detection (ECD) with a Cu or Au/Cu electrode is

commonly used for underivatised sugars [3, 4, 5]. Using these conditions, the determination of sugars in a chocolate beverage was described [6].

The employment of an alkaline borate buffer system improved the electrophoretic properties and absorption ability through formation of sugar-borate complexes. Simple sugars were separated and detected at 195 nm with an alkaline borate buffer system [7].

Table 4.1 ***pK values of some carbohydrates*** *[8, 9]*

Compound	pK at 25 °C	Compound	pK at 25 °C
N-acetylneuraminic acid	2.60	Glucose	12.28
Glucuronic acid	3.20	Arabinose	12.34
Galacturonic acid	3.48	Galactose	12.35
Fructose	12.03	Sucrose	12.51
Mannose	12.08	Raffinose	12.74
Xylose	12.15	Lactose	11.98
Maltose	11.94	Lyxose	12.29
2-Deoxyglucose	12.52	2-Deoxyribose	12.67
D-Mannitol	13.50 (18 °C)	D-glucitol	13.57
Sorbitol	13.6	Glycerol	14.40

Indirect detection was also possible by using high pH buffers containing strongly UV-absorbing or fluorescent anions as additives. This method is based on the displacement of these background electrolytes by saccharide analytes (Chapter 1, 1.7.3.2). The method was successfully applied in the determination of sugars in fruit juices [10]. The hydrolytes of fetuin were separated by CZE and detected with indirect UV by adding 2,6-pyridinecarboxylic acid in the buffer at pH 12.1 [11]. This allowed the simultaneous determination of neutral mono-sugars (ribose, mannose, xylose, glucose, galactose, fucose), uronic acids (mannuronic acid,

glucuronic acid and galacturonic acid) and *N*-acetylamino sugars (*N*-acetylglucosamine, *N*-acetylgalactosamine).

Sorbic acid [10, 12-14], tryptophan [15], *p*-nitrophenol [16], etc. were used as buffer additives for the same purpose. Coumarin 343 was used for indirect LIFD in the analysis of sugars (sucrose, glucose and fructose) by Yeung *et al.* [17].

CZE coupled with indirect detection is a simple and convenient separation mode for native saccharides having low molecular weight (MW). However, the detection methods described above generally lacks sensitivity. Hence, pre-column derivatisation of saccharides is usually necessary in order to obtain highly sensitive detection. Often, pre-column labelling also improves the saccharide electrophoretic behaviour, due to the characteristics of the derivatising reagent, and thus the compatibility with certain electrolyte systems. The commonly employed derivatising reagents and the reactions for saccharides were described in Chapter 3 (Table 3.1 and Table 3.2).

The choice of an appropriate tag is crucial because it will influence not only the electric charges of the derivatives but also the hydrophobic property of the derivatives and thus the effect on the choice of the buffer system and CE mode. For instance, monosacharides are, generally, too hydrophilic to be solubilised in ionic surfactant-based micellar systems. However, the labelling with hydrophobic tags such as 2-aminoacridone (2-AA), *p*-aminobenzonitrile (*p*-ABN) (Chapter 3, tag ii, tag iii) will enhance the hydrophobicity of the sugars and, thus micellar electrokinetic chromatography (MEKC) becomes possible. Eight sugars including *N*-acetylgalactosamine, galactose, mannose, fucose, glucose, *N*-acetylgalactosamine, ribose and xylose, were derivatised with 2-AA and separated

by MEKC [18]. This type of derivatisation was originally introduced by Jackson for the labelling and separation of mono- and oligo-saccharides by slab gel electrophoresis [19]. Using *p*-aminobenzonitrile (*p*-ABN, Chapter 3, tag iii), 24 sugars including mono-, di- and trisaccharides were separated by MEKC in an SDS micellar phase [20].

CZE is the main mode for separation of derivatised monosaccharides and a borate buffer system is most frequently employed as the borate complexation favours both separation and detection. The distinction between different sugar species originates not only from the molecular weight and the number of charges, but also from the stability of the complexes. The latter is determined by the configuration of the hydroxyl groups in the given saccharide. The more stable the complex is, the higher is its electrophoretic mobility. For a detailed discussion on the complexation of borate-saccharides, we refer to the references [21-23].

The UV absorbing reagents, such as 4-aminobenzoic acid (4-ABA, Chapter 3, tag ix) [24] and 6-aminoquinoline (6-AQ, Chapter 3, tag vi) [25], were used for the derivatisation of saccharides. Subsequently the derivatives were separated with an alkaline borate buffer system in bare fused silica capillaries. Vorndran *et al.* [26] obtained the separation of 30 sugars including neutral monosaccharides, sucrose, raffinose, and uronic acids with a 150-175 mM borate buffer (pH 10.0). The carbohydrates were analysed as their 2-aminopyridine (2-AP), *p*-aminobenzoic acid (*p*-ABA) and *p*-aminobenzoic acid ethyl ester (ABEE) derivatives.

Laser induced fluorescence detection (LIFD) is considered as the most sensitive detection method currently used in CE and the limit of detection (LOD) can be as low as 10^{-13} M [27]. The major fluorescence reagents used for saccharides, as well

as many other applications, were described in Chapter 3 (Table 3.1 and Table 3.2).

9-Aminopyrene-1,4,6-trisulfonate (APTS) is the most attractive fluorescence reagent because of its extensive conjugated system (four aromatic rings) in each molecule (Chapter 3, tag xviii) and thus, sugar-APTS derivatives have a substantially higher molar absorptivity and quantum efficiency than most of the other fluorophore sugar derivatives. When excited at 488 nm, the APTS derivatised sugars can be selectively detected while APTS itself has a much weaker fluorescence emission at that wavelength. Chen *et al.* [28] reported that the APTS derivatised sugars have significant absorption at 488 nm (35% of its 455 nm maximum absorbance), while APTS (λ_{max} = 424 nm) has only 4% of its λ_{max} absorption. Besides, three negatively charged sulfonic groups of APTS strongly influence the electrophoretic behaviour of the saccharide derivatives.

The CE separations of monosaccharides, derivatised with APTS and ABEE, and detected with LIF and UV, respectively, are presented.

4.2 Experimental

4.2.1 Chemicals

D-Mannose was obtained from Janssen Chimica (Beerse, Belgium). Sodium cyanoborohydride ($NaBH_3CN$), borax and all other sugar standards were purchased from Sigma-Aldrich (Steinheim, Germany). Water used in the experiments was produced by a Milli-Q water purification system (Millipore, Bedford, MA, USA). Acetic acid (99.7%) was obtained from Panreac (Barcelona, Spain) and sodium hydroxide from UCB (Leuven, Belgium).

9-Aminopyrene-1,4,6-trisulfonate (APTS) was obtained from Lambda Fluoreszenztechnologie GmbH (Graz, Austria) or from Molecular Probes (Leiden, The Netherlands). 4-Aminobenzoic ethyl ester (ABEE) was from Acros Organic (New Jersey, USA). The HPLC grade tetrahydrofuran (THF) was obtained from Lab-Scan Ltd. (Dublin, Ireland).

4.2.2 Derivatisation procedures

4.2.2.1 Monosaccharides derivatised with APTS

Two standard monosaccharide samples were used for the derivatisation with APTS. The first standard mix of monosaccharides was prepared by mixing 1 mg of the following monosaccharides: *N*-acetyl-D-galactosamine, *N*-acetyl-D-glucosamine, L-rhamnose, D-mannose, D-glucose, D-fructose, D-xylose, L-fucose and D-galactose. 1 mg of the mix was taken and 60 µL APTS (28 mM in 25% acetic acid solution) and 30 µL sodium cyanoborohydride (1 M in THF) were added. The mixture was then heated at 90 °C for 60 minutes. The derivatives were stored at −20 °C and diluted with water prior to injection. Fructose was individually derivatised by mixing 1 mg of fructose with 15 µL APTS (28 mM in 25% acetic acid) and 10 µL of a $NaBH_3CN$ solution (1 M in THF). The rest of the procedure was the same as for the mix of sugars.

The second mixture of 10 monosaccharides, i.e. L-rhamnose, D-glucose, D-galactose, D-xylose, D-fucose, D-glucuronic acid, D-ribose, L-arabinose, D-mannose and D-galacturonic acid was prepared as stock solution containing 0.0025 M of each monosaccharide. 10 µL of this solution was then mixed with 6 µL of APTS (95 mM in 25% acetic acid) and 4 µL sodium cyanoborohydride (1

M in THF). The heating procedure was the same as above and the sample was diluted with water prior to injection.

4.2.2.2 Monosaccharides derivatised with ABEE

A stock solution was prepared by dissolving ABEE (100 mg/mL) and acetic acid (100 mg/mL) in methanol. Immediately prior to use, 10 mg of sodium cyanoborohydride was added to 1 mL of this solution to obtain the ABEE reagent solution.

A mixture of ten monosaccharide standards, i.e. L-rhamnose, D-ribose, D-mannose, D-glucose, D-xylose, L-fucose, L-arabinose, D-galactose, D-glucuronic acid and D-galacturonic acid, was prepared as water solution containing 0.0625 M for each monosaccharide. 200 µL of the mixture was mixed with 2 mL of the reagent solution in a glass tube with screw cap. The mixture was heated at 80 °C for 60 minutes. The warm mixture was immediately diluted with 200 µL alkaline borate buffer (pH 8.5) and vortex-mixed vigorously for several seconds. During this step, excess ABEE reagent precipitated. After cooling to room temperature, the mixture was centrifuged. The resulting clear, colourless solution was analysed by CE within 24 hours to minimise degradation.

4.2.3 CE procedures

The separations were performed on two CE systems. System 1 was a P/ACE 2100 system equipped with a laser induced fluorescence detector (3 mW 488 nm argon ion laser) from Beckman Instruments, Inc. (Fullerton, CA USA). System 2 was an

HP^{3D} CE system with diode array detector from Hewlett Packard (Waldbronn, Germany).

Bare fused silica capillaries (Composite Metal Services LTD, Worcester, UK) with 20 µm i.d. and 27 cm in length (20 cm to the detector) (system 1) or 25 µm i.d. and 48.5 cm in length (40 cm to the detector) (system 2) were used.

The pH of the borate buffers was adjusted with sodium hydroxide. New capillaries were rinsed with 1 M sodium hydroxide solution for 15 minutes and then with water for 5 minutes. Between each run, the capillary was conditioned by rinsing with 1 M sodium hydroxide for 2 minutes and the run buffer for 4 minutes.

4.3 Results and discussion

4.3.1 Separation of monosaccharides derivatised with APTS

According to a report of Chen *et al.* [28], excitation with an argon ion laser at 488 nm coupled with a 520 ± 20 nm narrow band filter for emission, favours detection of the APTS-sugars adducts compared to the reagent.

Monosaccharides, as well as oligo- and polysaccharides with reducing ends can be derivatised with APTS by amination, as depicted in Figure 4.1. The reaction proceeds *via* chain opening by the acid catalyst followed by amination with APTS to form a Schiff base. Finally, reduction occurs through sodium cyanoborohydride obtaining the stable amine. The yield of derivatisation was usually ca. 95% for mono-, di- and higher DP oligosaccharides, while the yield of derivatisation of *N*-acetyl-galactosamine and *N*-acetyl-glucosamine were around 30-40% corresponding to the yields reported by Chen *et al.* [29].

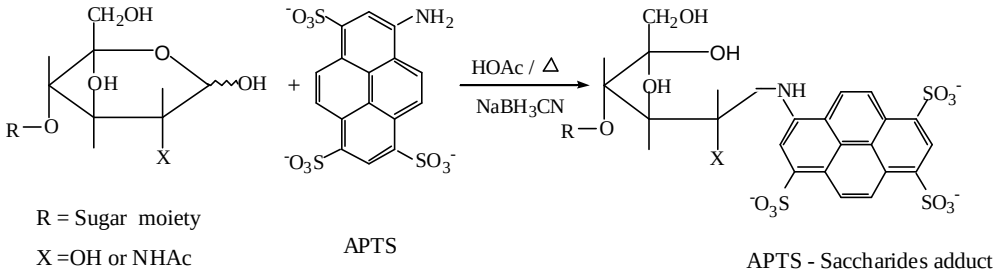

Figure 4.1 ***Reductive amination between reducing sugars and APTS***

Higher yields of *N*-acetyl-amino sugars with reductive amination could be obtained by using stronger organic acids as the acidic catalyst to promote the ring opening, such as citric acid [30]. Ketoses like fructose exhibit a much lower reaction yield compared to aldoses. As can be seen in Figure 4.2 a, the CE analysis of nine sugars resulted in only eight peaks. The peaks were identified by spiking with standards showing that fructose was missing in the separation profile. This is due to the much lower reactivity of ketoses compared to aldoses. The low activity of fructose could not compete with the aldoses to react with the APTS in the mixture. On the other hand, the fructose-APTS derivative could be obtained by individually reacting with APTS. The fructose-APTS derivative was added to the derivatised mixture shown in Figure 4.2 a. The separation of this mixture is shown in Figure 4.2 b.

The elution sequence of the sugars is governed by the apparent mobility which is determined by the electrophoretic mobility and the electroosmotic flow (EOF). At the high pH conditions applied, the apparent mobility is towards the cathode because of the high magnitude of the EOF. The higher is the electrophoretic

mobility (towards the anode), the lower is the apparent mobility and the longer is the migration time.

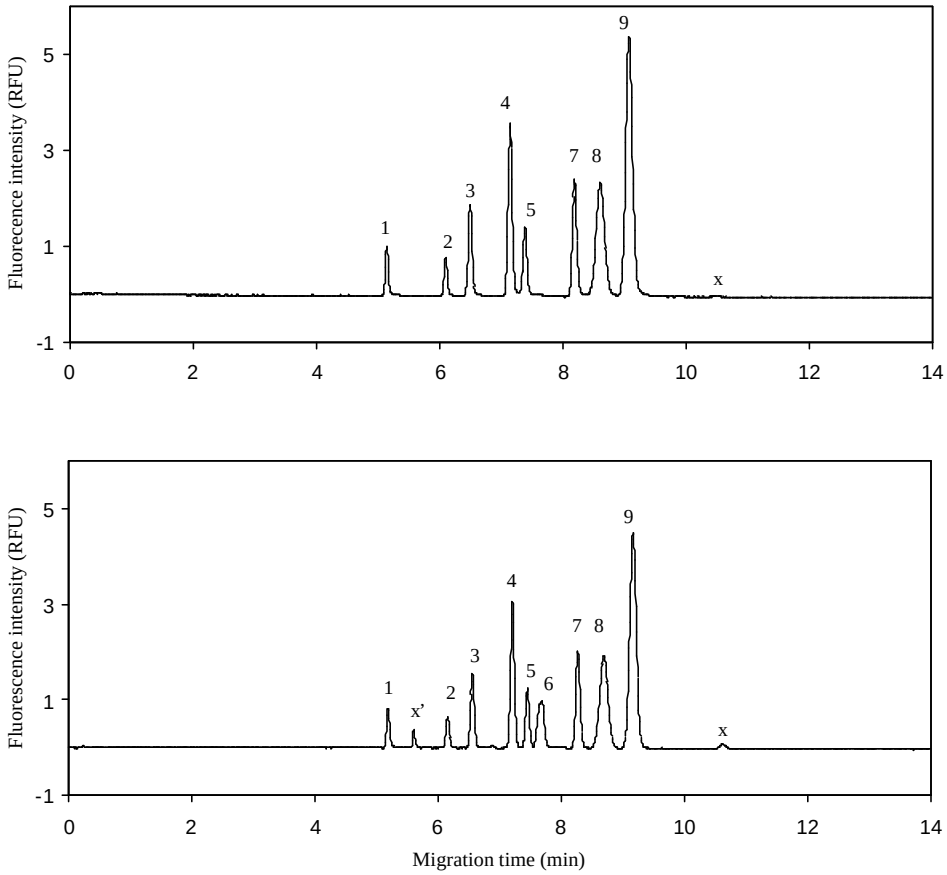

Fgure 4.2 ***Separation of nine monosaccharides derivatized with APTS***

Peaks: 1 = *N*-acetylgalactosamine, 2 = *N*-acetylglucosamine, 3 = rhamnose, 4 = mannose, 5 = glucose, 6 = fructose, 7 = xylose, 8 = fucose, 9 = galactose, x and x' are impurities of the derivatisation.
CE conditions: 20 µm i.d. and 27 cm in length (20 cm to the detector window) bare fused silica capillary, voltage +20 kV, 120 mM borate buffer, pH 10.2, 20 s injection at 0.5 psi, detection LIF at ex 488 nm/em 520 ± 20 nm.

The electrophoretic mobility of each individual sugar derivative is determined by its charge density after APTS reaction and the borate complexation. Because each

monosaccharide acquires the same charge (three) from the tag molecule (Figure 4.1), differences in charge density can only originate from the borate complexation for monosaccharides of the same molecular weight (MW). This is, for example, the case with glucose and galactose. Complex formation between sugars and borate can be described by [21]:

$$B^- + L \rightleftharpoons BL^- + H_2O \qquad (1)$$

$$BL^- + L \rightleftharpoons BL_2^- + H_2O \qquad (2)$$

where L is the polyol ligand and B^- is the tetrahydroxyborate $B[OH]^-_4$. In a pH range from 8 to 12, aqueous borate solutions contain not only tetrahydroxyborate ions but also more highly condensed polyanions such as triborate, $[B_3O_3(OH)_5]^{2-}$, and tetraborate, $[B_4O_5(OH)_4]^{2-}$. Whatever the chemicals are to prepare the buffer, the same species are obtained because of the equilibrium process.

The final structure of a polyol-borate complex is closely related to its stability in aqueous solution. High concentration of borate and high pH result in high stability of the complex. For any particular sugar molecule, the stability of the complexes also depends on the configuration, the number of hydroxyl groups, and the presence of substituents. The orientation of the vicinal hydroxyl groups of sugars is listed in Table 4.2.

Sugars with cis-oriented hydroxyl groups at C_3/C_4 form more stable complexes than those having trans-oriented hydroxyl groups at C_3/C_4. As can be seen in Figure 4.2, galactose elutes well after glucose because it has cis-oriented hydroxyl groups at C_3/C_4 and thus forms a stable borate complex. In contrast, glucose forms a less stable borate complex because it has trans-orientated hydroxyl groups at C_3/C_4. As a result, glucose has a shorter migration time than galactose.

Table 4.2 ***Eluting order, mobility and orientation of hydroxyl groups at C_3/C_4***

Saccharide derivatives	Eluting order		Mobility × 10^{-5} ($cm^2v^{-1}s^{-1}$)		-OH orientation at C_3/C_4
	APTS	ABEE	APTS	ABEE	
L-Rhamnose	1	1	2.42	13.6	*trans*
D-Mannose	2	5	3.03	18.6	*trans*
D-Glucose	3	4	3.25	18.3	*trans*
D-Ribose	4	2	3.50	16.0	*trans*
D-Xylose	5	3	3.93	17.6	*trans*
L-Fucose	6	7	4.22	20.4	*cis*
L-Arabinose	7	6	4.30	19.0	*cis*
D-Galactose	8	8	4.46	20.9	*cis*
D-Glucuronic acid		9		23.4	*trans*
D-Galacturonic acid		10		26.3	*cis*

Widmer *et al.* [21] advanced the following rules for complexation: (a) polyols can form 1:1 and 1:2 complexes with borate, (b) not only hydroxyl groups on adjacent carbon atoms but also those on alternate carbons are involved in complexation, (c) cis-1,2-diols are preferred over trans-diols, (d) an increase in the number of hydroxyl groups increases the stability, and (e) Coulombic repulsion destabilises the complex.

The migration sequence between hexoses and pentoses can be mostly explained using these rules. For instance, the fucose-borate complex is less stable than galactose because it has one hydroxyl group less at C_5 compared to galactose. Similarly, rhamnose also has one hydroxyl group less than mannose and glucose, and is thus eluting in front of mannose and glucose. However, the migration order of mannose and glucose remains unexplained.

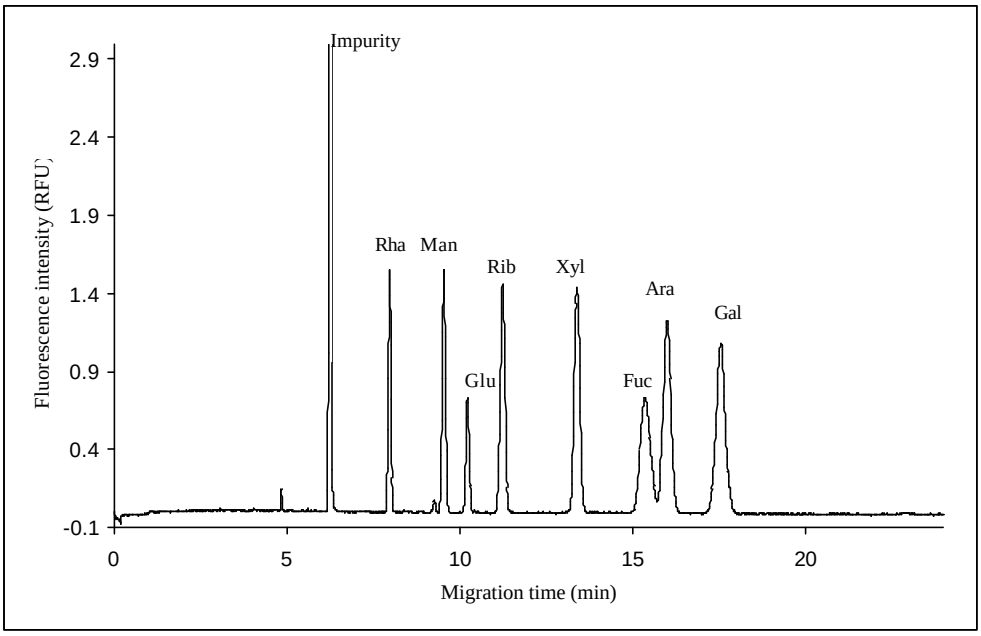

Figure 4.3 ***Separation of a mixture of monosaccharide-APTS derivatives***

Peaks: Rha = rhamnose, Man = mannose, Glu = glucose, Rib = ribose, Xyl = xylose, Fuc = fucose, Ara = arabinose, Gal = galactose.
CE conditions: 20 µm i.d. and 27 cm in length (20 cm to the detector window) bare fused silica capillary, voltage +30 kV, injection 10 s at 0.5 psi, 20 °C, 222 mM borate buffer at pH 9.6. Detection LIF at ex 488 nm/em 520 ± 20 nm.

Of the pentoses, arabinose forms the most stable complex because of its *cis*-hydroxyl groups at C_3/C_4 and thus exhibits the longest migration time, as illustrated in Figure 4.3.

The two *N*-acetylamino sugars shown in Figure 4.1 have a relatively high molecular weight compared to the other monosaccharides. Due to this low charge density, they migrated fast. Besides, the elution order of *N*-acetyl-galactosamine and *N*-acetyl-glucosamine is related to the position change of the *cis*-hydroxyl

groups at C_3/C_4, presumably due to the contribution of *N*-acetyl group at C_2 [26, 31].

However, it is still difficult to predict the migration order of some sugars, for example, arabinose and fucose. The APTS derivatives of fucose and arabinose could be baseline separated with the concentrated borate buffer used in Figure 4.3 but not with the relatively low concentrated borate buffer used for Figure 4.2. Despite the same *cis*-oriented –OH groups at C_3/C_4 (Figure 4.4), fucose has one hydroxyl group more at C_5 favouring the borate complexation whereas arabinose has a lower molecular weight than fucose. Consequently, the concentration of borate is very critical for the separation of fucose-APTS and arabinose-APTS as illustrated in Figure 4.4.

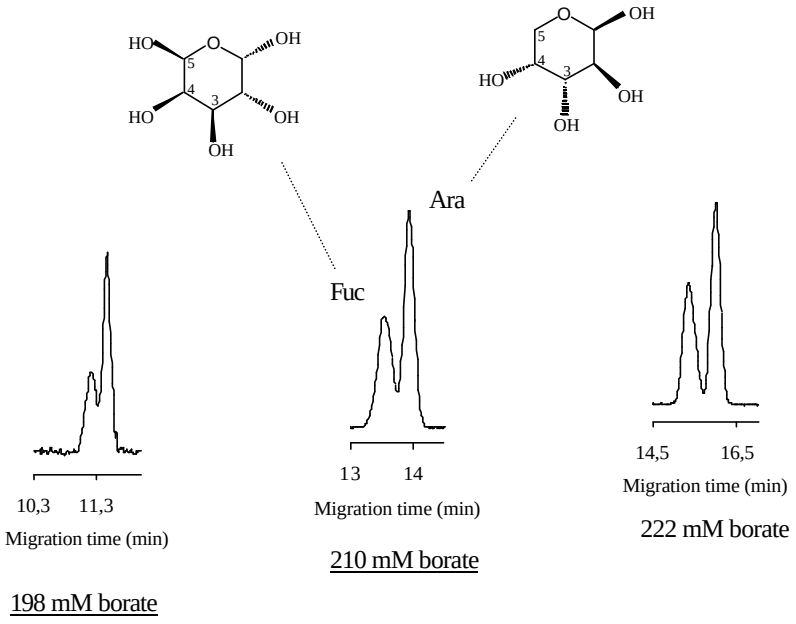

Figure 4.4 ***Separation of the APTS derivatives of fucose and arabinose with different concentration of borate buffer (pH 9.6).***

Other CE conditions as described in Figure 4.3

The APTS derivatives of glucuronic acid and galacturonic acid did not elute with the high buffer concentration because of their high negative charge density.

4.3.2 Separation of monosaccharides derivatised with ABEE

The separation of the ABEE derivatives of ten monosaccharides, including glucuronic acid and galacturonic acid, was accomplished in a single run with UV detection at 306 nm (Figure 4.5). Galacturonic acid has a longer migration time than glucuronic acid because it forms the most stable borate complex.

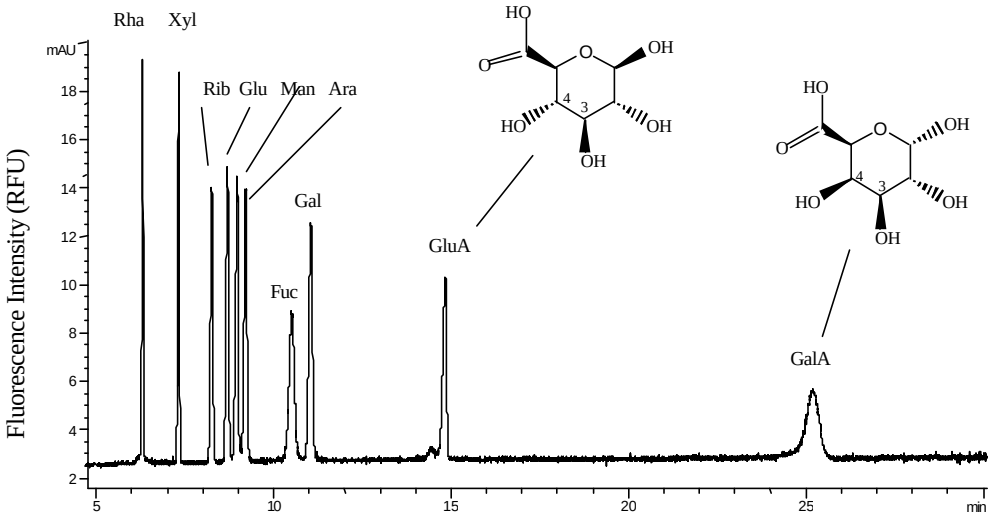

Figure 4.5 ***Electropherogram of ten monosaccharide-ABEE derivatives***

Peaks: Rha = rhamnose, Xyl = xylose, Rib = ribose, Glu = glucose, Man = mannose, Ara = arabinose, Fuc = fucose, Gal = galactose, GluA = glucuronic acid, GalA = galacturonic acid.
CE conditions: bare fused silica capillary with 25 μm i.d. × 48.5 cm in length (40 cm to the detector), run buffer 330 mM borate, pH 11.5, temperature 25 °C, injection 10 s at 50 mbar, voltage +30 kV, UV detection at 306 nm.

Contrary to APTS, ABEE inherently is neutral and the electrophoretic mobility of the sugar derivatives is only determined by the borate complexation. The apparent mobilities of sugar-ABEE derivatives are significantly higher than those with APTS as can be seen in Table 4.2. The migration of xylose shifted in front of ribose and, arabinose in front of fucose. However, the elution sequence of the neutral saccharides in Figure 4.5 is not the same as it is in Figure 4.3.

Hence, the derivatising reagents have a different influence on the complexation of the sugars. Sugar-APTS derivatives are subjected to a stronger steric hindrance and Coulombic repulsion than the sugar-ABEE derivatives upon borate complexation since APTS is a relatively large and highly negatively charged molecule.

4.4 Conclusion

The separation of monosaccharides could be accomplished by CE with LIF or UV detection by labelling with a suitable reagent. It has been demonstrated that the derivatisation reagent drastically influences the migration order.

References

[1] Journal of Chromatography Library – Volume 58, Carbohydrate analysis, high performance liquid chromatography and capillary electrophoresis, Ed. Z. El Rassi, Elseviers, Amsterdam, **1995**

[2] S. Suzuki and S. Honda, *Electrophoresis*, 19, **1998**, 2539

[3] J. Ye and R. P. Baldwin, *J. Chromatogr. A* 687, **1994**, 141

[4] R. M. Cassidy, W. Lu and V.-P Tse, *Anal. Chem.* 66, **1994**, 2578

[5] X. Huang and W.T. Kok, *J. Chromatogr. A* 707, **1995**, 335

[6] A. M. Fermier and L. A. Coló, *J. High Resol. Chromatogr.* 19, **1996**, 613

[7] S. Hofsttter-Kuhn, A. Paulus, E. Gassmann and H. M. Widmer, *Anal. Chem* . 63, **1991**, 1541

[8] A. Paulus and A. Klockow-Beck, Chromatographia, CE Series, Analysis of carbohydrates by capillary electrophoresis, K. D. Altria Ed. Elsvier, **1999**

[9] T. Soga and D. N. Heiger, *Anal. Biochem.* 261, **1998**, 73

[10] A. Klockow, A. Paulus, V. Figueiredo, R. Amadó and H. M. Widimer, *J. Chromatogr. A* 680, **1994**, 187

[11] T. Soga and D. N. Heiger, *Anal. Biochem.* 261, **1998**, 73

[12] A. Zemann, D. T. Nguyen and G. Bonn, *Electrophoresis*, 18, **1997**, 1142

[13] X. Xu, W. T. Kok and H. Poppe, *J. Chromatogr. A*, 716, **1995**, 231

[14] A. E. Vorndran, P. J. Oefner, H. Scherz and G. K. Bonn, *Chromatographia* 33, **1992**, 163

[15] B. Lu and D. Westerlund, *Electrophoresis* 17, **1996**, 325

[16] J. Plocek and J. Chmelik, *Electrophoresis* 18, **1997**, 1148

[17] T. W. Garner and E. S. Yeung, *J. Chromatogr.* 515, **1990**, 639

[18] M. Greenaway, G. N. Okafo, P. Camilleri and D. Dhanak, *J. Chem. Soc. Chem. Commun.* 14, **1994**, 1691

[19] P. Jackson, *Anal. Biochem.* 196, **1991**, 238

[20] H. Schwaiger, P. Oefner, C. Huber, E. Grill and G. K. Bonn, *Electrophoresis* 15, **1994**, 941

[21] S. Hoffsteter-Kuhn, A. Paulus, E. Gassmann and H. M. Widmer, *Anal. Chem*. 63, **1991**, 1541

[22] E. Grill, C. Huber, P. Oefner, A. Vorndran and G. Bonn, *Electrophoresis* 14, **1993**, 1004

[23] H. Schwaiger, P. J. Oefner, C. huber, E. Grill and G. K. Bonn, *Electrophoresis* 15, **1994**, 941

[24] C. Huber, E. Grill, P. Oefner and O. Bobleter, *Fresenius J. Anal. Chem.* 348, **1994**, 825

[25] X. Le, C. Scaman, Y. Zhang, J. Zhang, N. J. Dovichi, O. Hindsgaul and M. M. Palcic, *J. Chromatogr. A* 716, **1995**, 215

[26] A. E. Vorndran, E. Grill, C. Huber, P. J. Oefner and G. K. Bonn *Chromatographia* 34, **1992**, 109

[27] K. Swinney and D. Bornhop, *Critical Reviews in Analytical Chemistry* 30 (1), **2000**, 1

[28] R. A. Evangelista, M. Liu and F. A. Chen, *Anal. Chem.* 67, **1995**, 2239

[29] F. A. Chen and R. A. Evangelista, *Anal. Biochem.* 230, **1995**, 273

[30] R. A. Evangelista, F. A. Chen and A. Guttman, *J. Chromatogr. A* 745, **1996**, 273

[31] S. Honda, S. Iwase, A.Makino and S.Fujiwara, *Anal. Biochem*. 176, **1979**, 217

Chapter 5

CE Analysis of Oligosaccharides

Abstract

Oligosaccharides can be analysed by CE with UV or LIF detection after precolumn derivatisation. Two different CE modes have been applied to separate oligosaccharides and the mechanisms are discussed.

5.1 Introduction

The analysis of oligosaccharides derived from polysaccharides can be an alternative approach to the structural elucidation of polysaccharides. Sucrose and maltose have been analysed by CE using strong alkaline electrolytes and indirect UV detection [1]. Underivatised oligosaccharides including disaccharides (trehalose, sucrose, lactose, lactulose and cellobiose), trisaccharides (raffinose) and tetrasaccharides (stachyose) were also analysed by CE at high pH electrolyte conditions in combination with electrochemical detection (ECD) [2]. Baldwin and co-workers [3] separated maltooligosaccharides (Dextrin 15) and starch hydrolysates on bare fused silica capillaries using ECD with a Cu electrode. 10 mM cetyltrimethylammonium bromide (CTAB) was added to the 100 mM sodium hydroxide buffer to reverse the EOF. Under these conditions, however, baseline separation of the oligomers was not achieved. Analysis of disaccharide

constituents of glycosaminoglycans (GAGs), such as heparin, hyaluronic acid and chondroitin sulfate, was achieved by CE coupled with direct or indirect UV detection [4]. Structural differences among GAGs were demonstrated. After enzymatic degradation of GAGs with different lyases, e.g. heparinase, chondroitinase, disaccharides bearing unsaturated uronic acids at C_4-C_5, were obtained which allowed direct UV detection at 232 nm. Because of their ionic nature, the GAG-derived disaccharides could readily be analysed. Determination of the oligosaccharide composition of heparin and low-molecular-weight (LMW) heparins was achieved by using a borate/SDS buffer system at pH 8.8. Although it was not possible to identify and quantify all components in various LMW heparins, mainly because of lack of standards, comparison of the electropherograms allowed to elucidate differences or similarities in the oligosaccharides, reflecting hereby the microheterogeneity of different commercially available LMW heparins.

A comparative study on the composition of two sets of eight unsaturated disaccharide samples derived from heparin/heparan sulfate and chondroitin/dermatan sulfate was carried out using both normal and reversed polarity CE [5]. In reversed polarity CE, using a single buffer system composed of sodium phosphate with pH 3.48, the disaccharides were completely resolved. At this pH, the EOF is negligible and the solutes migrate by their electrophoretic mobility only towards the anode. In the same report, the separation of 13 heparin derived oligosaccharides ranging from di- to tetrasaccharides, using both normal and reversed polarity CE was described. The various oligosaccharides, which differed primarily in size by the number of disaccharide units, were better

resolved at normal polarity using 10 mM sodium borate, pH 8.8 containing 50 mM SDS. This may be due to some partitioning into the SDS micelles and to the fact that the EOF is in the opposite direction of the electrophoretic mobility of the analytes, thus decreasing their apparent mobility resulting in improved resolution. These oligosaccharides could be detected at 232 nm because of the unsaturated bond in the uronic acid residues. The CE analysis of sulfated synthetic LMW heparin fragments, however, necessitated the application of indirect UV detection [6]. Sulfated synthetic oligosaccharides exhibit low molar absorptivities as a result of the absence of the double bond in their structures. Indirect UV detection was performed by adding the chromophore containing 5-sulfosalicylic acid or 1,2,4-tricarboxybenzoic acid to the background electrolyte. The sensitivity of indirect UV detection was reported to be at least one order of magnitude higher than that of direct UV detection [6].

Looking for high sensitive detection and good electrophoretic properties for the CE analysis of neutral oligosaccharides, much attention has been paid to derivatise oligosaccharides with suitable tags. Most often, reductive amination (Chapter 3, scheme i) is used to derivatise oligosaccharides containing reducing ends. The separation of isomaltooligosaccharides up to 20 DP and derivatised with 2-aminopyridine (2-AP) on a polyacrylamide coated capillary column with an acidic electrolyte (100 mM phosphate buffer, pH 2.5) and UV detection has been described [7]. Several disaccharides including gentibiose, maltose, lactose, cellobiose and melibiose were labelled with APTS by reductive amination and subsequently separated by CE using MOPS (3-[*N*-morpholino]propanesulfonic acid) and borate buffers [8]. With MOPS, gentibiose migrated first, followed by

maltose, lactose, cellobiose and melibiose. This migration order is governed by differences in hydrodynamic volume arising from varying degrees of hydration due to the different position of hydroxyl groups in the non-reducing end pyranose. In borate buffer, the migration order was gentibiose, maltose, melibiose, cellobiose and lactose. This migration order is dictated by the magnitude of the stability constants of the formed disaccharide-borate complexes. In the same publication, two APTS-derivatised glucose tetrasaccharide isomers differing only in one linkage at the non-reducing end were well resolved in the MOPS buffer but not in the borate buffer. This means that the borate complexation with both isomers had no significant effect on their relative electrophoretic mobilities. The isomers were maltotetraose-APTS [glc-α(1-4)glc-α-(1-4)glc-α-(1-4)glc-α-(1-4)-APTS and glc-α(1-6)glc-α-(1-4)glc-α-(1-4)glc-α-(1-4)-APTS].

This chapter describes some applications in the separation of the oligosaccharides in malt extract and dextrin 15 using LIF and UV detection.

5.2 Experimental

5.2.1 Chemicals

9-Aminopyrene-1,4,6-trisulfonate (APTS) was purchased from Lambda Fluoreszenztechnologie (Graz, Austria). HPLC grade tetrahydrofuran (THF) and methanol were from Lab-Scan (Dublin, Ireland). Orthophosphoric acid was from Merck (Darmstadt, Germany) and acetic acid from Panreac (Barcelona, Spain). 4-Aminobenzoic ethyl ester (ABEE) was bought from Acros (New Jersey, USA). Sodium hydroxide was obtained from UCB (Leuven, Belgium). Malt extract and Dextrin 15 (from maize starch) were obtained from Fluka (Bornem, Belgium).

Maltooligosaccharide standards, sodium cyanoborohydride and borax were obtained from Sigma (Steinheim, Germany).

5.2.2 Derivatisation procedures

5.2.2.1 Derivatisation with APTS

1 mg of Dextrin 15 or malt extract was mixed with 10 µL APTS (38 mM in 15% acetic acid aqueous phase) and 3 µL sodium cyanoborohydride (1 M in THF). The mixture was heated at 95 °C for one hour and then diluted with 1 mL water prior to injection. The standard mixture was derivatised by the same procedure.

5.2.2.2 Derivatisation with ABEE

A stock solution was prepared by dissolving ABEE (100 mg/mL) and acetic acid (100 mg/mL) in methanol. Prior to use, 10 mg of sodium cyanoborohydride was added to 1 ml of the stock solution to obtain the ABEE reagent solution. 200 µL of a standard mixture containing glucose, maltose, maltotriose, maltotetraose, maltopentaose, maltohexaose and maltoheptaose with a concentration of 0.05 M for each sugar, was mixed with 2 mL of the reagent solution in a glass tube with screw cap. The reaction mixture was heated at 80 °C for 60 minutes. The warm sample was immediately diluted with 200 µL alkaline borate buffer (pH 8.5) and vortex-mixed. During this step, excess ABEE precipitated in the form of a fine white powder. After cooling to room temperature, the mixture was centrifuged. The resulting clear, colourless solution was analysed by CE within 24 hours after the preparation.

5.2.3 CE procedures

Fused silica capillaries with 50 and 75 μm i.d. and with 50 cm effective length from Composite Metal Services (Worcester, UK) were used. New capillaries were rinsed with water and 1.0 M sodium hydroxide solution for 15 minutes prior to use. Between each run, the capillary was conditioned with 1.0 M sodium hydroxide solution for 2 minutes and then with run buffer for 4 minutes. Borate and phosphate buffers were prepared by using sodium hydroxide to adjust the pH.

5.3 Results and discussions

5.3.1 Oligosaccharides in the malt extract with LIF detection

Figure 5.1 shows the separation of the APTS derivatised malt extract together with the analysis of some standards. The separations were obtained in the negative polarity mode with an acidic phosphate buffer (pH 2.2).

The migration is controlled only by the electrophoretic mobilities (charge to mass ratio) because the EOF is negligible at a pH of 2.2. The main malt extract constituents are glucose (DP 0), maltose (DP 1), maltotriose (DP 2), maltotetraose (DP 3), maltopentaose (DP 4), maltohexaose (DP 5), maltoheptaose (DP 6) and maltooctaose (DP 7). Only low amounts of oligomers with DP higher than 7 were present as shown in the insert in Figure 5.1.

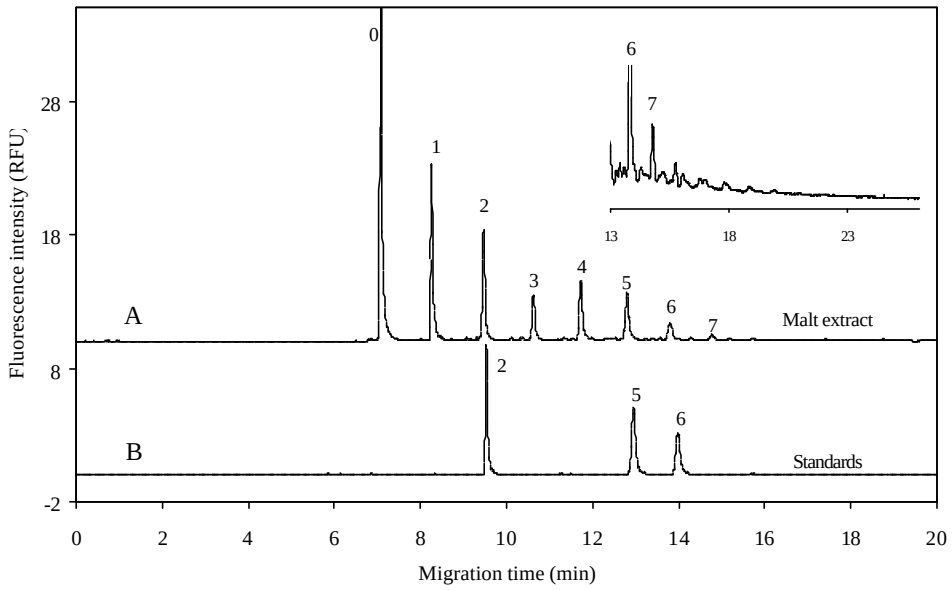

Figure 5.1 ***Separation of a malt extract (A) and a standard mixture of maltose, maltohexaose and maltoheptaose (B)***

Peaks: 0 = glucose, 1 = maltose, 2 = maltotriose, 3 = maltotetraose, 4 = maltopentaose, 5 = maltohexaose, 6 = maltoheptaose, 7 = maltooctaose.
CE conditions: 75 µm i.d. and 57 cm in length (50 cm to the detector window) bare fused silica capillary, 20 °C, 4 s injection at 0.5 psi, voltage -20 kV, 50 mM phosphate buffer, pH 2.2, detection LIF at ex 488 nm/em 520 ± 20 nm.

5.3.2 Oligosaccharides in Dextrin 15 with LIF detection

Dextrin 15 is a maltooligosaccharide mixture with a typical chain length distribution. Figure 5.2A shows the separation on a bare fused silica capillary with a 50 mM phosphate buffer at pH 2.2 in the negative polarity mode. The oligosaccharides elute as in Figure 5.1 with increasing DP number i.e. from DP 0 to DP 15. The separation is based on the differences of their charge to mass ratios.

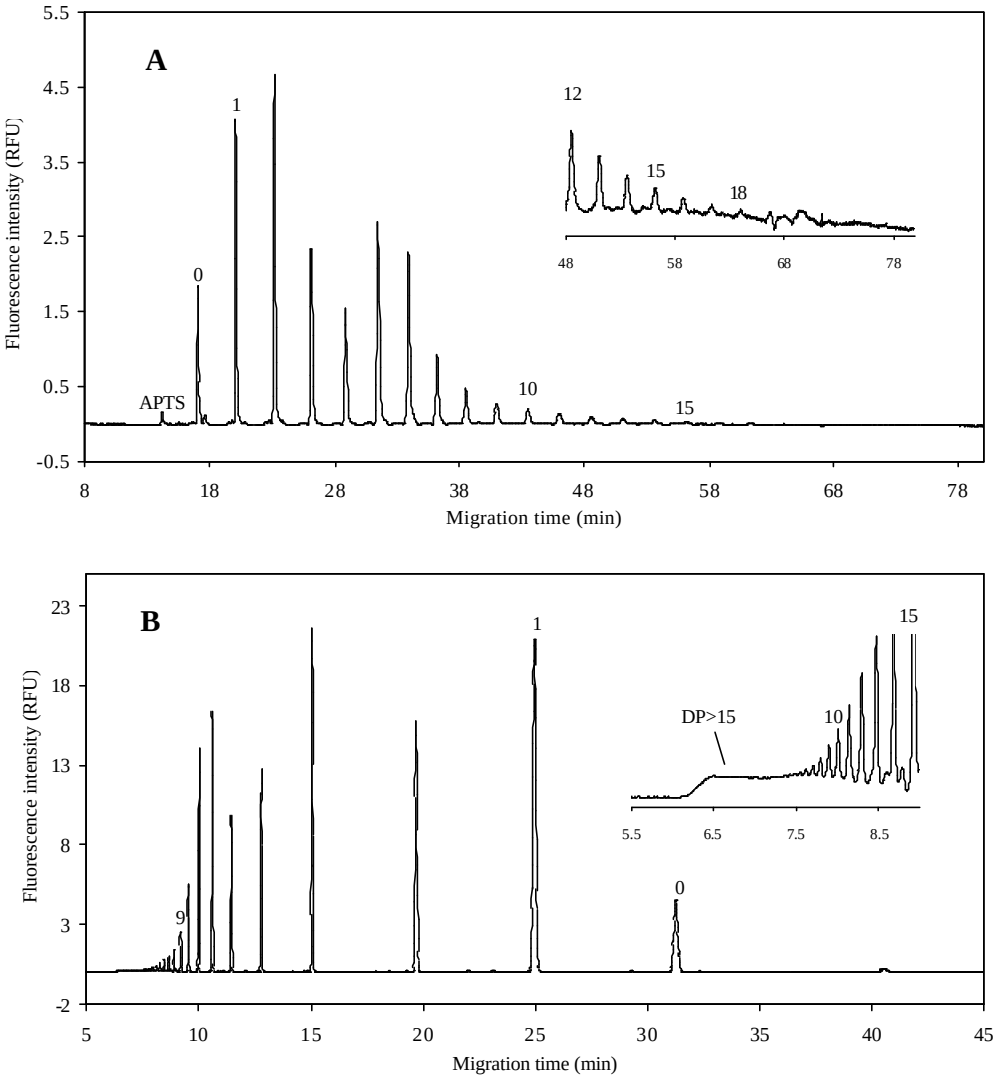

Figure 5.2 ***CE separation profiles of dextrin 15 with normal (A) and reversed polarity (B) mode***

Peaks: 0 = glucose (DP 0), 1 = maltose (DP 1), 9 = DP 9, 10 = DP 10, 15 = DP 15.
CE conditions: 50 µm i.d. and 57 cm in length (50 cm to the detector window) bare fused silica capillary, 20 °C, 4 s injection at 0.5 psi, detection LIF at ex 488 nm/em 520 ± 20 nm.
A. voltage -20 kV, 80 mM phosphate buffer, pH 2.2
B. voltage +20kV, 100 mM borate buffer, pH 10.2.

An increase in the charge to mass ratio results in a higher electrophoretic mobility and a shorter migration time. The migration of the ATPS derivatives is directed towards the anode because they carry negative charges. Each oligomer reacts with only one molecule of the reagent (APTS) at the reducing terminal group, and therefore, each oligomer possesses the same charge by derivatisation. Hence, the larger the mass of the oligosaccharide, the longer is the migration time.

Figure 5.2 B shows the separation with an alkaline pH and in the positive polarity mode. The electroosmotic flow towards the cathode is now controlling the migration (upstream). The electrophoretic mobility of the solutes is now downstream and compounds with the highest charge to mass ratio have the longest migration times. The oligosaccharide derivatives also form complexes with borate and thus the charge density on the derivatives originates from both the tag and the complexation.

The complete reversal in migration order is of substantial interest because it shows that both modes are complementary to each other. A graphical representation how these mirror images are created is given in Figure 5.3. These two separation modes result in different separatio n efficiency and resolution of oligosaccharides (from DP 0 to DP 6), which will be discussed in Chapter 6, Table 6.1 and Table 6.2.

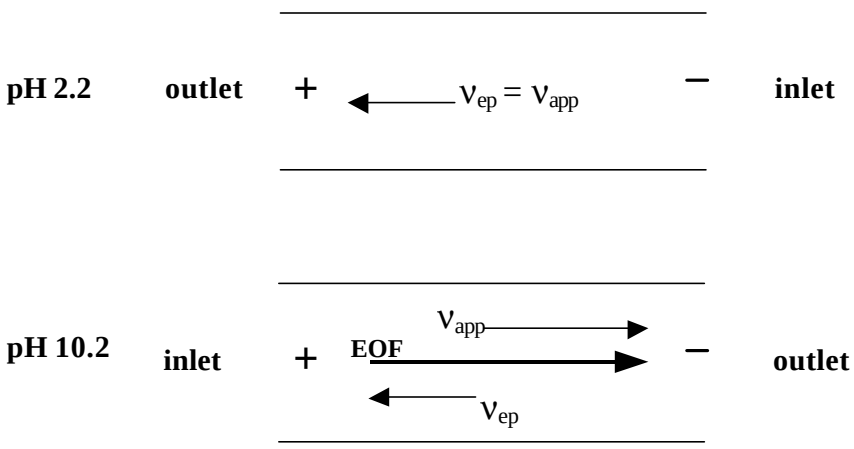

Figure 5.3 ***Separation schemes of the two CE modes***

5.3.3 CE analysis of oligosaccharide standards with UV detection

LIF detection is a rather expensive approach for oligosaccharide CE analysis. Therefore, the possibilities of UV detection were evaluated by forming ABEE derivatives. Figure 5.4 shows the CE separation of seven maltooligosaccharides derivatised with ABEE on a bare fused silica capillary with UV detection at 306 nm.

The separation was performed in the positive polarity mode with an alkaline borate buffer at pH 11.5. As described in 5.3.2, the oligosaccharides with the high mass migrate through the detector window faster than those with low mass.

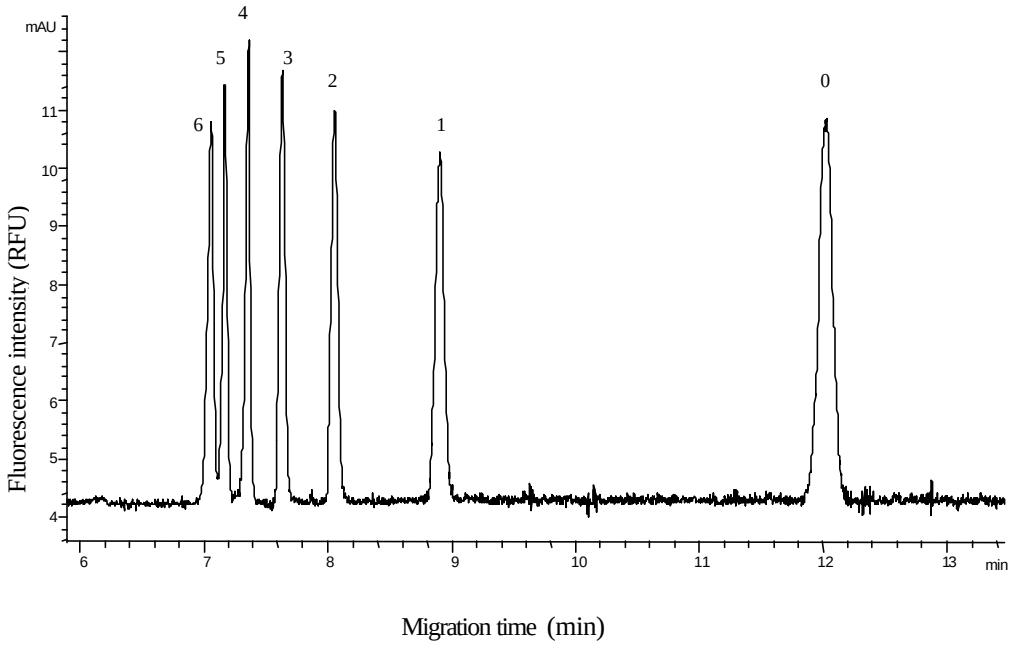

Figure 5.4 ***Separation of seven maltooligosaccharides by CE after ABEE derivatisation***

Peaks: 0 = glucose (DP 0), 1 = maltose (DP 1), 2 = maltotriose (DP 2), 3 = maltotetraose (DP 3), 4 = maltopentaose (DP 4), 5 = maltohexaose (DP 5) and 6 maltoheptaose (DP 6)
CE conditions: 25 µm i.d. × 48.5 cm (40 cm to the detector window) bare fused silica capillary, run buffer 450 mM borate at pH 11.5, voltage +30 kV, temperature 25 °C, injection for 30 s at 50 mbar, detection at 306 nm.

5.4 Conclusion

Oligosaccharides can be analysed by CE after formation of appropriate derivatives i.e. APTS for LIF detection and ABEE for UV detection. Mirror images are obtained by applying two electrolytes. At low pH and with reversed polarity, oligosaccharides elute in order DP 0 to DP x whereas at high pH in the normal

polarity mode, the elution order is DP x to DP 0. The two modes are providing complementary information as will also be illustrated in the following chapters.

References

[1] X. Xu, W. T. Kok and H. Poppe, *J. Chromatogr. A* 716, **1995**, 231

[2] L. A. Colón, R. Dadoo and R. N. Zare, *Anal. Chem.* 65, **1993**, 478

[3] J. Ye and R. P. Baldwin, *Anal. Chem*. 65, **1993**, 3525

[4] S. A. Ampofo, H. M. Wang and R. J. Linhardt,
Anal. Biochem. 199, **1991**, 249

[5] U. R. Desai, H. Wang, S. A. Ampofo and R. J. Linhardt,
Anal. Biochem. 213, **1993**, 120

[6] A. Pervin, A. Al-Hakim and R. J. Linhardt,
Anal. Biochem. 221, **1994**, 182

[7] J. B. L. Damm and G. T. Overklift, *J. Chromatogr. A*, 678, **1994**, 151

[8] S. Honda, A. Makino, S. Suzuki and K. Kakehi,
Anal. Biochem. 191, **1990**, 228

[9] F. A. Chen and R. A. Evangelista, *Anal. Biochem* . 230, **1995**, 273

Chapter 6

Investigation on the Quantitative Aspects of Oligosaccharide Analysis by CE-LIFD

Abstract

Maltooligosaccharides with DPs ranging from 0 to 6 were derivatised with 9-aminopyrene-1,4,6-trisulfonic acid (APTS) and analysed using capillary electrophoresis (CE) in combination with laser induced fluorescence detection (LIFD). The separations were performed both in the normal and in the reversed polarity mode. The separation parameters were optimised and compared. Quantitative analysis by CE-LIFD was investigated.

6.1 Introduction

The determination of the degree of polymerisation (DP) of oligosaccharides and polysaccharides is a great challenge to analysts due to problems such as the lack of suitable standards, the need for a high resolving technique and the derivatisation methods required to elute the solutes. Derivatisation is most often involved in CE analysis because it is necessary for both sensitive detection and improvement of the electrophoretic properties of the saccharides. Quantitative analysis is mostly done based on measurement of the basic units of saccharides such as neutral monosaccharides and uronic acids [1-4]. Chemical or enzymatic hydrolysis is necessary to break down the chains before derivatisation,

unfortunately, the completion of hydrolysis is often questionable, which is complicating quantitative analysis.

Although many applications were reported for mapping the chain length distribution of oligo- and polysaccharides [5], quantitative analysis of DP numbers to the best of our knowledge has not yet been performed.

Maltooligosaccharides with a DP from 0 to 6 after derivatisation with the fluorescence reagent 9-aminopyrene-1,4,6-trisulfonic acid (APTS) were used as model compounds for a quantitative study. In the labelling reaction, the amino group of the reagent reacts with the carbonyl group of the reducing end of a sugar to form a Schiff base, which is further reduced with sodium cyanoborohydride to form a stable amine (see Chapter 3, Scheme i). According to Chen and Evangelista [6], the derivatisation yields for monosaccharides and oligosaccharides with APTS are larger than 95%. Moreover, labelling yields were found to be highly reproducible and independent of the average chain length between DP 3 and 135 [7].

6.2 Experimental

6.2.1 Chemicals

APTS was purchased from Molecular Probes (Leiden, the Netherlands). Sodium cyanoborohydride, borax and all oligosaccharide standards were purchased from Sigma-Aldrich (Steinheim, Germany). The purity of maltotriose, maltohexaose and maltoheptaose was higher than 93%. The purity of the other standards was above 97%. Sodium hydroxide was obtained from UCB (Leuven, Belgium). HPLC grade tetrahydrofuran (THF) was obtained from Lab-Scan Ltd. (Dublin,

Ireland). Ortho-phosphoric acid was purchased from Merck (Darmstadt, Germany). Acetic acid was from Panreac (Barcelona, Spain). Water used in all the experiments was produced by a Milli-Q water purification system (Millipore, Bedford, MA, USA).

6.2.2 Labelling procedure

A sample of seven standards was prepared by dissolving glucose, maltose, maltotriose, maltotetraose, maltopentaose, maltohexaose, and maltoheptaose in equal amounts in water with a final concentration of 0.01 M for each saccharide.

10 µL of the stock solution was pipetted into an Eppendorf vial, followed by addition of 30 µL of APTS solution (0.095 M in 15% acetic acid solution) and 5 µL of sodium cyanoborohydride (1 M in THF). The mixture was heated at 90 °C for 1 hour and diluted to 5 mL with Milli-Q water. Series of standard solutions with different concentrations were prepared by diluting the above concentrated samples.

6.2.3 CE procedures

The analyses were performed on a P/ACE 2100 CE system equipped with a laser induced fluorescence detector (3-mW 488 nm argon-ion laser from Beckman Instruments, Inc. (Fullerton, CA, USA). Peak integration was done by using the Beckman gold chromatography software. Bare fused silica capillaries were obtained from Composite Metal Services (Worcester, UK). New capillaries were washed with 1 M sodium hydroxide solution for 15 minutes and then with water for 15 minutes. Before each run, the capillaries were rinsed with 1 M sodium

hydroxide for 2 minutes and conditioned by the run buffer for 4 minutes. Borate buffers were prepared by adjusting the pH with sodium hydroxide. Phosphate buffer was prepared by using sodium hydroxide to adjust the ortho-phosphoric acid solution.

The CE conditions were as follows. A bare fused silica capillary with 50 μm i.d. and 47 cm length (40 cm to the detector window) was applied in all the experiments. The temperature was set at 20 °C. Injection was performed hydrodynamically for 20 s at 0.5 psi and detection was done with LIF at ex 488 nm/em 520 ± 20 nm. Both the positive and negative polarity mode were applied:

1) positive polarity, voltage +30 kV, 100 mM borate buffer pH 10.2.

2) negative polarity, voltage -25 kV, 80 mM phosphate buffer pH 2.2.

6.3 Results and discussion

6.3.1 Separation of the mixture of seven saccharides

Separation profiles of the oligosaccharides were obtained with the alkaline borate buffer for the positive polarity mode and the acidic phosphate buffer for the negative polarity mode.

The peaks were identified by spiking with individual standards. In this batch of APTS, large amounts of impurities, indicated by the asterisks (*) in Figure 6.1, were observed. However they did not disturb the quantitative analyses.

When the alkaline borate buffer conditions were used (positive polarity, condition 1), the elution order was from the DP 6 to DP 0 (Figure 6.1 A). In the case of the acidic phosphate buffer conditions (negative polarity, condition 2), a reversed

order was obtained (Figure 6.1 B). The mechanisms of these two modes have been explained in Chapter 5 (5.3).

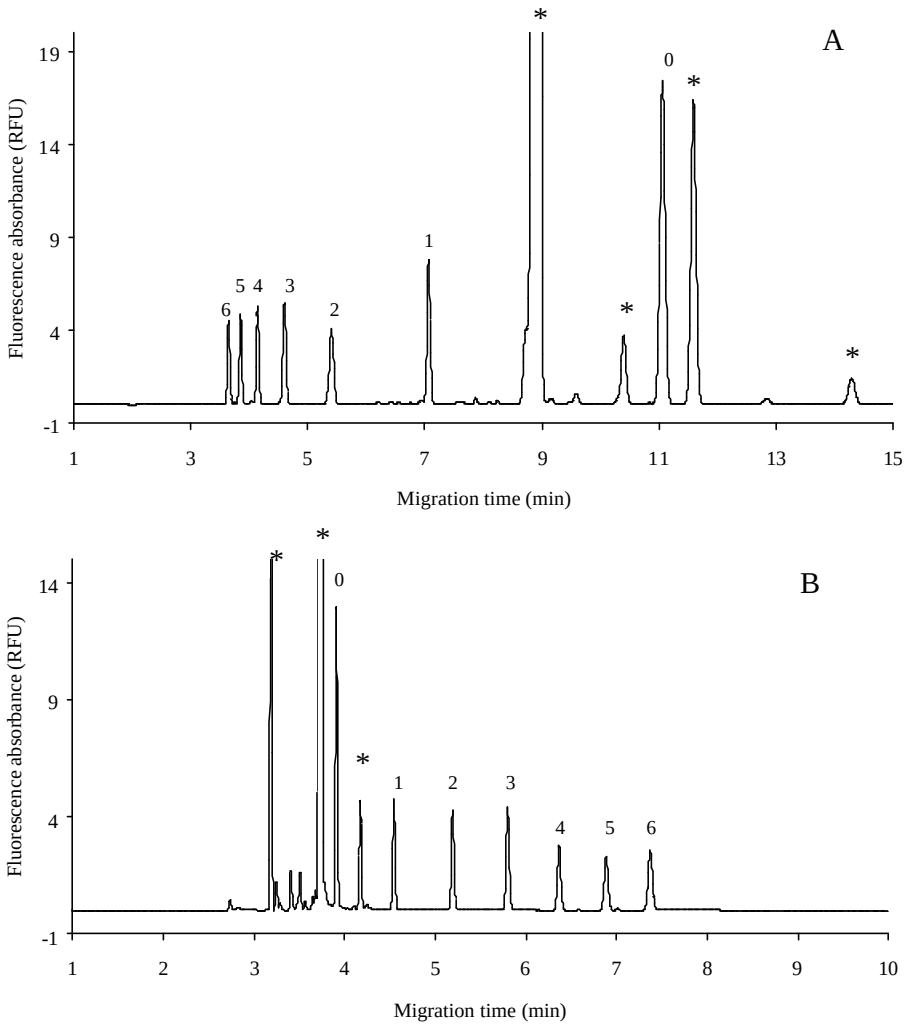

Figure 6.1 ***Electropherograms of maltooligosaccharides-APTS with positive polarity (A, condition 1) and negative polarity (B, condition 2)***

Peaks: 0 = DP 0 (glucose), 1 = DP 1 (maltose), 2 = DP 2 (maltotriose), 3 = DP 3 (maltotetraose), 4 = DP 4 (maltopentaose), 5 = DP 5 (maltohexaose), 6 = DP 6 (maltoheptaose), * = impurities.
CE conditions: see text (6.2.3).

6.3.2 Comparison of the separation with two CE conditions

6.3.2.1 Limits of detection (LOD)

When the sensitivity of the analyses in both separation modes was studied, an LOD of 5×10^{-9} M was obtained with the borate buffer (Table 6.1). This appeared to be one order of magnitude lower than for the phosphate buffer (Table 6.2). The same behaviour was observed in the analysis of monosaccharides with UV detection, and this is possibly caused by the effect of complexation between borate and saccharides. Hofftester-Kuhn and co-workers [8] reported that underivatised mono- and oligosaccharides could be detected with a 2 to 50 times higher sensitivity in an alkaline borate buffer compared to other buffers when detection was performed at a wavelength of 195 nm.

6.3.2.2 Resolution (R_s)

The resolution between oligosaccharide pairs decreased with increasing DP number. The resolution obtained with the alkaline borate buffer was very high between DP 1 and DP 2, and decreased rapidly to a resolution of 2.20 between DP 5 and DP 6 (Table 6.1). On the other hand, the resolution between DP 1 and DP 2 for the acidic phosphate buffer was 9.37 which is substantially lower than for the alkaline borate buffer, whereas between DP 5 and DP 6, the resolution is still 4.37 (Table 6.2).

In conclusion, for oligosaccharides with DP $\leq$ 2, the resolution with the borate buffer system is higher than the one obtained with the acidic phosphate buffer system. On the other hand, for oligomers with the DP $\geq$ 3, the resolution with the

acidic phosphate buffer is higher than the one obtained with the alkaline borate buffer system.

Table 6.1 ***Repeatability of migration (RSD), efficiency (N), resolution (R_s) and limit of detection (LOD) obtained for the separation of maltooligosaccharides in the positive polarity mode with borate buffer***

Saccharides	DP	RSD (n = 8) (migration time)	N	R_s	LOD (M)
Glucose	0	0.62	70,497		5×10^{-9}
Maltose	1	0.29	67,391	24.37	5×10^{-9}
Maltotriose	2	0.85	48,200	13.34	5×10^{-9}
Maltotetraose	3	0.84	47,120	6.90	5×10^{-9}
Maltopentaose	4	0.67	45,199	4.29	5×10^{-9}
Maltohexaose	5	0.58	32,975	2.92	5×10^{-9}
Maltoheptaose	6	0.48	29,522	2.20	5×10^{-9}

Table 6.2 ***Repeatability of migration (RSD), efficiency (N), resolution (R_s) and limit of detection (LOD) obtained for the separation of maltooligosaccharides in the negative polarity mode with phosphate buffer***

Saccharides	DP	RSD (n = 8) (migration time)	N	Rs	LOD (M)
Glucose	0	0.32	133,947		5×10^{-8}
Maltose	1	0.50	146,174	9.37	5×10^{-8}
Maltotriose	2	0.50	157,786	8.92	5×10^{-8}
Maltotetraose	3	0.53	121,602	7.23	5×10^{-8}
Maltopentaose	4	0.53	112,266	5.98	5×10^{-8}
Maltohexaose	5	0.73	103,752	5.09	5×10^{-8}
Maltoheptaose	6	0.76	96,399	4.37	5×10^{-8}

6.3.2.3 Efficiency (N)

The separation efficiencies obtained with the acidic phosphate buffer system were two or three times those obtained with the alkaline borate buffer system (Table 6.1

and Table 6.2). With the alkaline borate buffer system, the separation efficiency drastically decreased with increasing DP number (Table 6.1).

Hence, it can be concluded that the acidic phosphate buffer system is preferred to reach high DP separation profiles of oligosaccharides and polysaccharides due to the higher efficiency and resolution for oligosaccharides with DP ≥ 3. On the other hand, the alkaline borate buffer system can be used to reach higher detection sensitivity, which is especially useful to monitor very high DP chains. Illustrative examples are discussed in Chapter 7, 7.3.

6.3.3 Injection

The precision of the measurements particularly depends on the repeatability of injection.

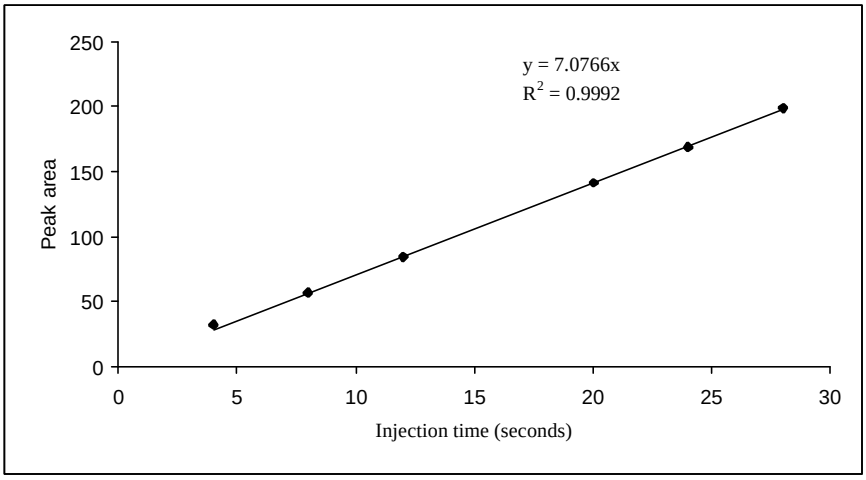

Figure 6.2 ***Linearity of injection volume and peak area***

Maltopentaose-APTS derivative (5×10^{-7} M) was used as test sample.
CE condition: see text (6.2.3), condition 1 was applied.

Hydrodynamic sampling was used in the experiments since it is based strictly on volume loading of the sample, thus providing the most precise injection. Figure 6.2 shows the linear relationship between injection volume and peak area for maltopentaose-APTS. The linearity is satisfactory (R^2 = 0.9992) ensuring good precision of measurements.

6.3.4 Linear range of the calibration curves

A wide linear range with good regression coefficients ($R^2 \geq 0.99$) was found in three to four orders of magnitude of the concentration for both buffer systems (Table 6.3, Table 6.4). It can be seen that the slopes of the calibration curves with the borate buffer system were systematically higher than those obtained with the phosphate buffer. For example, the slopes of the calibration curve for maltose is 6×10^8 with borate buffer and is only 2×10^8 with phosphate buffer. This is another expression of the enhanced sensitivity obtained with borate buffer.

The effect is also visible in Figure 6.3 for a series of experiments performed with a narrower range of concentration.

It is thus shown that it is possible to quantify the individual oligomers with good sensitivity and precision (as expressed by the good correlation coefficients). A continuous problem is, however, as already mentioned, the lack of standards available for the quantitation of each DP number. Because they are not commercially available, it is not possible to construct calibration curves for each DP number. Hence, it is impossible to quantify the total amount of this type of saccharides in the sample by this approach.

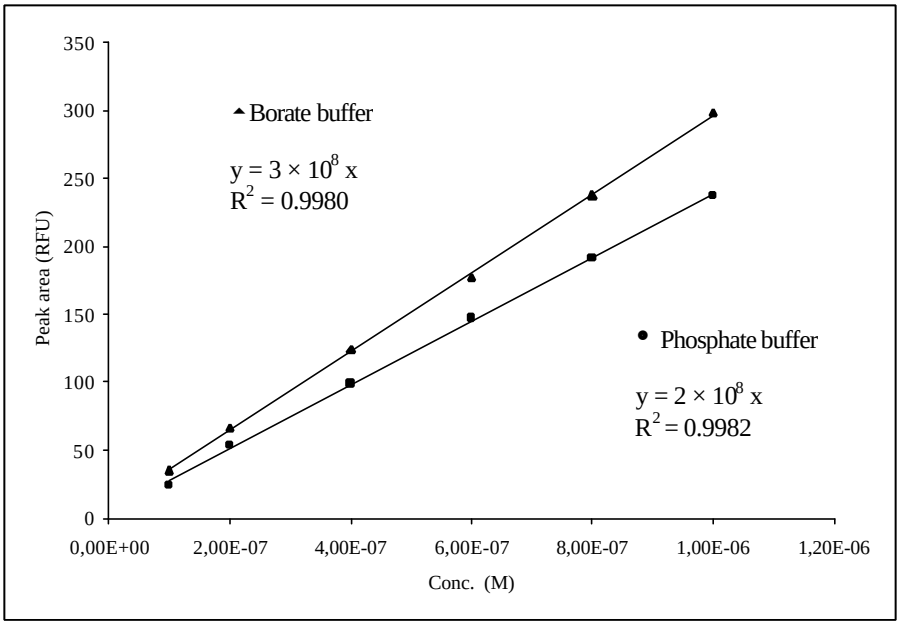

Figure 6.3 ***Calibration curve of maltopentaose-APTS obtained with two CE conditions described in 6.2.3.***

Therefore, our further interest focused at the investigation of the relative response factors (RRF). This is the ratio of the normalised peak area of the compounds of interest to the peak area of an internal standard. A normalised peak area is the area divided by its migration time. This is often used in CE because it allows to correct for run to run variation in migration time and hence, in peak area of a given product. In these experiments maltose (DP 1) was taken as the internal standard. If it could be shown that the RRF of all compounds in the standard mixture were close to 1, this would be of tremendous interest for the quantitation of the total amount of a saccharide in a sample.

Table 6.3 ***Linear range of maltooligosaccharides obtained with the borate buffer***

Oligosaccharides	Linear range (M)	Regression equation	Regression coefficient (R^2)	RRF
Glucose	5×10^{-9} - 1×10^{-5}	$y = 2 \times 10^{9} x$	0.9995	
Maltose	5×10^{-9} - 5×10^{-6}	$y = 6 \times 10^{8} x$	0.9994	1.00
Maltotriose	5×10^{-9} - 5×10^{-6}	$y = 4 \times 10^{8} x$	0.9996	1.25
Maltotetraose	5×10^{-9} - 5×10^{-6}	$y = 4 \times 10^{8} x$	0.9998	1.26
Maltopentaose	5×10^{-9} - 5×10^{-6}	$y = 3 \times 10^{8} x$	0.9997	1.29
Maltohextaose	5×10^{-9} - 5×10^{-6}	$y = 3 \times 10^{8} x$	0.9997	1.13
Maltoheptaose	5×10^{-9} - 5×10^{-6}	$y = 3 \times 10^{8} x$	0.9998	1.19

Table 6.4 ***Linear range of maltooligosaccharides obtained with the phosphate buffer***

Oligosaccharides	Linear range (M)	Regression equation	Regression coefficient (R^2)	RRF
Glucose	5×10^{-8} - 5×10^{-6}	$y = 4 \times 10^{8} x$	0.9990	
Maltose	5×10^{-8} - 1×10^{-5}	$y = 2 \times 10^{8} x$	0.9997	1.00
Maltotriose	5×10^{-8} - 1×10^{-5}	$y = 2 \times 10^{8} x$	0.9986	0.97
Maltotetraose	5×10^{-8} - 1×10^{-5}	$y = 2 \times 10^{8} x$	0.9980	1.00
Maltopentaose	5×10^{-8} - 1×10^{-5}	$y = 2 \times 10^{8} x$	0.9959	0.84
Maltohextaose	5×10^{-8} - 1×10^{-5}	$y = 2 \times 10^{8} x$	0.9958	0.76
Maltoheptaose	5×10^{-8} - 1×10^{-5}	$y = 2 \times 10^{8} x$	0.9892	0.61

In that case the total concentration of each type of saccharide (with DP number 0 to ∞) could be known by simply taking the summed areas of all saccharide peaks (even not resolved ones) and comparison versus the calibration line of a single standard. Besides, the DP numbers involved in a hump like elution, representing many unseparated polymers, could be evaluated by dividing the peak area of the hump like peak by the peak area of an internal standard.

However, from the results obtained, which are summarised in Table 6.3 and Table 6.4, it cannot be concluded that the response of each oligosaccharide is the same. This is rather strange and intensive experimental work is needed to study this further.

Two opposite effects seem to control the response factors. Firstly, it is known that the derivatisation efficiency decreases upon increasing chain length. This is not surprising considering the increasing steric hindrance of the saccharide chain lowering the accessibility for the derivatising agent. This can clearly be seen in the RRF values listed in Table 6.4.

The second effect that appears to control the RRF values can be deduced from Table 6.3. The borate buffer that has been used in this case is, as already mentioned, enhancing the sensitivity of the saccharides by complexation. For this reason the values in Table 6.3 are larger than 1. This enhancement seems, unfortunately, not to be constant.

Hence, it can be concluded that it will be difficult to obtain RRF values close to 1 with the borate buffer. It could be possible to obtained better values with the phosphate buffer, if the derivatisation procedure can be improved, e.g. by using higher amounts of the derivatising reagents, etc. However, the expensive fluorescence reagent hampered this study.

6.4 Conclusion

Calibration curves for maltooligomers with a DP from 0 to 6 were linear in a concentration range varying over three to four orders of magnitude using both an alkaline borate buffer and an acidic phosphate buffer. It was observed that borate

complexation increases the detection sensitivity of the analytes. Analysis of the independent DP chain lengths is feasible given the standard is available. Quantification of each saccharide in a given mixture by comparison with a single standard is erratic and further research is required.

References

[1] T. Soga and D. N. Heiger, *Anal. Biochem*. 261, **1998**, 73

[2] C. Huber and E. Grill, P. Oefner, O. Bobleter, *Fresenius J. Anal. Chem*. 348, **1994**, 825

[3] A. Rydlund and O. Dahlman, *J. Chromatogr. A* 738, **1996**, 129

[4] O. Dahlman, A. Jacobs, A. Liljenberg and A. I. Olsson, *J. Chromatogr. A* 891, **2000**, 157

[5] S. Suzuki and S. Honda, *Electrophoresis* 19, **1998**, 2539

[6] F. A. Chen and R. A. Evangelista, *Anal. Chem.* 230, **1995**, 273

[7] M. G. Oshea, M. S. Samuel, C. M. Konik and M. K. Morell, *Carbohydr. Res*. 307, **1998**, 1

[8] S. Hofstetter-Kuhn, A. Pulaus, E. Gassmann and H. M. Widmer, *Anal. Chem*. 63, **1991**, 1541

Chapter 7

CE Analysis of a High Molecular Weight Reducing Neutral Polysaccharide

Abstract

Amylose, a neutral reducing polysaccharide, was separated after APTS derivatisation in a bare fused silica capillary either with the alkaline borate buffer (pH 10.2) at normal polarity or with the acidic phosphate buffer (pH 2.2) at reversed polarity. Linear polyacrylamide coated capillaries with gel free buffer (tris-borate buffer, pH 8.65) or a gel buffer system (tris-citrate mixed with linear polyacrylamide gel, pH 3.0) were used.

7.1 Introduction

To obtain good separation of neutral polysaccharides with a high degree of polymerisation (DP) and a broad distribution in chain lengths, several prerequisites should be met. High resolving power is essential in the electromigration process of high molecular weight polysaccharides. Sufficient difference in the charge to mass ratio between the chains is critical. Sensitive detection is necessary to detect the high DP polymers because of the low amount of sample load in CE resulting in extremely small amounts of these high mass polymers.

Neutral polysaccharides are not electrically charged unless strong alkaline conditions leading to the ionisation of hydroxyl groups are used. Baldwin and his coworkers described separation profiles of dextran with different average molecular weight (MW), namely 1500, 6000, 9300 and 18300, in a bare fused silica capillary by using 200 mM sodium hydroxide buffer [1]. Electrochemical detection (ECD) with a Cu-electrode was applied. The EOF was reversed through addition of the positively charged surfactant cetyltrimethylammonium bromide (CTAB). The saccharides thus moved towards the anode. This approach, however, turned out to give poor DP separation even for dextran with average MW 1500 (DP < 10).

Using a pre-column derivatisation approach (Chapter 3), a drastic improvement of DP separation was reached as reported by the group of Novotny [2, 3]. After labelling dextran and amylose with the fluorescence reagent 8-aminonaphthalene-1,3,6-trisulfonate (ANTS, Table 3.2, tag xvi) and detection by laser induced fluorescence (LIFD), separations up to DP 70 were obtained in a linear polyacrylamide coated capillary with a tris-borate gel free buffer system. The separation of amylose with DP>30 in an untreated bare fused silica capillary with an acidic pH buffer (pH 2.5) after labelling with 9-aminopyrene-1,4,6-trisulfonic acid (APTS, Table 3.2, tag xvii) was reported by Soini and Novotny [4].

It is particularly important to choose a suitable tag in order to impart high charge contents to the neutral polysaccharides. Both ANTS and APTS contain three negatively charged sulfonic groups and thus contribute to a relatively high charge density on the derivatised polysaccharides.

The aim of this part was to reach a DP separation as high as possible of amylose by CE. The structure of amylose was illustrated in Chapter 2 (2.4.2).

7.2 Experimental

7.2.1 Chemicals

9-Aminopyrene-1,4,6-trisulfonate (APTS) was obtained from Lambda Fluoreszenztechnologie (Graz, Austria). Amylose (from potato, type III), sodium cyanoborohydride, citric acid, borax, (γ-methacryloxypropyl)trimethoxysilane, ammonium persulfate and N,N,N',N'–tetramethylethylenediamine (TEMED) were obtained from Sigma-Aldrich (Steinheim, Germany). HPLC grade tetrahydrofuran (THF) was from Lab Scan Ltd. (Dublin, Ireland). Ortho-phosphoric acid and acrylamide were purchased from Merck (Darmstadt, Germany). Acetic acid was obtained from Panreac (Barcelona, Spain). Tris-(hydroxymethyl)aminomethane (tris) was from Acros Organics (Geel, Belgium). Sodium hydroxide was obtained from UCB (Leuven, Belgium) and HPLC grade dichloromethane from Alltech (Lokeren, Belgium). Methanol was purchased from Biosolve Ltd (Valkenswaard, The Netherlands). Linear polyacrylamide (LPAA) (MW 700,000-1,000,000, 10 % aqueous solution) was from Polyscience Inc. (Warrington, PA, USA). Water used in all experiments was produced by a Milli-Q water purification system (Millipore, Bedford, MA, USA).

7.2.2 Derivatisation procedure

1 mg amylose was mixed with 15 µL of APTS (38 mM in 15% acetic acid) followed by the addition of 2 µL of sodium cyanoborohydride (1M in THF). Since

this was a qualitative analysis, no excess of reagent was required. The reaction mixture was heated at 95 °C for 3 hours and then diluted to 4.5 mL with water prior to injection.

7.2.3 Capillary coating

The coating procedure was performed according to Stefansson [5], which is a slightly modified version of the Hjertén method [6]. A new capillary was treated with 0.1 M NaOH for 1 hour and then rinsed with water and methanol for 30 minutes. Next, (γ-methacryloxypropyl)trimethoxysilane (10 µL/mL dissolved in dichloromethane containing 0.02 M acetic acid) was coupled to the silica wall during a 60 minute treatment performed under nitrogen pressure. The capillary was then rinsed with methanol and water for 30 minutes. A 4 % (w/w) acrylamide solution, containing 1 µL/mL N,N,N',N'– tetramethylethylenediamine (TEMED) and 1 mg/mL ammonium persulfate, was then passed through the capillary under nitrogen pressure for 30 minutes. Finally, the capillary was rinsed with water and dried under a stream of nitrogen.

7.2.4 CE instrumentation

The employed CE instrument was a P/ACE 2100 CE equipped with laser induced fluorescence detector (3-mW 488 nm argon-ion laser module from Beckman Instruments, Inc. (Fullerton, CA, USA). Bare fused silica capillaries with 50 µm and 75 µm i.d. (50 cm to the detector window) were obtained from Composite Metal Services Ltd (Worcester, UK). New fused silica capillaries were rinsed with 1.0 M sodium hydroxide solution for 15 minutes and water for 10 minutes prior to

use. Between runs, capillaries were washed with 1.0 M sodium hydroxide solution for 2 minutes and with the run buffer for 4 minutes, respectively. The coated capillary was flushed with the run buffer for 10 minutes before the first run and was conditioned with the run buffer between each run. Detection was performed with LIFD at λ_{exc} = 488 nm and λ_{em} = 520 ± 20 nm.

7.3 Results and discussion

7.3.1 Separation of amylose under acidic CE conditions

Figure 7.1 shows the amylose profile obtained with the phosphate buffer (pH 2.2) in the reversed polarity mode on a bare fused silica capillary. Under these conditions, migration depends only on the electrophoretic mobility and thus on the charge density because the EOF is negligible at such a low pH. The peaks eluting in front of glucose (DP 0) come from APTS residues in the mixture. Polymer chain lengths with a DP up to 60 were separated. The charge to mass ratio decreases with increasing molecular weight because the amount of charges received from the tag is constant (three charges) for every polymer chain. The resolution depends on the differences of charge to mass ratio. After DP 60, the baseline is recovered only after 200 minutes (Figure 7.1, insert). This means that many unseparated chains with DP higher than 60 are present.

Hence, the separation of neutral polysaccharides under these conditions depends mainly on the magnitude of the charge to mass ratio and the difference of the charge to mass ratio of the polymer chains.

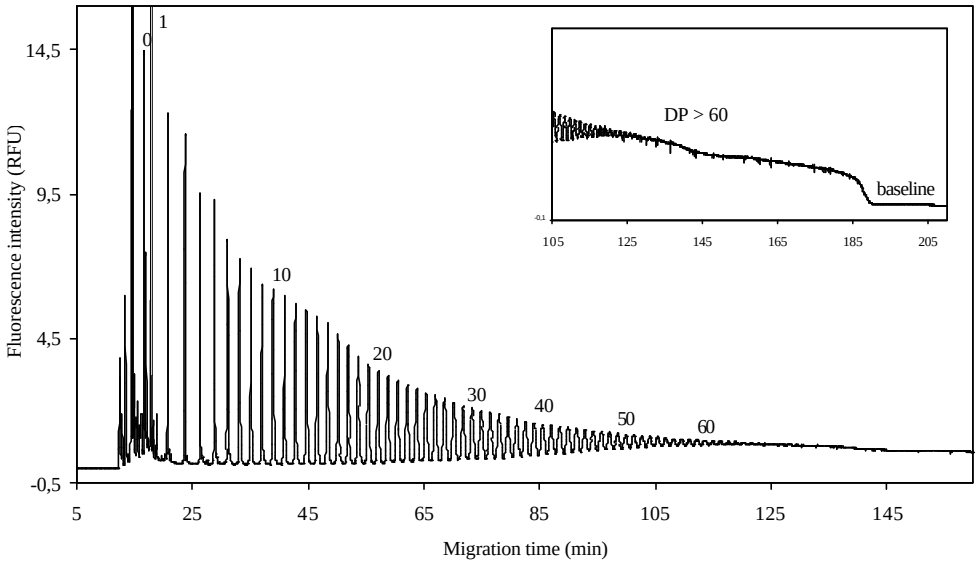

Figure 7.1 ***Separation profile of amylose-APTS with acidic phosphate buffer in the reversed polarity mode***

Peak: The number indicates the DP, 0 = DP 0 (glucose), 1 = DP 1 (maltose), etc.
CE conditions: 75 µm i.d. and 57 cm in length (50 cm to the detector window) bare fused silica, voltage -10 kV, 20 °C, 10 s injection at 0.5 psi, 160 mM phosphate, pH 2.2.

7.3.2 Separation of amylose under alkaline CE conditions

Using the alkaline borate buffer in the normal polarity mode, amylose is completely eluted in a relatively short time on a bare fused silica capillary (Figure 7.2) since the major driving force is the EOF which is high in the alkaline buffer (pH 10.2). As explained in Chapter 5 (5.3.2), the migration order of the polymers with alkaline borate buffer is opposite to that with the phosphate buffer.

The first eluting hump-like peak indicated by the arrow represents the contents of the high DP chains. The use of borate buffer imparts higher fluorescence

absorbance (Chapter 6, Figure 6.3). The main advantage of using the borate buffer is that it offers more information about the high DP chain lengths than a phosphate buffer.

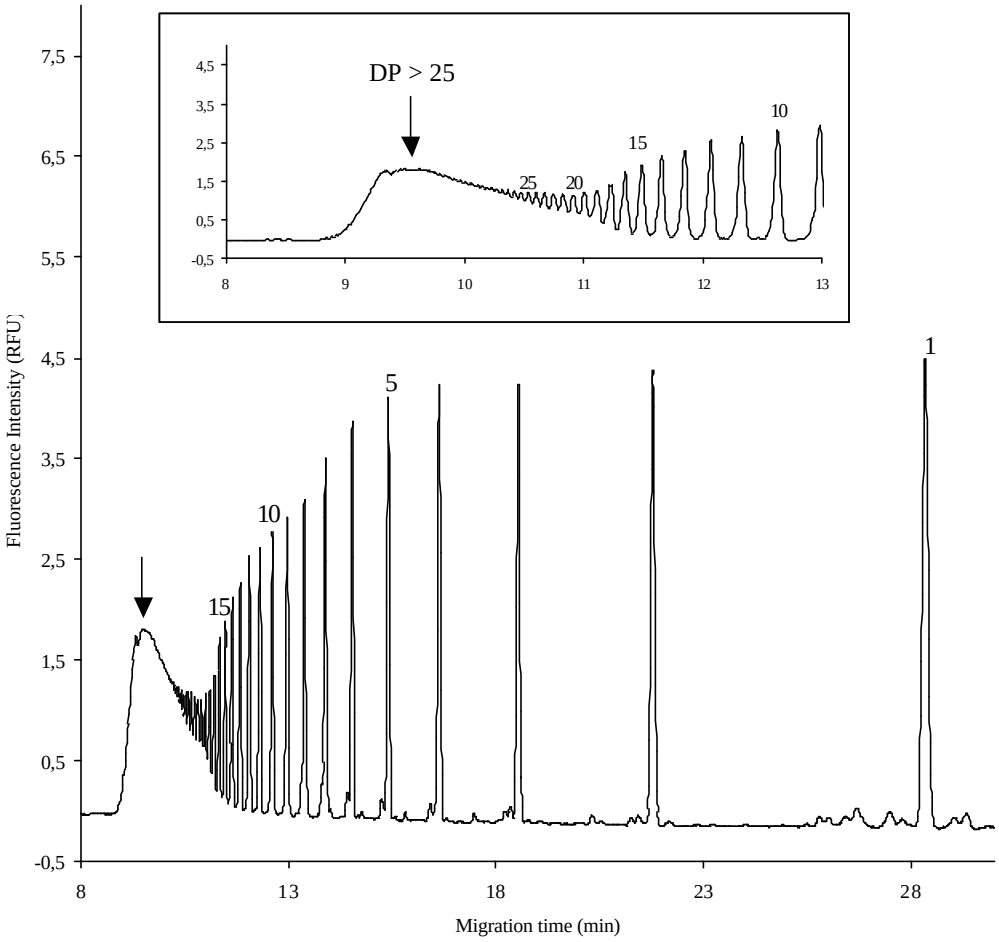

Figure 7.2 ***Separation profile of amylose-APTS with the alkaline borate buffer in the normal polarity mode***

Peaks: The number indicates the DP, 1 = DP 1 (maltose), 5 = DP 5 (maltohexaose), etc.
CE conditions: 50 µm i.d. and 57 cm in length (50 cm to the detector window) bare fused silica, voltage +15 kV, 20 °C, 4 s injection at 0.5 psi, 100 mM borate buffer, pH 10.2.

As extensively discussed in the precedent chapter, further investigation on the derivatisation procedure is required such as to obtain the same relative response factors (RRF) for each DP number of the chain. If this could be obtained, the technique could be used to quantify even the amount of unresolved peaks.

Under these conditions, only polymer chains with a relatively low DP (< 25) are separated (Figure 7.2, insert). DP differentiation under these conditions is thus much smaller compared to the acidic buffer (see Figure 7.1). This was also shown in Chapter 6 (Table 6.1 and Table 6.2).

Alkaline conditions contribute to high resolution for the oligomers with DP 0, DP 1, and DP 2, but resolution is reduced rapidly and the resolution for DP 5/DP 6 is only 2.20. On the other hand, the resolution of DP 5/DP 6 is 4.37 under acidic phosphate conditions.

Hence, acidic conditions have the advantage to separate polymer chains with higher DP than alkaline conditions, whereas the alkaline conditions offer more sensitivity for the high DP polymer chains.

7.3.3 Separation of amylose in a coated capillary with gel free buffer

In a linear polyacrylamide coated capillary, negatively charged polysaccharide derivatives move towards the anode only by their electrophoretic mobility because the silanol groups that generate the EOF are shielded by the coating layer. Figure 7.3 shows the separation profile of amylose-APTS derivatives on the coated capillary with a mild pH buffer.

Under these conditions, the polymer chains of amylose-APTS are resolved up to a DP of 30. Stefansson and coworkers reported [5] that a polyacrylamide coated

capillary and a gel free buffer gives fast separation of amylose-ANTS derivatives, but it was impossible to resolve saccharides with a high DP. This is confirmed by our experiments.

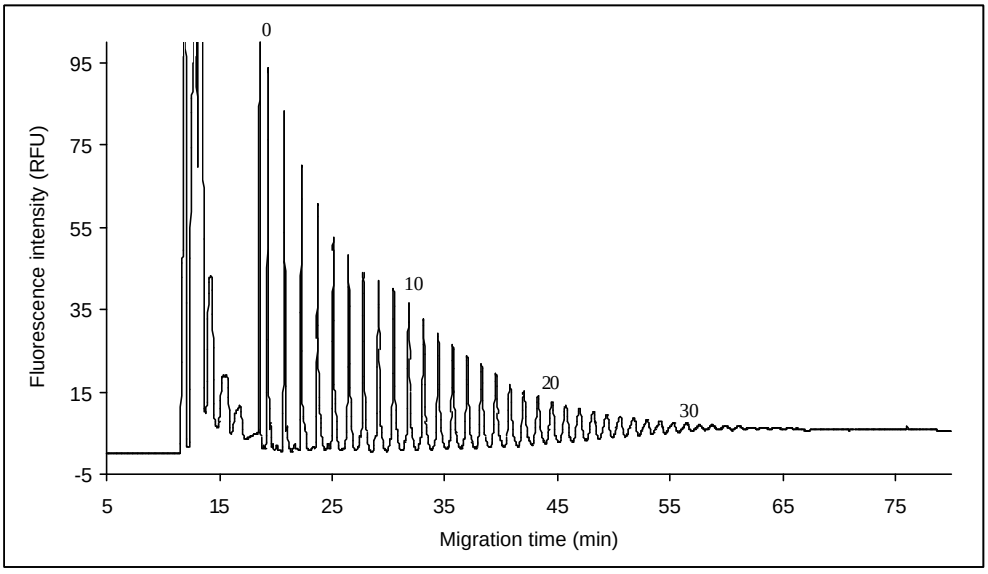

Figure 7.3 ***Separation profile of amylose-APTS on a coated capillary***

Peaks: The number indicates the DP number of the polymer chains
CE conditions: 75 µm i.d × 57 cm (50 cm to the detector) linear polyacrylamide coated capillary, 100 mM tris-borate buffer, pH 8.65, voltage - 20 kV, 20 °C, 20 s injection at 0.5 psi. pressure.

7.3.4 Separation of amylose with a linear polyacrylamide gel buffer (CGE)

By introducing a linear polyacrylamide (LPAA) gel in the coated capillary, a significant improvement in the elution of DP numbers could be achieved. The separation of hyaluronic acid (HA) up to DPs ≈190 was demonstrated by Hong *et al.* [8]. The separated DP numbers for the neutral polysaccharides obtained with a gel system (Figure 7.4) are slightly less than those obtained with CZE and the

fluorescence absorbance is lower. It should be noted that the sample batches were different for Figure 7.1 and Figure 7.4. Using CZE, the derivatives for Figure 7.4 gave a separation with DP > 80 (data not shown). Applying CGE, less DP numbers were observed (DP $\leq$ 80) and the analysis time was longer (Figure 7.4) compared to CZE, presumably due to an increase of the buffer viscosity.

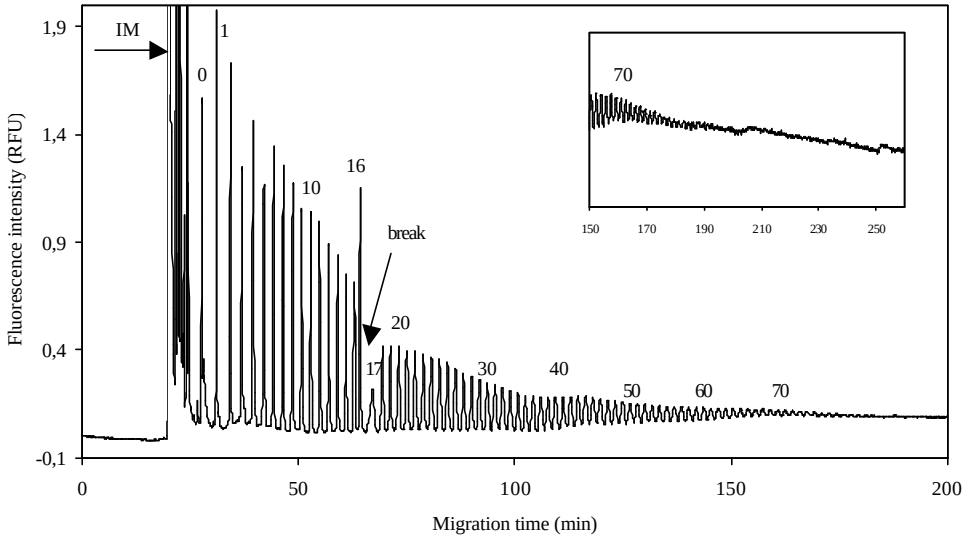

Figure 7.4 ***Separation profile of amylose-APTS on a coated capillary with gel buffer***

Peaks: see Figure 7.3.
CE conditions: 75 µm i.d × 57 cm (50 cm to the detector) linear polyacrylamide coated capillary, buffer, 25 mM citric acid and 12.5 mM tris in 5% LPAA (10 % of an aqueous solution, of linear polyacrylamide, MW 700,000 – 1,000,000), pH 3.0, voltage -10 kV, 10 s injection at 0.5 psi, 20 °C.

However, the gel buffer slightly increases the resolution due to the polymeric sieving medium [8]. This was beneficial to the very high DP numbers of the negatively charged polysaccharides which possess an inherently lower charge density difference than low DP numbers.

The reason of the migration break at DP 16 to DP 17, as the arrow indicates in Figure 7.4, is not clear yet. An important reproducible phenomenon is the sharpening and broadening of DP 16 and DP 17, respectively. This forms the subject of an independent study because this occurs frequently in CGE.

7.4 Conclusion

Good separation of neutral polysaccharides derivatised with APTS could be obtained in bare fused silica capillaries. Acidic conditions offer the advantage of reaching high DP separation while alkaline conditions give more information about the total high DP content. From these results it can be concluded that the use of a coated capillary with either a gel free buffer system or a gel buffer system does not substantially improve the high DP separation of neutral polysaccharides.

References

[1] W. Zhou and R. P. Baldwin, *Electrophoresis* 17, **1996**, 319

[2] J. Chemelík, J. Chmelíková and M. V. Novotny, *J. Chromatogr. A* 790, **1997**, 93

[3] M. Stefansson and M. Novotny, *Carbohydr. Res.* 258, **1994**, 1

[4] H. A. Soini and M. V. Novotny, *Proc. 20 th, Int. Symp. Capillary Chromatography*, Riva Del Garda, keynote lecture, May 25-29, **1998**

[5] M. Stefansson and M. Novotny, *Anal. Chem.* 66, **1994**, 1134

[6] S. Hjertén, *J. Chromatogr.* 347, **1985**, 191

[7] S. Hofstetter-Kuhn, A. Pulaus, E. Gassmann and H. M. Widmer, *Anal. Chem*. 63, **1991**, 1541

[8] M. Hong, J. Sudor, M. Stefansson and M. Novotny, *Anal. Chem.* 70, **1998**, 568

Chapter 8

CE Analysis of High Molecular Weight Non-reducing Neutral Polysaccharides

Abstract

Inulin, a non-reducing polysaccharide, was taken as a model compound for the separation by capillary electrophoresis (CE) with laser induced fluorescence detection (LIFD). Derivatisation was performed with fluorescein isothiocyanate (FITC). High separation efficiency in an acceptable analysis time was obtained on a polyacrylamide (PAA) coated capillary. More than one hydroxyl group of the sugar reacted with the derivatisation reagent, leading to more than one peak per polymer. However, the degree of polymerisation (DP) could be elucidated and DP profiling of inulin after enzymatic degradation became feasible.

8.1 Introduction

Fructose based oligo- and polysaccharides are low caloric sweeteners that also exhibit a number of dietary fiber-like effects. They stimulate the growth of colonic Bifidobacteria, a family of bacteria considered to be highly beneficial for human health [1]. Inulin and inulin hydrolysates are potentially of medical interest because of their anti-tumor activity. It is believed that inulin plays an important role in anti-tumor defense [2].

Inulin has a linear molecular structure with β (2→1) fructosyl-fru linkages (G-F-(F)n) [3], where n is the degree of polymerisation (DP) (Figure 8.1). When n is zero (GF), we have sucrose. When n is 1, the oligosaccharide is named 1-kestose or kestotriose (GFF_1), 1,1-kestotetraose (GFF_2) when n is 2, 1,1,1-kestopentaose (GFF_4) when n is 3, and so on.

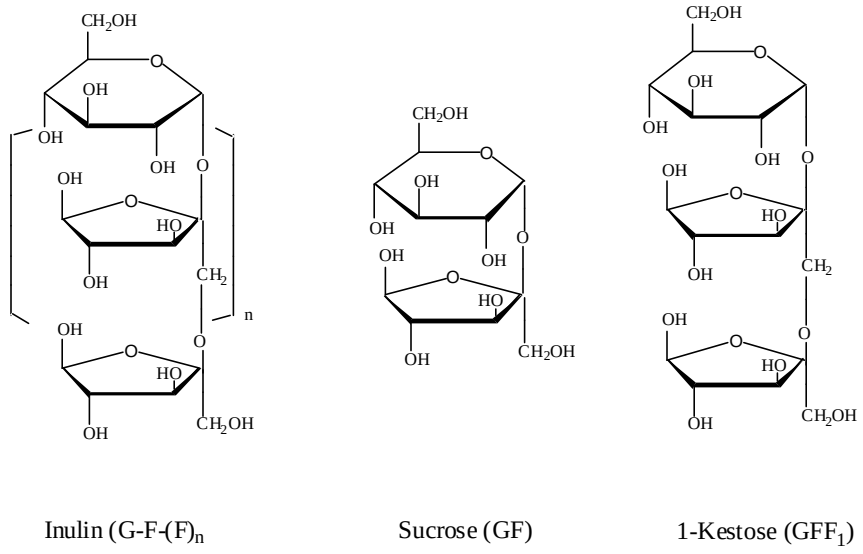

Figure 8.1 ***Structure of inulin, sucrose and 1-kestose***

Inulin is commonly analysed by high performance liquid chromatography (HPLC) [4-6]. Anion exchange chromatography (AEC) with pulsed amperometric detection (PAD) is the most effective technique to separate inulin up to chain lengths of 50 [7, 8].

Capillary electrophoresis (CE) with laser induced fluorescence detection (LIFD) is a powerful technique for the separation of saccharides as demonstrated in recent years [9,10]. The success of the separation strongly depends on the appropriate

choice of derivatising reagent as outlined in Chapter 3. Most of the fluorescence tags (Chapter 3, Table 3.1 and 3.2), however, only react with saccharides containing aldehyde groups, i.e. aldoses such as glucose, amylose, etc. Ketoses, like fructose, have a very low reactivity for amination with those reagents (see Chapter 4). Consequently, inulin, the polymer of ketose (Figure 8.1) can not be properly labelled with these tags.

Inulin can be labelled with fluorescein isothiocyanate (FITC) *via* its hydroxyl groups (Figure 8.2). FITC is a well known derivatisation reagent for the analysis of amino acids [11] and efficiently introduces fluorescence groups in most structures lacking chromophoric compounds. Moreover, at appropriate pH, the carboxylic function of FITC contributes to the electrophoretic characteristics of the derivatised solutes. This part presents the successful profiling of inulin and derived samples *via* FITC derivatisation and CE-LIFD analysis.

8.2 Experimental

8.2.1 Chemicals

Tris(hydroxymethyl)-aminomethane (tris) was obtained from Merck (Darmstadt, Germany) and borate from Pleuger (Wijnegem, Belgium). Fluorescein isothiocyanate (FITC), commercial inulin-FITC derivative, sucrose (GF), boric acid and sodium hydroxide were from Sigma (Steinheim, Germany). Pyridin was from UCB (Leuven, Belgium), dibutyltin dilaurate from Fluka (Steinheim, Germany), ethanol from Chem-Lab (Lichtervelde, Belgium), dimethyl sulfoxide (DMSO) from Riedel-de Haën (Seelze, Germany) and ethyl acetate from Ferak (Berlin, Germany). Water was obtained from a Milli-Q water purification system

(Millipore, Bedford, MA, USA). The fructooligosaccharides GFF1, GFF2 and GFF3 standards were obtained from Megazyme (Bray, Ireland). The inulin samples (HP, LS and ST) were kindly donated by the Tiense Suiker Raffinaderij (Tienen, Belgium).

8.2.2 CE-LIFD

CE separations were performed on a P/ACE 2100 system equipped with a laser induced fluorescence system (3 mW 488 nm argon laser) from Beckman (Fullerton, CA, USA). A polyacrylamide (PAA) coated capillary was purchased from Beckman. The bare fused silica capillary was from Composite Metal Services Ltd (Worcester, UK). The running buffer was 120 mM boric acid adjusted with tris (500 mM) to pH 7.4 or a 100 mM borate buffer adjusted to pH 10.2 with sodium hydroxide. The coated capillary was conditioned with running buffer for 10 minutes before the first run and for 3 minutes prior to each injection. The bare fused silica capillary was rinsed with 1 M sodium hydroxide for 15 minutes and with water for 5 minutes before the first injection. Between runs, the capillary was conditioned using 1 M sodium hydroxide solution for 2 minutes and then with run buffer for 4 minutes. Detection was performed at an excitation wavelength of 488 nm and an emission wavelength of 520 ± 20 nm. The separations were performed with the following conditions:

1. Bare fused silica capillary with 50 µm i.d. × 57 cm in length (50 cm to the detector window), 100 mM borate buffer (pH 10.2), voltage +10 kV, temperature 20 °C, injection 4 s at 0.5 psi pressure.

2. PAA coated capillary with 50 µm i.d. × 57 cm in length (50 cm to the detector window), 120 mM tris-borate buffer with pH 7.4, voltage –30 kV, temperature 20 °C, injection 4 s at 0.5 psi pressure.

8.2.3 Derivatisation procedure

The derivatisation was performed according to the method described by de Belder and Granath [12] with minor modifications. 10 mg of inulin sample was dissolved in 0.1 mL of DMSO containing 1 mg of FITC and 0.05 mL of pyridine. 0.05 mL of dibutyltin dilaurate was added to the mixture which was then heated at 95 °C for two hours. After heating, the resulting solution was processed in two different ways to remove unreacted FITC, namely the classical way with ethanol precipitation or alternatively by ethyl acetate washing. The derivatised carbohydrates were then diluted 100 times with water prior to injection.

8.3 Results and discussion

8.3.1 Derivatisation

de Belder and Granath [12] reported that FITC reacts with dextran in dimethyl sulphoxide (DMSO) at elevated temperature to give O-(fluoresceinyl-thiocarbamoyl)dextran (FITC-dextran). The reaction is catalysed by dibutyltin dilaurate.

Similarly, inulin forms derivatives with FITC (Figure 8.2) via the hydroxyl groups. The isothiocyanate group can react with any of the hydroxyl groups of a polysaccharide although it is known that primary hydroxyl groups react faster than secondary ones.

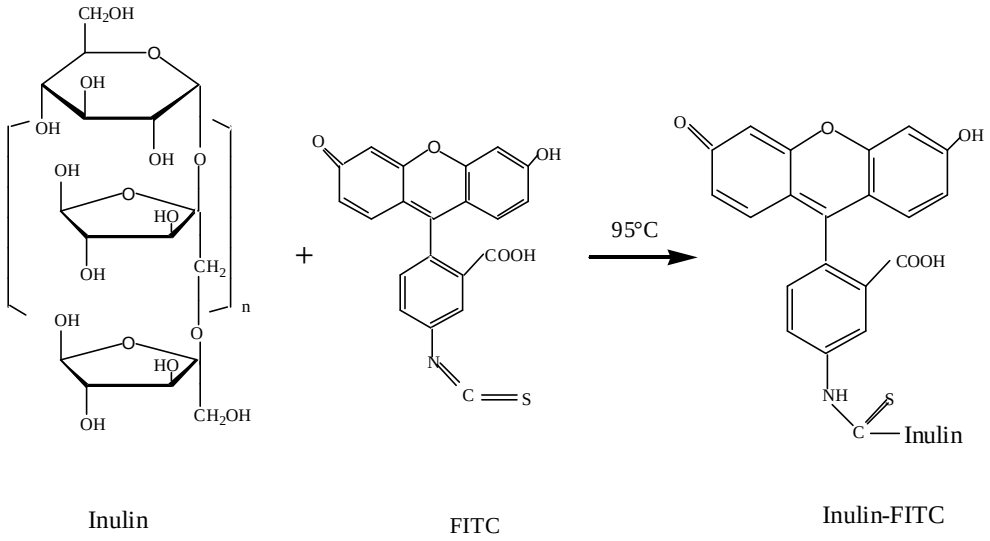

Figure 8.2 ***Reaction of inulin with FITC***

Multiple peaks can be seen in the electropherograms of the derivatives, e.g. in Figure 8.3 B and in the insert. This is a common problem when FITC is used for derivatisation of saccharides. This multiple peak formation could not be avoided, whatever the molar ratio of FITC and inulin was used in the reaction. This was also the case in other studies. For example, multiple tagging also occurs in the derivatisation of myoglobin with FITC because the multiple amino groups are involved in the reaction. This has been illustrated with CE by Banks and Paquette [13].

8.3.2 Separation of commercial inulin-FITC derivative by CE

Inulin-FITC derivative could not be well separated according to DP number on a bare fused silica capillary. Figure 8.3A shows the best separation of a commercial

inulin-FITC derivative on a bare fused silica capillary with the alkaline borate buffer. Under these conditions, the high EOF causes fast elution of the whole inulin content in 12 minutes. Only a series of partly separated peaks representing relatively low DP chains is noted.

In order to increase resolution, a PAA coated capillary was used. The EOF is suppressed by the coating layer and reversed polarity had to be used. Moreover, a wide pH range can be chosen for ionisation of the acidic functions of the derivatives. As a result, very good separation of the chain length distribution of the commercial inulin-FITC derivative was obtained at pH 7.4 with 120 mM tris-borate as shown in Figure 8.3 B.

The minor signals eluting early are reagent impurities. Inulin samples can thus be separated according to distinction of the charge to mass ratio of their FITC derivatives. Multiple peaks are observed and this particularly for the relatively low DP oligomers. Single main peaks appear when the DP became relatively high (Figure 8.3 B, insert). Multiple tagging definitely also occurs for high DP polymers. However, they cannot be separated from the main peaks because of the small differences in electrophoretic mobility. The higher the MW is, the lower is the difference in electrophoretic mobility between the different polymer chains. Combined with an increasing longitudinal diffusion for high DP numbers, this led to a single peak for each high MW polysaccharide.

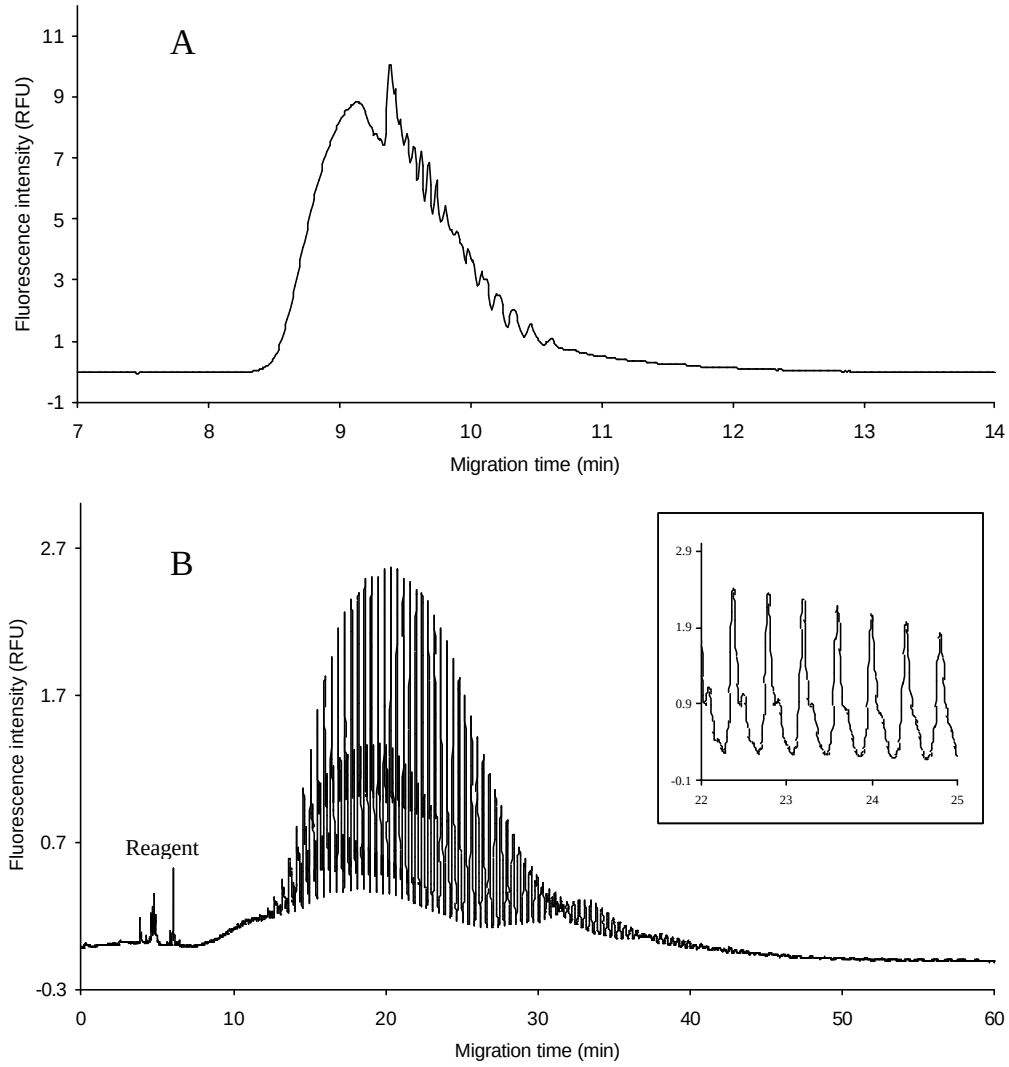

Figure 8.3 ***Electropherograms of commercial inulin-FITC***

CE conditions as described in 8.2.2.
A: condition 1, B: condition 2.

8.3.3 Separation of inulin samples after ethanol washing

Three inulin samples, named HP, LS and ST, were derivatised with FITC and analysed on the PAA coated column. Unreacted FITC was removed by extracting

the reaction mixture with ethanol. As can been seen in Figure 8.4, the separation profiles of these three inulin samples are very similar and only the peak heights are different. LS and ST inulin show lower peak heights than HP inulin.

A series of peaks with low peak height eluting after sucrose and between 8 and 13 minutes, is observed in the profiles of the samples LS and ST but not in the sample HP. They are oligomers with a DP from 0 to about 10. The samples were spiked with sucrose (DP 0) to mark the initial elution of the oligomers.

8.3.4 Separation of inulin samples after ethyl acetate washing

FITC-inulin oligomers with relatively low chain lengths (GF, GFF_1, GFF_2, GFF_3, etc.) were observed to dissolve in ethanol. Consequently, the electropherograms in Figure 8.4 show no significant difference in chain length distribution between the three inulin samples. Instead of ethanol, ethyl acetate was used to extract the reagent residues. The separation profiles of the three inulin samples are displayed in Figure 8.5. LS and ST inulin give profiles that are drastically different from those obtained after ethanol extraction. LS and ST inulin turned out to contain high amounts of oligomers with relatively low DP ranging from 0 to about 10.

This proved that the low DP oligomers were removed during the precipitation process when ethanol was used whereas these oligomers remained in the water solution upon washing with ethyl acetate.

The separation of inulin derivatives obtained by the classical ethanol extraction process [13] did thus not reflect the real content and distribution of the chains of the samples.

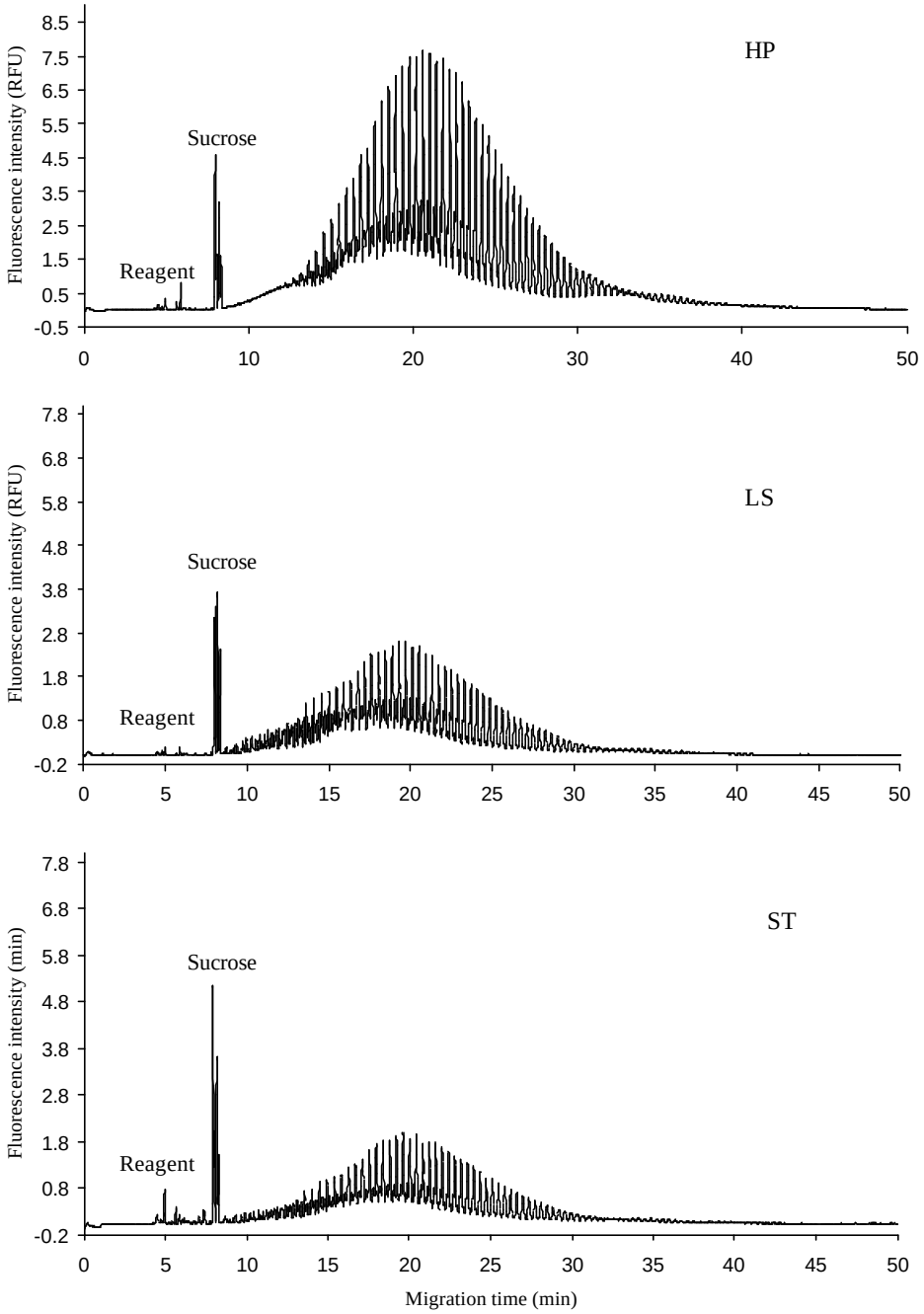

Figure 8.4 ***Separation profiles of inulin-FITC after washing with ethanol***

CE conditions: see section 8.2.2. Condition 2 was applied.

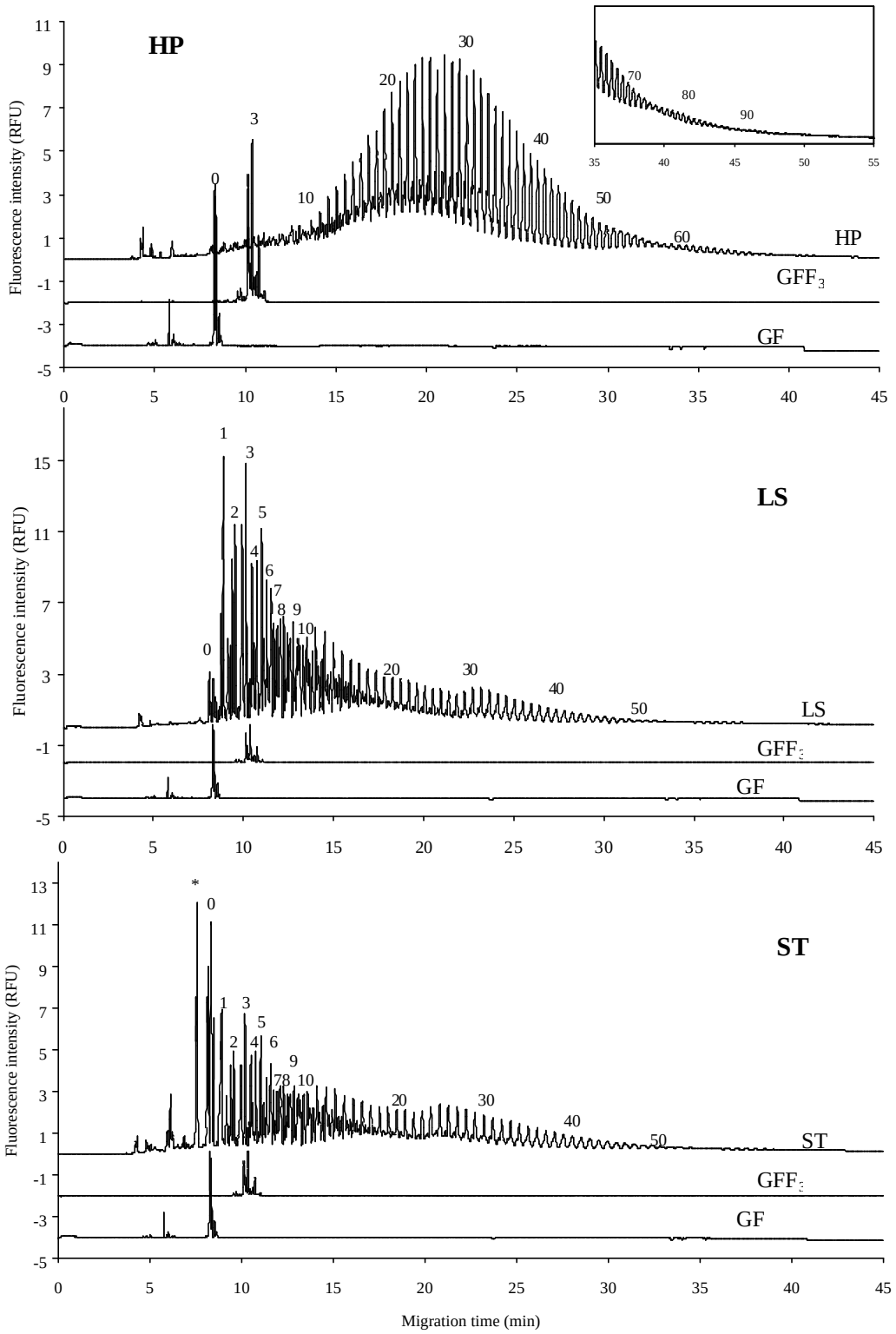

Figure 8.5 ***Separation of inulin-FITC after washing with ethyl acetate***

CE conditions: see section 8.2.2. Condition 2 was applied.

The separation profile of the HP sample after ethyl acetate washing (Figure 8.5 HP) had nearly the same shape as that after ethanol extraction (Figure 8.4 HP). Only some small additional peaks eluting between 8 to 13 minutes, and thus low DP oligomers from 0 to 10, were noted.

The separation profile of HP inulin (Figure 8.5) was obviously different from those of LS and ST but is nearly the same as the commercial inulin-FITC (Figure 8.3 B). Indeed after the experiments we have been informed that the HP sample was pure inulin, whereas LS and ST were enzymatic degradation products.

Elucidation of the DP numbers was established by using some commercial available oligomers, namely GF (DP 0), GFF_1 (DP 1), GFF_2 (DP 2) and GFF_3 (DP 3). HP inulin was separated up to DP 90 (Figure 8.5 HP, insert).

Degraded inulins, namely LS and ST, both contained high amounts of low DP oligomers from 0 to about 10 compared to HP inulin, as illustrated in Figure 8.5. Differences between the profiles of LS and ST inulin were observed by comparing the peak heights. In the profile of LS inulin, a relatively low peak height is noted for GF (DP 0) and the highest peak is GFF_1 (DP 1), whereas the highest peak height in the profile of ST inulin is GF (DP 0). The peak in front of sucrose (DP 0), indicated with an asterisk in Figure 8.5 ST, is an unknown impurity probably originating from the hydrolysis. Therefore, it can be assumed that LS and ST inulin samples are produced by different degradation procedures.

Hence, upon evaluation of CE profiles prepared after ethyl acetate washing instead of ethanol precipitation, it is possible to differentiate inulin samples obtained after different enzymatic treatments.

8.4 Conclusion

Characterisation between different inulin samples could be done by using FITC derivatisation and CE-LIFD even though the derivatisation reaction led to more complex profiles than e.g. APTS derivatisation.

References

[1] H. Hidaka, M. Hirayama and K. Yamada, *J. Carbohydr. Chem.* 10, **1991**, 509

[2] A. Fuchs, *Biochem. Soc. Trans.* 19, **1991**, 555

[3] D. H. Lewis, *New Phytol*. 124, **1993**, 583

[4] W. Praznik and R. H. F. Beck, *J. Chromatogr.* 303, **1984**, 417

[5] P. J. Simms, M. H. Rebecca and K. B. Hicks, *J. Chromatogr. A* 684, **1993**, 131

[6] J. O. Metzger, R. Woisch, W. Tuszynski and R. Angermann, *Fresenius, J. Anal. Chem* . 349, **1994**, 473

[7] J. W. Timmermans, M. B. Van Leeuwen, H. Tournois, D. De Wit and J. F. G. Vliegenthart, *J. Carb. Chem*. 13, **1994**, 881

[8] W. Van Den Ende, Ph. D thesis, "Fructan metabolism in chicory roots (*Cichorium intybus* L.)", **1996**, Catholic University Leuven, Belgium,

[9] S. Suzuki and S. Honda, *Electrophoresis* 19, **1998**, 2539

[10] J. C. M. Waterval, H. Lingeman, A. Buit, and W. J. M. Underberg, *Electrophoresis* 21, **2000**, 4029

[11] S. P. D. Lalljie and P. Sandra, *Chromatographia* 40, **1995**, 513

[12] A. N. de Belder and K. Granath, *Carbohydr. Res*. 30, **1973**, 375

[13] P. R. Banks and D. M. Paquette, *J. Chromatogr. A* 693, **1995**, 145

Chapter 9

CE Analysis of Gums

Abstract

Gums were derivatised with the fluorescence reagent, 9-aminopyrene-1,4,6-trisulfonic acid (APTS) followed by microcentrifuge filtering. The resulting high mass fractions were analysed by capillary electrophoresis (CE) on a polyacrylamide (PAA) coated capillary with laser induced fluorescence detection (LIFD). A wide range of electrolytes was used. The effect of the pH on the electrophoretic mobilities and the peak shapes for the gum constituents was found to be significant. The separation of a mixture of five commercial gums, namely iota carrageenan, kappa carrageenan, alginic acid, xanthan and carboxymethyl cellulose (CMC) was achieved at pH 3.2 with a 25 mM trisodium citrate buffer. A mixture of arabic gum, karaya gum and CMC could be separated at pH 7.8.

9.1 Introduction

Gums represent a largely unexplored source of valuable materials. The structures and the constituents of some important gums, important in relation with e.g. biological activities in drugs, functional properties in foods, etc. have been outlined in Chapter 2 (2.4.4). An analytical technique for their effective characterisation is highly demanded. Because of the compositional and structural

diversity, combined with the high molecular weight (MW) (Chapter 2, Table 2.1 and Table 2.1), it is a great challenge to achieve this goal.

The classical approach is chemical or enzymatic decomposition followed by chromatographic separation of the constituting monosaccharides. Schneider *et al.* [1] used capillary electrophoresis (CE) to analyse several commercial thickeners, including arabic gum, pectin, sodium alginate, tragacanth gum and xanthan gum, after hydrolysing the gums with sulfuric acid and tagging the monosaccharides with 9-aminopyrene-1,4,6-trisulfonate (APTS). A poly(methyl methacrylate) capillary was used because of its stability in a highly alkaline buffer system. The identification and quantification of gums based on their basic constituents, however, has limited application. For example, acid hydrolysis of a mixture of the galactomannans in guar gum and locust bean gum (LBG) will yield mannose, galactose and arabinose. Because there is a rather large variability in the ratio of mannose to galactose in locust bean gum (LBG), quantification of LBG in a mixture with guar gum will be erratic [2].

Although capillary electrophoresis allows separation of polysaccharides with a high degree of polymerisation (DP) (see Chapter 7 and 8), full separation of the chain lengths in gums is not yet possible. This is due to the extremely high molecular weight (MW) (Chapter 7), the compositional heterogeneity and the poor electrophoretic properties of gums. For example, carboxymethyl cellulose (CMC), both native and enzymatically decomposed, can only be partially resolved on a linear polyacrylamide coated capillary by using buffer additives [3] or by applying 18% instacryl gel [4]. Partially hydrolysed kappa-carrageenan was studied by Sudor and co-workers [5] using both gel and gel free buffers and

separation was only achieved to approximately 30 DP. The majority of solutes, appeared as a hump-like peak, indicating that the separation of chain lengths was far from complete.

Alternatively, the analysis of polysaccharides as a single peak by CE, regardless their chain length distribution and compositional heterogeneity, became an interesting approach in recent years for the characterisation of polysaccharides. Brewster and Fishman [6] reported that amylose and amylopectin could be resolved in 10 minutes by using iodine containing buffers in an unmodified capillary column. Iodine imparted charges and allowed UV-detection at 560 nm. Derivatisation steps were avoided in this method but the sensitivity was low.

Another example of the intact separation by CE was contributed by Zhong *et al.* [7] through the analysis of large pectin molecules (DP 200-1000). The separation of pectins with different degree of esterification (DE) was performed simply in a bare fused silica capillary with phosphate buffer (pH 7.0). The migration time was a function of the DE, and a linear relationship was found between the pectin charge and the mobility. The separation was achieved in less than 20 minutes and derivatisation was not necessary. The relatively high limit of detection (LOD) of 0.5 mg/ml of this method was due to the low UV absorption coefficient of the solutes. Calibration was difficult because of lack of pectin standards with different DE.

Recently, the three types of carrageenan, namely iota, kappa and lambda carrageenan, were separated as intact peaks by CE [8]. Carrageenan was derivatised with APTS and then fractionated using microcentrifuge filters. The high MW fractions of carrageenan-APTS (retentates) were separated in a bare

fused silica capillary and detected with LIFD. The separation of iota and kappa carrageenan was achieved in 5 minutes by setting the analysis temperature at 50 °C. Lambda carrageenan, although not baseline resolved from kappa- and iota-carrageenan, could be clearly identified through its migration time and specific peak shape.

The aim of this work was to analyse a series of gums of commercial interest as single peaks on a polyacrylamide (PAA) coated capillary by CE-LIFD.

9.2 Experimental

9.2.1 Chemicals

All the commercial gums, citric acid, trisodium citrate and sodium cyanoborohydride were obtained from Sigma-Aldrich (Steinheim, Germany). Carrageenan samples were kindly provided by Rhodia, Centre de Recherches d'Aubervilliers (France). Natural and synthetic guar samples were from Quest International (Naarden, The Netherlands). 9-Aminopyrene-1,4,6-trisulfonate (APTS) was from Lambda Fluoreszenztechnologie (Graz, Austria). HPLC grade tetrahydrofuran (THF) was from Lab-Scan Ltd. (Dublin, Ireland). Acetic acid and sodium hydroxide were obtained from Panreac (Barcelona, Spain). The water used through the experiments was produced by a Milli-Q purification system (Millipore, Bedford, MA, USA).

9.2.2 Sample preparation

1 mg gum was mixed with 15 µL APTS (38 mM in 15% acetic acid) and 4 µL of sodium cyanborohydride (1 M in THF). The mixture was then heated at 95 °C for

3 hours. After heating, the mixture was diluted with Milli-Q water to 2 mL. For each sample, 60 µL of the diluted solutions was then transferred in the micro-concentrators (Millipore, Bedford, MA, USA) with 3×10^4 molecular mass cut-off filters followed by addition of 300 µL of Milli-Q water. The micro-concentrators were used for all samples unless indicated otherwise. Centrifugation was performed for 20 minutes at 6000 rpm and repeated twice after addition of 300 µL of Milli-Q water. The retentates were then collected by inversing the micro-concentrators and performing centrifugation at 4000 rpm for 5 minutes. Finally, 60 µL of Milli-Q water was added to dilute the retentates.

9.2.3 CE procedures

All experiments were carried out on a P/ACE 2100 CE system equipped with laser induced fluorescence (LIF) detection (3 mW 488 nm argon laser from Beckman Fullerton, CA, USA) at 488 nm excitation wavelength and 520 ± 20 nm emission wavelength.

A polyacrylamide (PAA) coated capillary with 50 µm i.d. × 40 cm effective length (Beckman, Fullerton, CA, USA) or a bare fused silica capillary with 50 µm i.d. × 50 cm effective length (Composite Metal Service, Worcester, UK) were used. Between runs, capillaries were conditioned by rinsing with Milli-Q water for 2 minutes, and then with run buffer for 4 minutes. 25 mM trisodium citrate buffers were adjusted to different pHs by using 1 M citric acid. Sodium hydroxide was used to adjust 25 mM trisodium citrate to pH 7.8.

The separations were carried out at a voltage of -30 kV (anode outlet) and at a temperature of 30 °C. Electrokinetic injection was applied because it provided

much higher sensitivity than pressure injection for the APTS-derivatised carrageenans [8].

9.3 Results and discussion

9.3.1 Separation of carrageenans

9.3.1.1 Separation without fractionation

The structures of the three types of carrageenan are depicted in Figure 2.6 (Chapter 2). These three forms differ discretely in their charges and are therefore amenable to electrophoretic separation. The three types of the carrageenan are negatively charged across a broad pH range (pH >1) [8] due to the strong acidic nature of the sulfate groups and should therefore migrate towards the anode under a condition of low electroosmotic flow (EOF).

The separations of kappa and iota carrageenan-APTS derivatives before centrifugation are shown in Figure 9.1. As can be seen, interference from the derivatising reagent strongly complicates the recognition of the analytes of interest. This is especially the case for iota carrageenan that contains a high native charge density with a migration time of less than 4.5 minutes. Kappa carrageenan, although showing a profile different from iota, could be separated only as a broad peak accompanied by some small peaks, as the arrow indicates in Figure 9.1 Kappa.

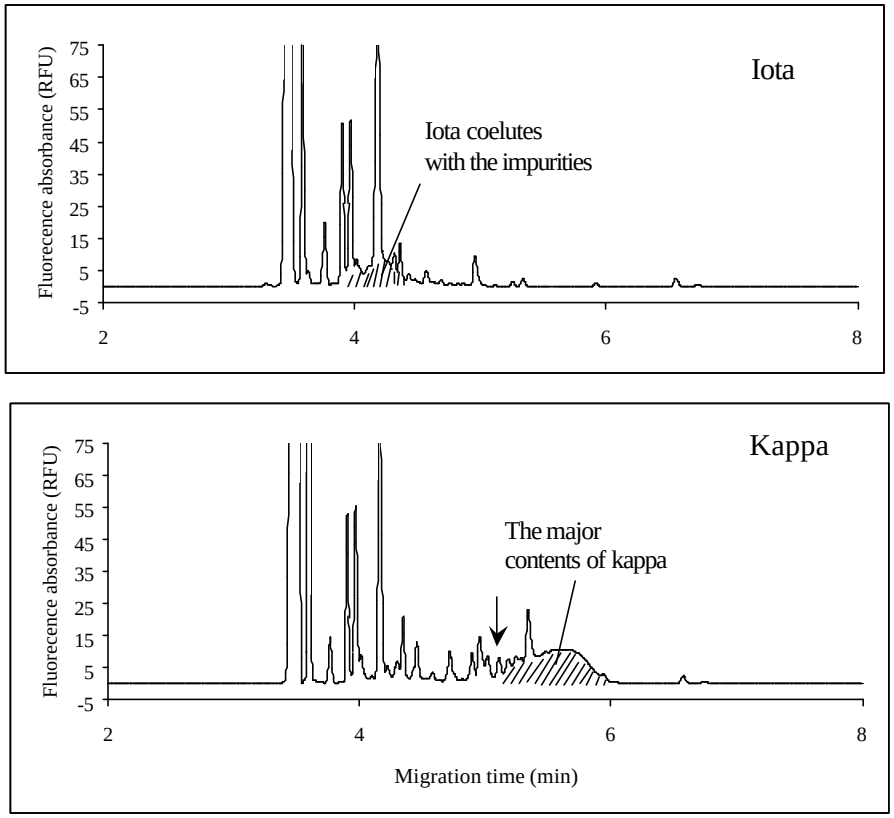

Figure 9.1 ***Separation profiles of iota and kappa carrageenans without centrifugation***

CE conditions: 50 µm i.d. × 50 cm effective length of a bare fused silica capillary, voltage –30 kV, temperature 30 °C, run buffer 25 mM trisodium citrate, pH 3.0, injection, 2 s of water at 0.5 psi, 5 s of sample at -10 kV, 1 s of water at -3 kV.

9.3.1.2 Separation of carrageenans after micro centrifugation

In order to remove excess labelling reagent and the small DP fraction, a micro-centrifuge filter was employed. A micro-centrifuge filter with 3×10^4 molecular mass cut-off was chosen because the molecular weight of carrageenans is above this cut-off.

The derivatised carrageenan samples are thus divided into two fractions namely the eluates (MW lower than 3×10^4) and retentates (MW higher than 3×10^4). The electropherograms of the retentates using the same CE conditions as for the total separation (Figure 9.1) are shown in Figure 9.2. The three types of standard carrageenan samples clearly show a characteristic migration time and peak shape after treatment with the centrifuge filters. The lambda standard sample, however, was of concern. It seems to be polluted with iota carrageenan as will be discussed further.

Compared to Figure 9.1, most of the labelling reagent and low DP saccharides are removed. The first visible minor peak in Figure 9.2 represents APTS residues which are useful as a mobility standard to guard against any shift in migration time. The relative migration times, i.e. the migration time of the carrageenans over the APTS marker, as measured from Figure 9.2, are 1.19 for iota, 1.24 for lambda and 1.66 for kappa, respectively. These values can only be used for differentiation of iota/lambda from kappa. The peak shapes of the carrageenans differ, while iota is characterised by a nearly Gaussian shape, Lambda shows tailing and kappa leading. The tailing factor defined as a/b ラ 100 in which a is the half peak width at the leading part and b is the half peak width at the tailing part measured at 10% of the peak height are 103 for iota, 31 for lambda and 162 for kappa, respectively. The peak shape also helps in characterising the carrageenans.

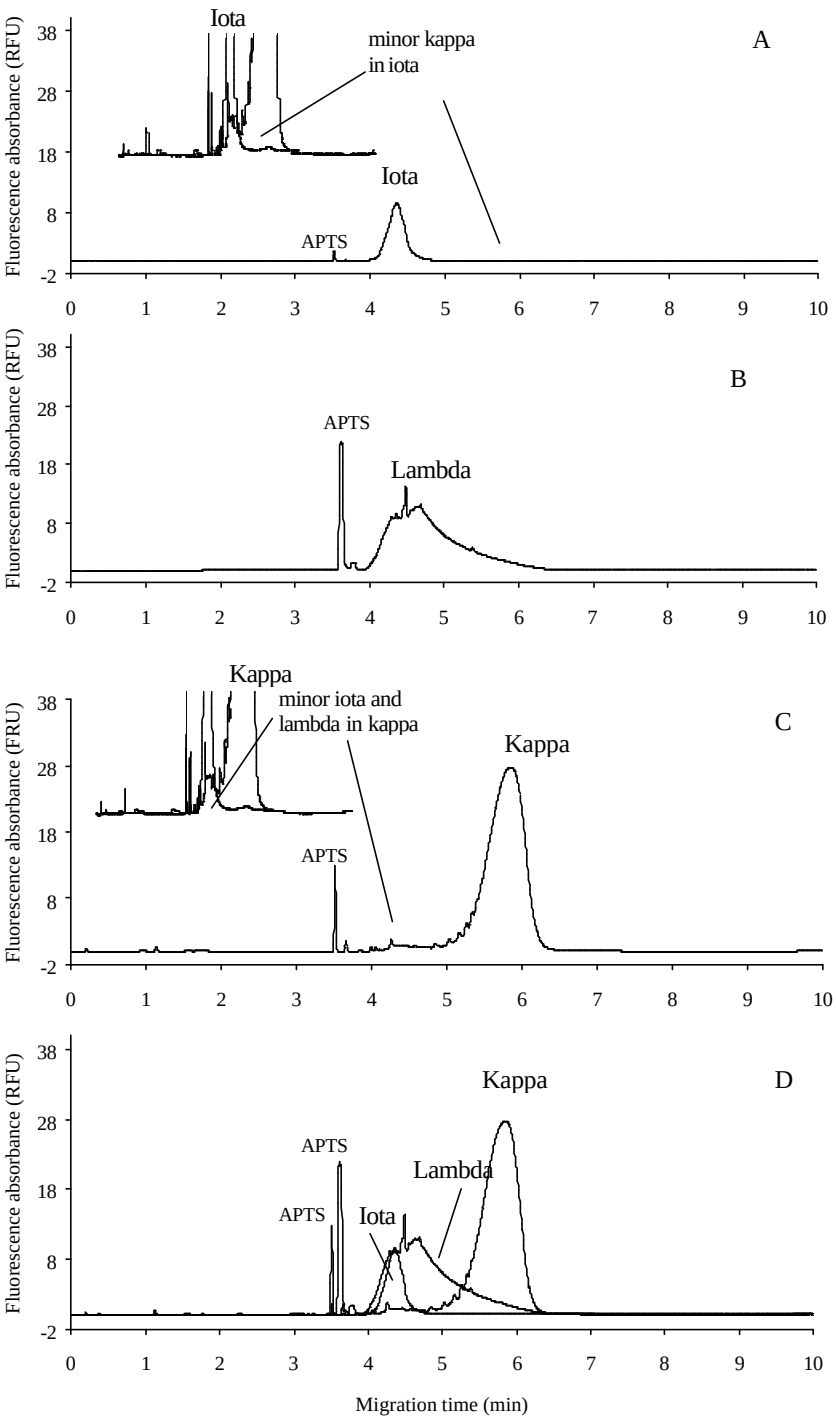

Figure 9.2 ***Separation of the retentates of commercial (A) iota, (B) lambda and (C) kappa carrageenan. (D) superimposed electropherograms of iota, lambda and kappa carrageenan***

CE conditions as described in Figure 9.1.

The APTS peak area or height indicates the high filtration efficiency. Another important effect of using a microcentrifuge filter was the concentration of the analytes of interest. This is demonstrated by the increase in the relative fluorescence intensity scales of the retentates (Figure 9.2) compared to the unfiltered carrageenan samples (Figure 9.1) of kappa. Hence, this improves the detection limit, which is critical for detection of high MW polysaccharides tagged only at their reducing terminals. It is noted that the kappa standard contained some minor traces of iota carrageenan (Figure 9.2).

The peaks of all types of carrageenan retentates are relatively broad (Figure 9.2). This is because polysaccharides inherently constitute a wide range of chain lengths and thus a broad distribution of charge to mass ratio.

A temperature of 30 °C during the electrophoretic process results in an analysis time of less than 7 minutes. Roberts *et al.* [8] reported that by increasing the temperature, migration time was drastically reduced while only a slight reduction in efficiency and resolution was observed. This is because the conformational states of carrageenan polysaccharides are a function of the temperature. At a relatively high temperature, the polymer chain can be a random coil rendering the structure looser and hence, due to lower electrostatic interaction, more free charged sites exist in solution, resulting in higher mobility. A temperature as high as 50 °C was used to separate iota and kappa carrageenan in 4 minutes [8].

9.3.1.3Separation of the carrageenan eluates

The separation profiles of the eluates from iota- and kappa-carrageenan after the centrifuge filtration show the low molecular mass portion (Figure 9.3). The

commercial available Beckman carbohydrate gel buffer was used because this buffer contains an anti-convective additive that improves peak efficiency.

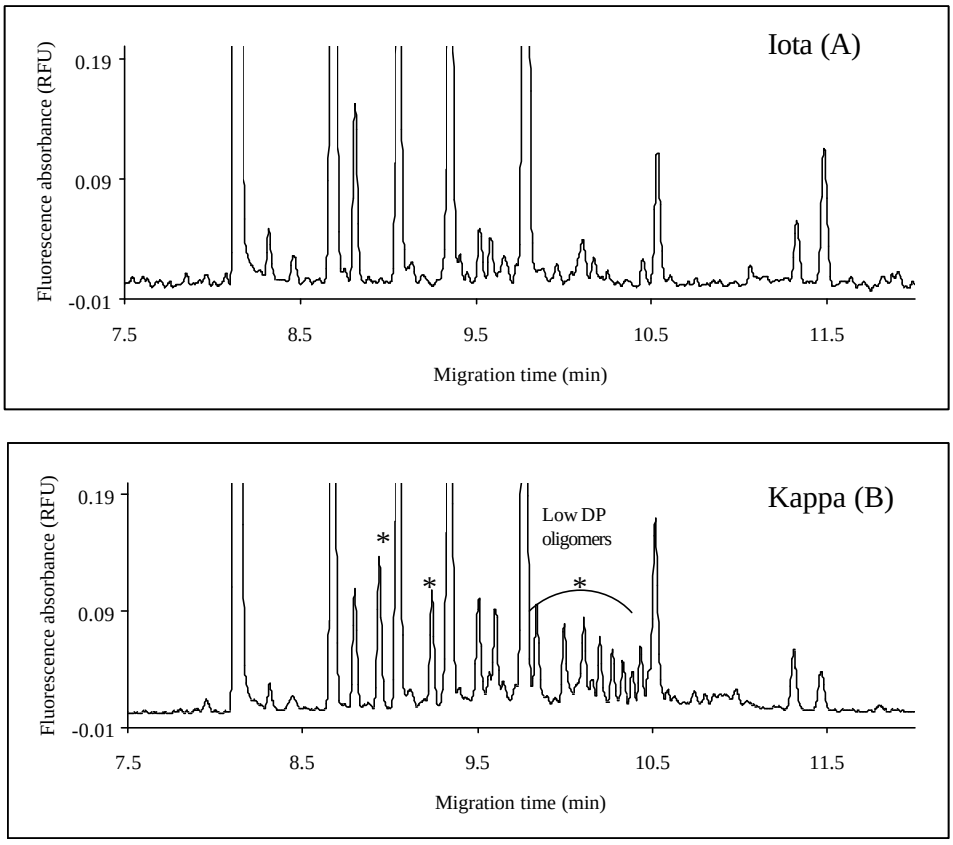

Figure 9.3 ***Separation of the eluates of (A) iota and (B) kappa carrageenan***

CE conditions: bare fused silica capillary with 50 µm i.d. × 57 cm in length (50 cm to the detector window), voltage -30 kV, 30 °C, the first injection, 2 s of water at 0.5 psi, the second injection, 5 s of sample at −10 kV and the third injection, 1 s of water at −3 kV, Beckman carbohydrate separation gel buffer (Beckman, Fullerton, CA, USA).

Through comparison of the blank with both the iota and kappa profiles, low DP oligomers were observed in kappa carrageenan, as indicated by the asterisks in Figure 9.3 B while the profile of iota carrageenan was the same as the blank

which indicates that no low DP oligomers are present in iota carrageenan (Figure 9.3 A). The impurities are certainly present in very low concentration compared to the parent carrageenan with high MW. Since the concentration of APTS tag is directly proportional to the concentration of the reducing end, the compounds with low molecular weight have a relatively high concentration of APTS compared to those with high molecular weight. Therefore, the fluorescence signal of the small DP compounds will be many times higher than the signal of an equal amount of high DP compounds.

9.3.1.4 Analysis of some other carrageenan samples

The method described above was successfully employed for the analysis of five carrageenan samples given for identity confirmation and purity check. The samples were considered to be

$1^{\#}$, kappa carrageenan, $2^{\#}$, kappa carrageenan, $3^{\#}$, lambda carrageenan,

$4^{\#}$, lambda carrageenan, $5^{\#}$, iota carrageenan.

The separation obtained with the five samples are given in Figure 9.4, 9.5, 9.6 and 9.7, respectively.

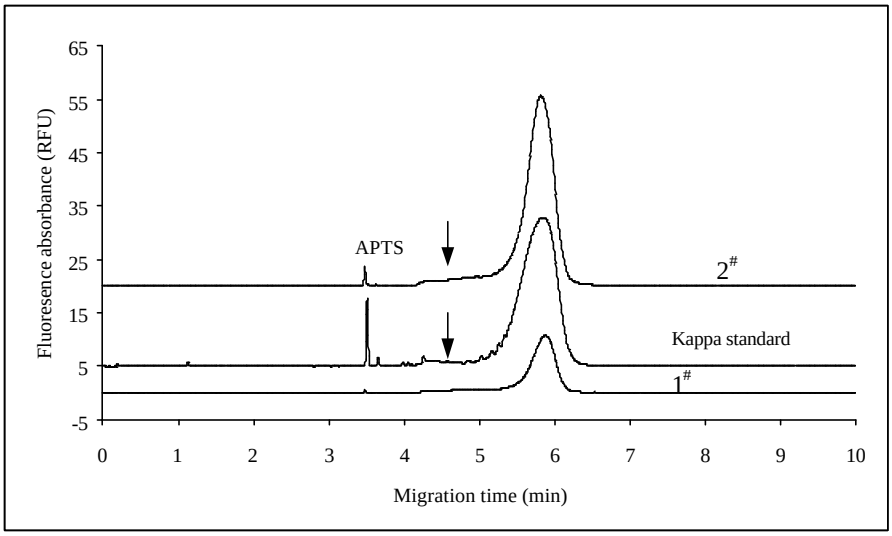

Figure 9.4 ***Separation of APTS derivatised 1# and 2# after filtration***

CE conditions as described in Figure 9.1

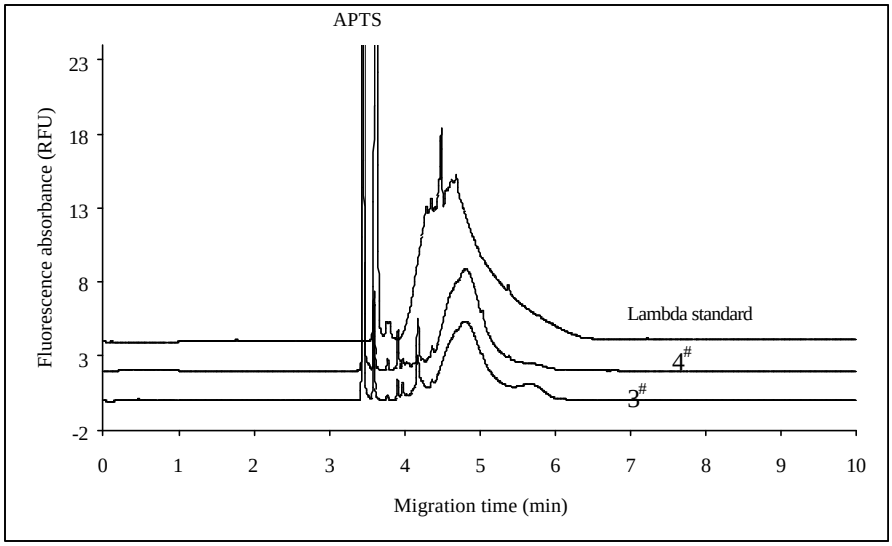

Figure 9.5 ***Separation of APTS derivatised 3# and 4# after filtration***

CE conditions as described in Figure 9.1

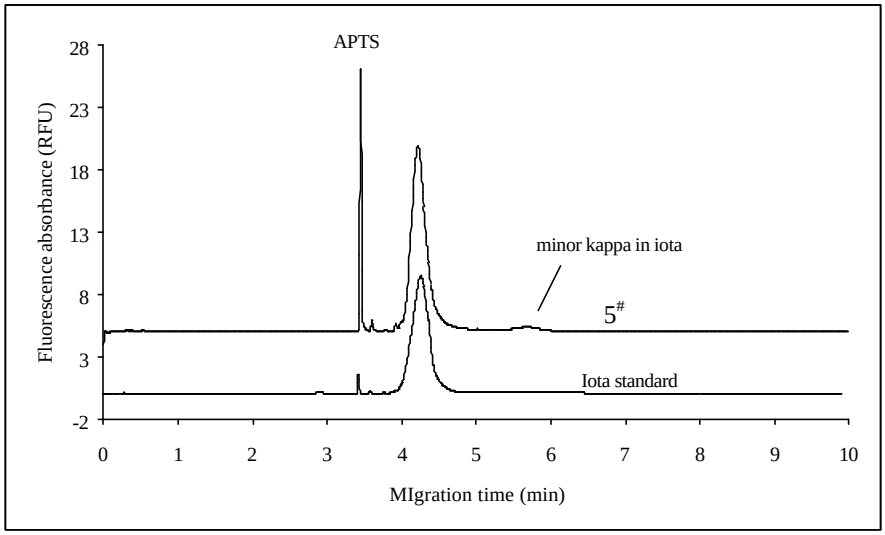

Figure 9.6 ***Separation of APTS derivatised 5# after filtration***

CE conditions as described in Figure 9.1.

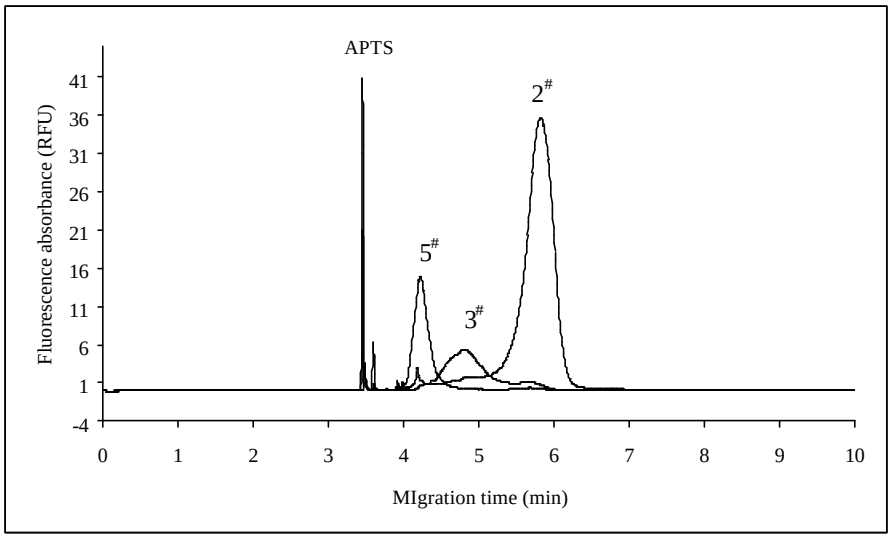

Figure 9.7 ***Differentiation of the retentates from the three APTS derivatised samples after centrifigution***

Peaks: 2# = kappa carrageenan, 3# = lambda carrageenan, 5# = iota carrageenan.
CE conditions as described in Figure 9.1.

1# and 2# give the typical kappa carrageenan separation profile as confirmed by the kappa carrageenan standard (Figure 9.5). These two samples also contain minor traces of iota and lambda carrageenan as the arrows indicate in Figure 9.4. 3# and 4# are assumed to mainly contain lambda carrageenan through comparison with the standard (Figure 9.5). However, they elute between 1# (or 2#) and 5# with much better resolution than in Figure 9.2. This lambda sample is indeed contaminated with iota! A much better resolution between iota, lambda and kappa is noted in Figure 9.7 compared to Figure 9.2. Recalculating the relative migration time for iota and lambda gives in 1.19 and 1.24, respectively, with tailing factors of 83 and 120, respectively. It is observed that 3# also contains iota carrageenan (Figure 9.7) but 4# does not. Besides, a higher amount of kappa carrageenan is present in 3# compared to 4# (Figure 9.5).

5# is iota carrageenan containing a minor amount of kappa carrageenan (Figure 9.6).

9.3.1.5 Separation of carrageenans on a PAA coated capillary

By using a polyacrylamide (PAA) coated capillary, the separation of the three carrageenans could be achieved more rapidly (in 4 minutes) using the same buffer system as for the uncoated capillary with the exception that a higher pH (pH 3.2) was applied (Figure 9.8). The migration time repeatability was very good for iota (RSD = 0.22%, n = 6) and kappa (RSD = 0.37%, n= 6) carrageenan. Besides, the separation efficiency was raised when the buffer pH was increased. When the pH was above 4.4, peak splitting was observed for kappa carrageenan and this is not desired. Hence, a buffer with pH < 4.4 was used. At pH 4.4, the separation efficiency (N) of iota carrageenan was 20,000. This was much higher than that

measured on an uncoated capillary (N = 2,300) reported by Roberts *et al.* [8]. The efficiency for kappa carrageenan (N = 9,514) was also higher than that obtained on a bare fused silica capillary (N = 5,700) [8].

Moreover, the buffer pH could be varied over a wide range from 3.0 to 7.8 offering advantages for the analysis of gums like CMC, xanthan gum, arabic gum, etc. This allowed to control the degree of deprotonation and thus to improve the electrophoretic properties of gums.

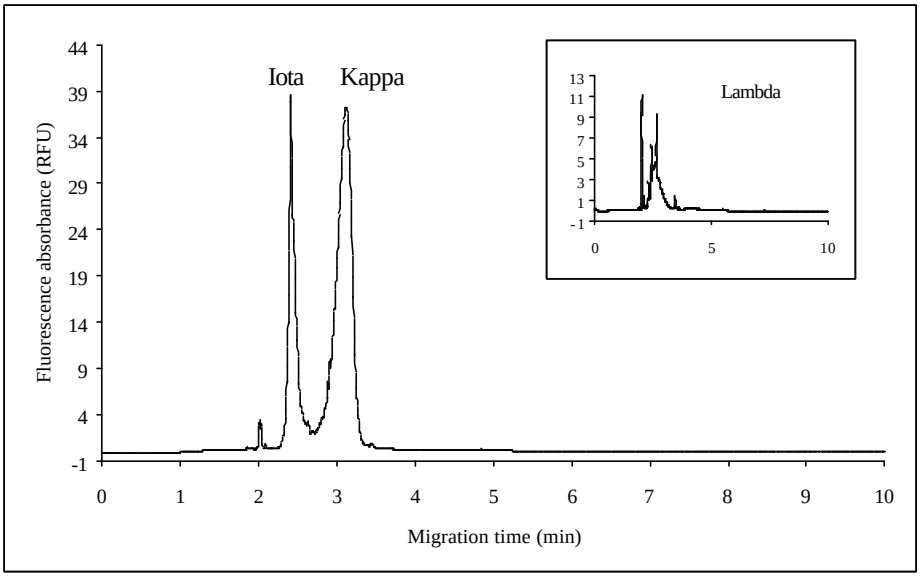

Figure 9.8 ***Analysis of iota, kappa and lambda standard carrageenans on a PAA coated capillary***

CE conditions: 50 µm i.d. × 40 cm in effective length of PAA coated capillary, 25 mM trisodium citrate buffer, pH 3.2, voltage -30 kV, 30 °C, injection 2 s of water at 0.5 psi, 5 s of sample at -10 kV and 1 s of water at -3 kV.

9.3.2 CE analysis of alginic acid and agar gums from seaweeds

Like carrageenan, alginic acid is a gum extracted from seaweed. It is a highly negatively charged polysaccharide. Alginic acid is composed of mannosyluronic and gulosyluronic acid. A mixture of iota carrageenan, kappa carrageenan and alginic acid could be well separated on the coated capillary with 25 mM trisodium citrate buffer at pH 3.2 as illustrated in Figure 9.9.

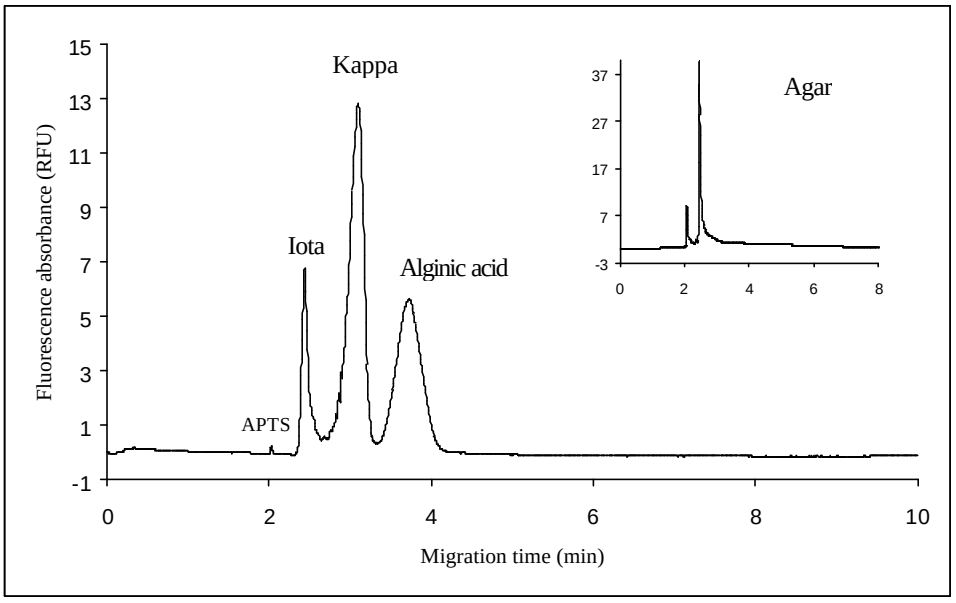

Figure 9.9 ***Separation of the mixture of iota carrageenan, kappa carrageenan and alginic acid.***

CE conditions as described in Figure 9.8.

Mannosyluronic and gulosyluronic acid present in alginic acid have a weaker acidity than the sulfate groups of carrageenans, hence alginic acid eluted as the last solute. Further increase of the buffer pH resulted in shorter migration times and alginic acid eluted between iota and kappa carageenan. Agar, as shown in the

insert of Figure 9.9, had the same migration time as iota carrageenan and could thus not be separated from iota carrageenan.

The mixture of five gums, i.e. xanthan and CMC, alginic acid, iota and kappa carrageenan, was separated in 10 minutes as illustrated in Figure 9.10. The later the elution is, the broader is the peak, i.e. CMC has the longest migration time and thus the broadest peak. The amount of deprotonated carboxyl groups of CMC is low at pH 3.2, which causes a relatively low charge density of CMC and thus a low mobility.

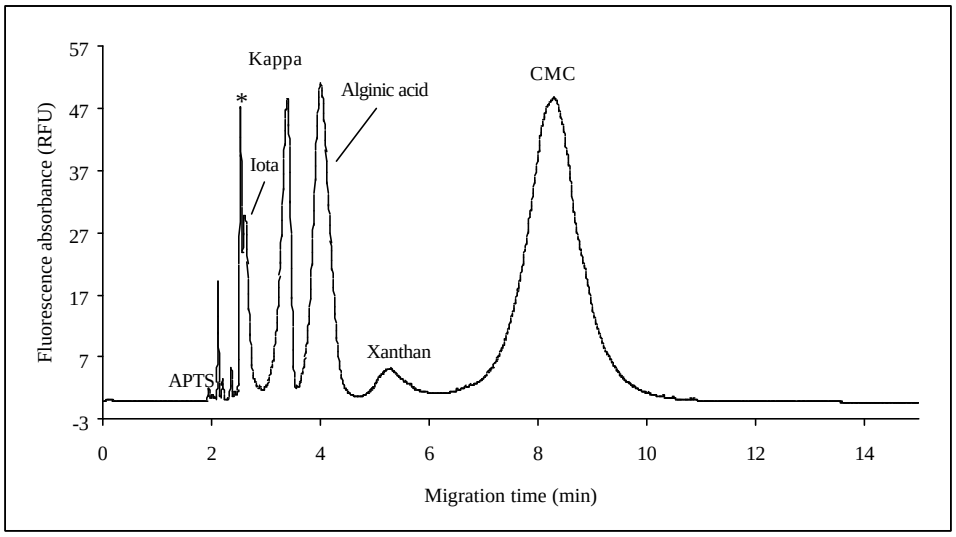

Figure 9.10 ***Separation of the mixture of iota and kappa carrageenan, alginic acid, xanthan and CMC***

CE condition: as described in Figure 9.8.

The peak partly co-eluting with iota carrageenan, indicated by the asterisk, is a portion of xanthan with a relatively high charge density. The molecular weight of this fraction of xanthan was demonstrated to be from 1×10^4 to 3×10^4 by

employing microcentrifuge filters with 3×10^3, 1×10^4 and 3×10^4 molecular mass cut-off, respectively.

9.3.3 Further experiments with CMC

The peak shape and migration time of CMC in function of the buffer pH on the PAA coated capillary were also studied. The profiles are shown in Figure 9.11.

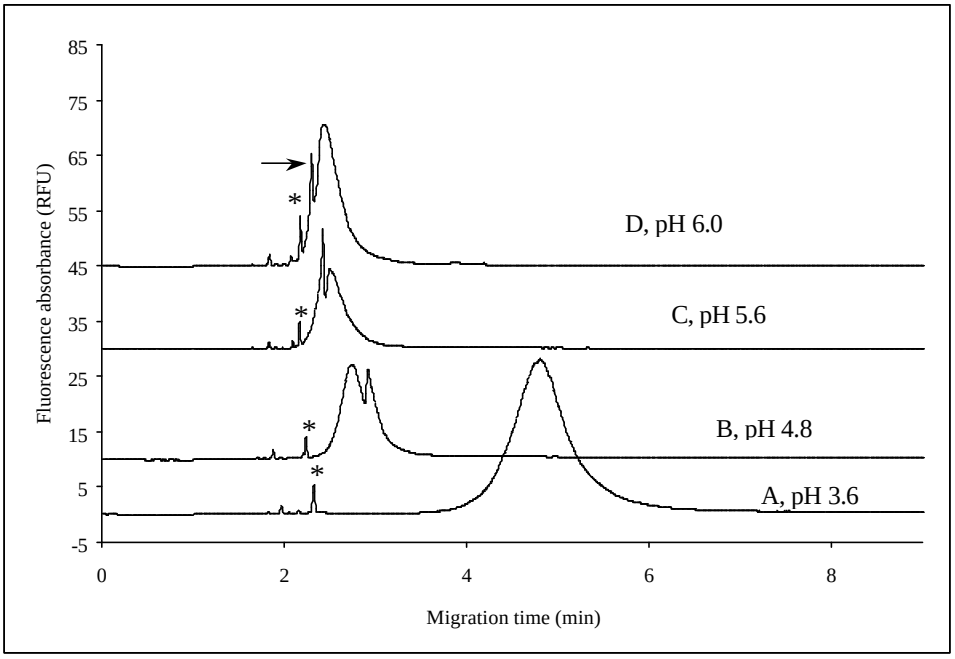

Figure 9.11 ***Electropherograms of CMC at different buffer pH***

CE conditions: same as in Figure 9.8 except for the buffer pH that was (A) 3.6, (B) 4.8, (C) 5.6 and (D) 6.0, respectively.

The migration time is strongly reduced (see also 9.8) and the peak becomes narrower by increasing the pH from 3.6 to 4.8 because dissociation of the carboxyl groups is encouraged. A slight reduction of migration time of CMC was further observed from pH 4.8 to 6.0 while the migration time as well as the peak

shape remained constant from pH 6.0 to 7.8. This indicates that at a pH higher than 6.0 deprotonation is complete and a maximum mobility is obtained.

Above pH 4.0, the major peak of CMC appeared to split. With increasing pH, the split position moved to the beginning of the peak until only a slightly split peak is observed at pH 6.0 as indicated by the arrow in Figure 9.11 D. Such an un-consecutive migration pattern could indicate structural heterogeneity in carboxymethylation. Incomplete reac tions may indeed result in products of questionable uniformity [9].

9.3.4 Gum Arabic, karaya and ghatti (gums from trees)

Compared to the gums from seaweed, the gums in this group are structurally more complex (Chapter 2, Table 2.2). Galacturonic acid is known to be one of the constituents of all these exudate gums. The acidic residues provide negative charges and thus the electrophoretic migration in an electric field. Increasing the pH of the run buffer has a significant effect on the migration times and on the peak shapes of these gums as well. The separation of the gums obtained at pH 7.8 are shown in Figure 9.12 (arabic and karaya gum) and Figure 9.13 (ghatti gum).

Arabic gum shows a broad peak besides one early eluting solute while karaya and ghatti gums show inconsecutive migration patterns. This could reflect a structural heterogeneity in the composition of these gums. The characteristic profiles can be used for their differentiation. The separation of the mixture of CMC, gum Arabic and gum karaya at pH 7.8 in 9 minutes is shown in Figure 9.14. The high pH was necessary to obtain the fast migration and good peak shape.

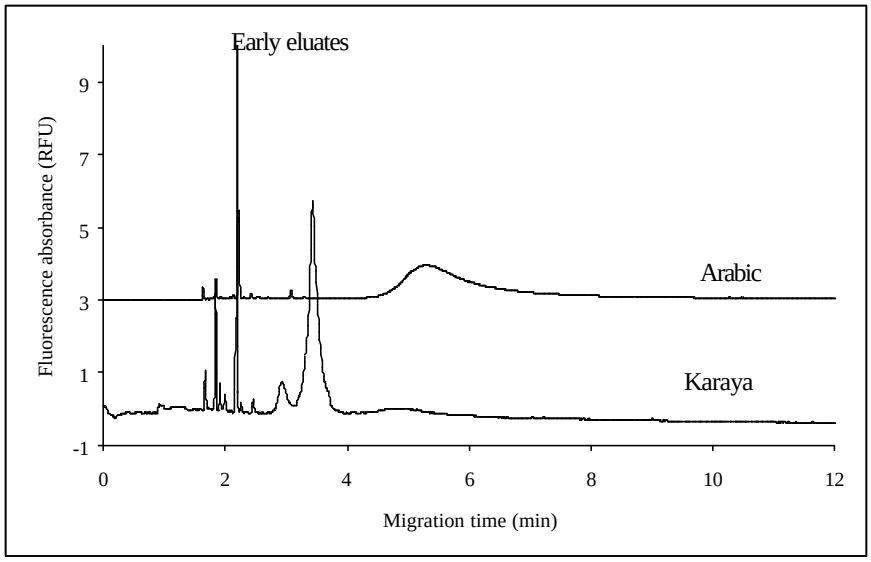

Figure 9.12 ***Electrophoretic separation profiles of gum Arabic and karaya***

CE conditions: 50 µm i.d. × 47 cm in length (40 cm to the detector window) of a PAA coated capillary, 25 mM trisodium citrate buffer pH 7.8, -30 kV, 30 °C, the first injection 2 s of water at 0.5 psi, the second injection 5 s of sample at −10 kV and the third injection 1 s of water at −3 kV.

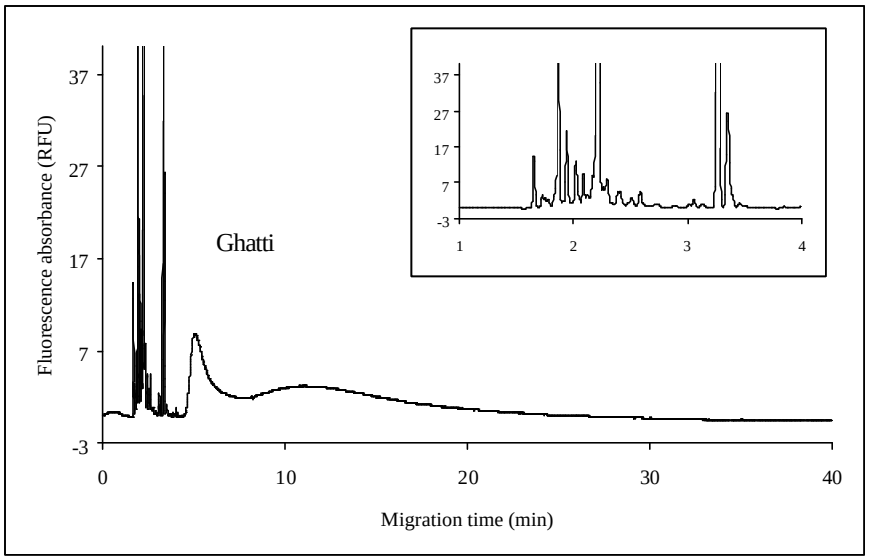

Figure 9.13 ***Electrophoretic separation profile of ghatti gum***

Insert: the early eluting from 1 to 4 min.
CE conditions as described in Figure 9.12.

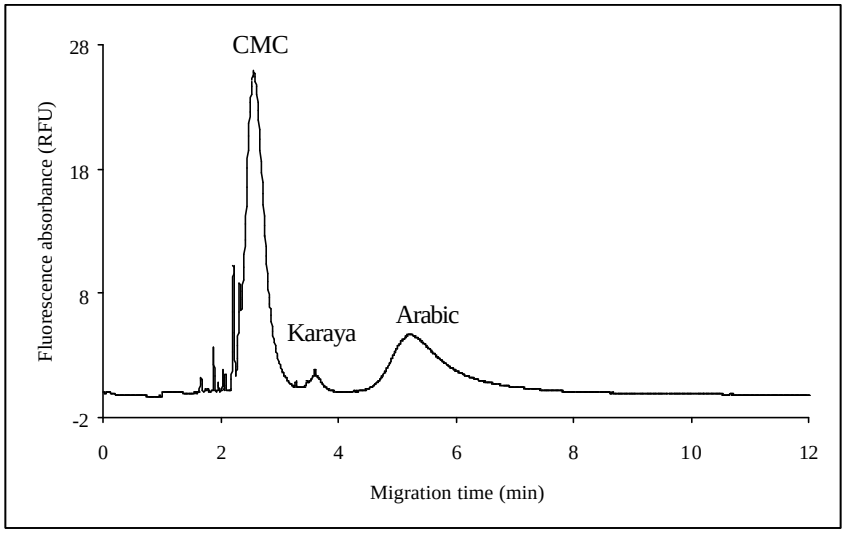

Figure 9.14 ***Separation of a mixture of CMC, karaya and arabic gum CE conditions*** as described in Figure 9.12

9.3.5 Guar gum (gum from seed flour)

Guar gum, which consists mainly of mannose and galactose (Chapter 2, 2.4.4.3), did not elute under the CE conditions described above. Only some early eluting peaks with a relatively low MW were detected. This is because guar and LBG are naturally neutral and the limited amount of negative charges introduced by the derivatising reagent (APTS) are not sufficient to obtain enough electrophoretic migration of these high mass polymers.

The separation of a synthetic guar gum on a bare fused silica capillary with a low pH (2.2) phosphate buffer gave the profile shown in Figure 9.15. Only a small amount of low DP oligomers is recorded. The natural guar sample has the same separation profile as the synthetic one.

The elution profile of the main peaks probably represents the guar backbone constructed by linear chains of β-1,4-D-mannopyranosyl units, while the relatively small peaks accompanying every main peak correspond to branched chains of D-galactopyranosyl units attached by α-1,6-linkages [10].

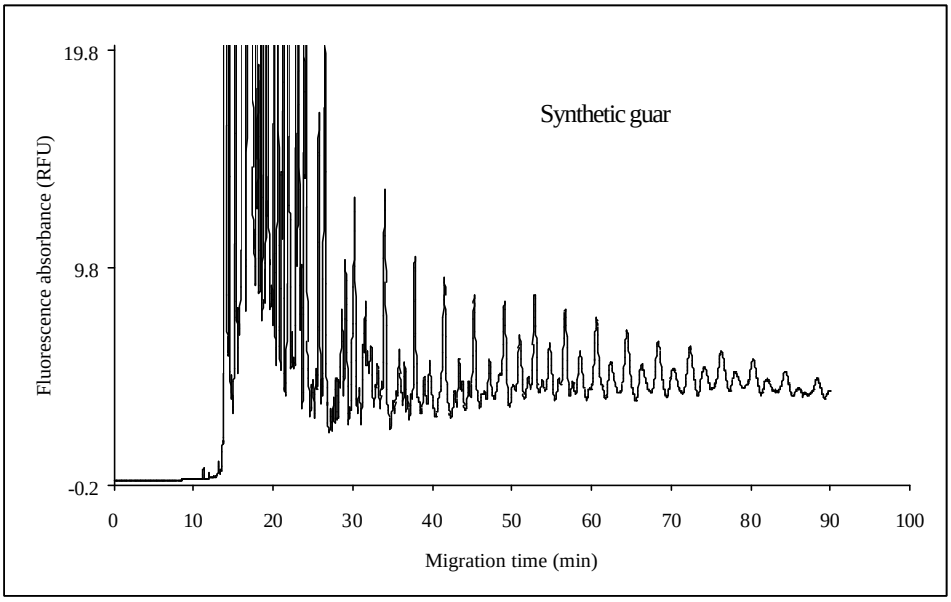

Figure 9.15 ***Separation of synthetic guar gum derivatised with APTS***

CE conditions: bare fused silica capillary 75 µm i.d. × 57 cm in length (50 cm to the detector window), 80 mM phosphate buffer pH 2.2, voltage -10 kV, injection 10 s at 0.5 psi, 20 °C.

9.3.6 Pectins

Three commercial available pectins with different degrees of esterification (DE) were analysed on the PAA coated capillary (Figure 9.16). The lower is the DE, the shorter is the migration time and the narrower is the peak. The migration is based on the free galacturonic acid groups of the pectin samples.

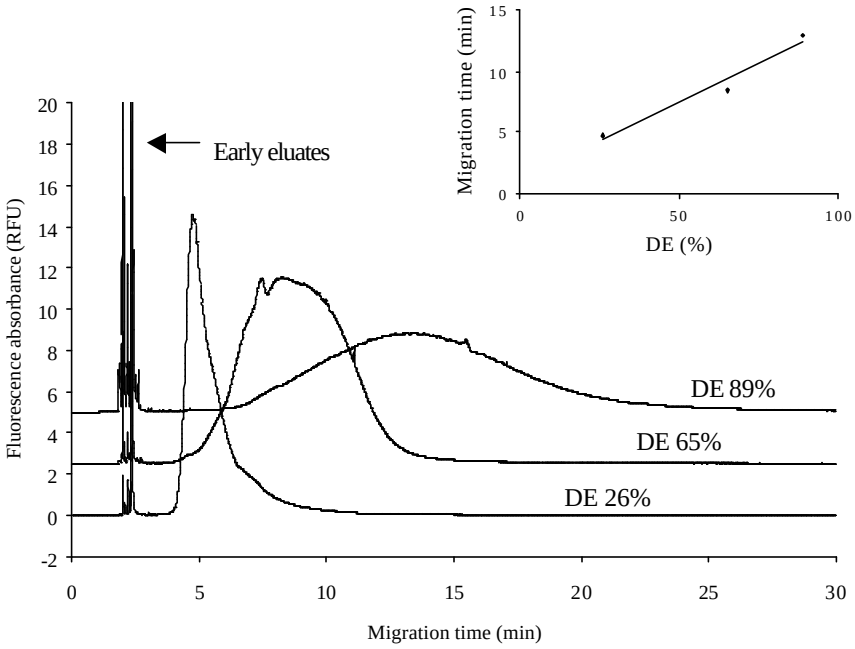

Figure 9.16 ***Electropherograms of three pectins with DE 26%, 65% and 89% CE conditions*** as described in Figure 9.8.

A partial overlap of the peaks occurred. A linear relationship could be observed between the migration time of the different pectins and their DE, as is shown in the insert of Figure 9.16. Hence, by using a more extensive set of standards, the DE for pectins could be measured in this way. The broad peak shape implies the broad distribution of esterification along the chain lengths. The pectin with highest DE (89%) gives the broadest peak shape, which means it has the largest distribution of esterification among these three standards. In addition, inconsecutive migration was also observed for pectins when the buffer pH was increased, which reflects the heterogeneous esterification.

9.4 Conclusion

For the first time, the separation of intact high MW polysaccharides on a PAA coated capillary is described. Short analysis time can be obtained by adjusting the buffer pH. For example, highly negatively charged polysaccharides such as carrageenans and alginic acid were best separated at low pH 3.2 while a high pH like 7.8 is needed to separate Arabic, karaya, and ghatti gum. Inconsecutive migration was observed on several occasions. This indicates structural heterogeneity of the analysed gums.

References

[1] P. J. Schneider, O. Grosche and H. Engelhardt, *J. High Resol. Chromatogr.* 22, **1999**, 79

[2] D. M. W. Andreson, *The American Associaton of Cereal Chemists, Inc.*, Vol. 33, No.10, **1988**, 844

[3] M. Stefansson and M. Novotny, *Anal. Chem.* 66, **1994**, 3466

[4] J. Sudor and M. Novotny, *Proc. Natl. Acad. Sci. USA* 90, **1993**, 9451

[5] J. Sudor and M. V. Novotny, *Anal. Chem.* 67, **1995**, 4205

[6] J. D. Brewster and M. L. Fishman, *J. Chromatogr. A* 693, **1995**, 382

[7] H.-J. Zhong, M. A. K. Williams, R. D. Keenan, D. M. Goodall and C. Rolin, *Carbohydr. Polym*. 32, **1997**, 27

[8] M. A. Roberts, H.-J. Zhong, J. Prodolliet and D. M. Goodall, *J. Chromatogr. A* 81, **1998**, 353

[9] M. Stefansson and M. V. Novotny, *Anal. Chem*. 66, **1994**, 3466

[10] M. Stefansson and M. V. Novotny, *Carbohydr. Res.* 258, **1994**,1

Chapter 10

Analysis of Hemicellulose and its Hydrolysates by CE-LIFD

Abstract

Hemicellulose (xylan) was derivatised with 9-aminopyrene-1,4,6-trisulfonic acid (APTS) and the solutes were separated by CE as borate complexes on a bare fused silica capillary coupled with laser induced fluorescence detection (LIFD). Profiles of xylan during enzymatic degradation were monitored. Identification and quantitative determination of neutral monosaccharides derived from enzymatic hydrolysis by xylanase and from chemical hydrolysis by trifluoroacetic acid was performed and the results were compared. This is only a preliminary study.

10.1 Introduction

Besides cellulose and lignin, hemicellulose is the most important constituent of terrestrial plant cell walls [1-3]. It is built up from different monosaccharide constituents, mainly D-glucose, D-galactose, D-mannose, D-xylose, L-arabinose, L-fucose, L-rhamnose, D-glucuronic acid, D-galacturonic acid and 4-*O*-methyl-D-glucuronic acid (see Chapter 2, 2.4.3). The amount of these principal residues present in hemicellulose differs depending on the source.

Determination of the kind and quantity of basic units present in hemicellulose is usually the first step in its characterisation.

Hemicellulose is commonly hydrolysed by using mineral acids, formic acid or trifluoroacetic acid. Trifluoroacetic acid is preferred since it can be removed by evaporation, and hence neutralisation is not necessary. Enzymatic hydrolysis of hemicellulose is still expensive and the completion is questionable. The subsequent determination of the component monosaccharides has been performed by gas chromatograhy (GC) [4] which offers the advantage that it can easily be coupled with mass spectrometry (MS). It suffers from the drawback, however, that carbohydrates need to be converted into volatile derivatives prior to analysis. Derivatisation may therefore be incomplete and can lead to the formation of multiple peaks per analyte. A number of high performance liquid chromatographic (HPLC) techniques have been used to analyse the carbohydrates present in hemicellulose. Although higher resolution can be realised by means of HPLC separation of carbohydrates on a strong anion-exchange resin using a sodium hydroxide gradient, the method has some shortcomings. One is that neutral saccharides and uronic acids cannot be analysed under the same conditions and another is that elaborate sample pretreatment is needed in order to remove contaminants usually encountered in biomass degradation samples, such as lignins, tannic acids, trifluoroacetic acid, and various hydroxylated components, which otherwise interfere either with the retention or with the pulsed amperometric detection of carbohydrates [5, 6]. Capillary electrophoresis (CE) was shown to be a valuable tool for analysing carbohydrates present in hemicellulose after either chemical hydrolysis using trifluoroacetic acid [7, 8] or

enzymatic hydrolysis [8, 9]. In the work of Huber and coworkers [7], the monosaccharides present in xylan obtained from the hydrolysis with trifluoroacetic acid were tagged with *p*-aminobenzoic acid (*p*-ABA) and then separated by CZE. Galacturonic acid and glucuronic acid could be separated but not rhamnose and mannose because rhamnose was masked by the reagent peak and mannose co-eluted with glucose. In addition, loss of the total yields of carbohydrates was reported in this study.

Dahlman *et al.* [9] studied the carbohydrate composition of hemicellulose by CZE with UV detection. The polysaccharides were first hydrolysed using a mixture of cellulase and hemicellulase (xylanase and endoglucanase). The hydrolysate was then derivatised with 4-aminobenzoic acid ethyl ester (ABEE). Both neutral monosaccharides and uronic acids could be separated in a single run with the detection at 306 nm wavelength. The total yields of carbohydrates (93-97%) reported were high. L-rhamnose and L-fucose, however, were not investigated in this work.

The aim of this work was to use CE with LIF detection for the analysis of enzymatic degradation profiles of commercial xylan and the basic constituents derived from both chemical and enzymatic hydrolysis.

10.2 Experimental

10.2.1 Chemicals

Trifluoroacetic acid and sodium cyanoborohydride, borax, xylan from birchwood and oat spelts, xylanase (β-1,4-D-xylanxylanohydrolase) from *Aureobasidium pullulans,* the standard monosaccharides, L-rhamnose, D-glucose, D-galactose, D-

xylose, L-fucose, D-ribose, D-galacturonic acid and D-glucuronic acid monohydrate were obtained from Sigma-Aldrich (Steinheim, Germany). D-mannose was from Janssen Chimica (Beerse, Belgium). L-arabinose was obtained from Ega-Chemie (Steinheim/Albuch, Germany). The purity of the standards was 99% except for D-galacturonic acid (97%). Xylooligosaccharides were obtained from Megazyme (Bray, Ireland). Glacial acetic acid was from Panreac (Barcelona, Spain). Sodium hydroxide was obtained from UCB (Leuven, Belgium). HPLC grade tetrahydrofuran (THF) was obtained from Lab-Scan Ltd. (Dublin, Ireland). 9-Aminopyrene-1,4,6-trisodium sulfonate (APTS) was purchased from Molecular Probes (Leiden, the Netherlands). The water used through all the experiments was produced by a Milli-Q purification system (Millipore, Bedford, MA, USA).

10.2.2 Sample preparation

10.2.2.1 Chemical hydrolysis

The chemical hydrolysis with trifluoroacetic acid was performed according to the method reported by Rydlund and Dahlman [8]. Briefly, 5 mg of xylan were mixed with 1 mL of trifluoroacetic acid (2 mol/L), then degassed with nitrogen for 10 seconds in order to remove oxygen, and thereafter heated in a boiling water bath for 4 hours. The obtained hydrolysates were dried with nitrogen gas. 1 mL of water, containing 2×10^{-4} M of ribose as the internal standard, was used to dissolve the dried hydrolysate. The blank sample for the chemical hydrolysis was prepared in the same way but without the addition of xylan.

10.2.2.2 Enzymatic hydrolysis

Conditions of enzymatic hydrolysis were according to the report of Dahlman *et al.* [9]. 0.5 mL of the stock solutions of xylan (2 mg/mL) was mixed with 30 units of xylanase (1,4-β-D-xylanxylanohydrolase, from *Aureobasidium pullulans*). The incubation was performed at 40 °C in 25 mM sodium acetate buffer at pH 4.0 for 0.25, 0.5, 1, 2, 4, 8 and 30 hours. The resulting hydrolysates were then derivatised with APTS.

In addition, the hydrolysate obtained from 30 hour incubation was dried with nitrogen gas and then dissolved with 0.2 mL of water containing 2×10^{-4} M of ribose (the internal standard). The obtained solution was then used for the quantitative determination of monosaccharides. Blanks, without the addition of xylan, were prepared using the same procedure.

10.2.3 Derivatisation procedures

1. 5 μL of enzymatic hydrolysate was mixed with 8 μL of APTS (95 mM in 25% acetic acid aqueous phase) and 4 μL of sodium cyanoborohydride (1 M in THF). Heating was processed at 90 °C for 1 hour. The reaction mixture was diluted to 1 mL prior to injection. The resulting derivatives were used to investigate the enzymatic degradation of xylan from birchwood.

2. For the investigation of the monosaccharide constituents of hemicellulose after 30 hour incubation, 5 μL of the chemical hydrolysates and enzymatic hydrolysates were mixed with 8 μL of 95 mM APTS in 25% acetic acid, respectively, followed by the addition of 4 μL of sodium cyanoborohydride (1M in THF). Then the

reaction mixtures were heated at 90 °C for 1 hour and then diluted with water to 5 mL.

3. A mixture of 10 standard monosaccharides, i.e. L-rhamnose, D-glucose, D-galactose, D-xylose, L-fucose, D-glucuronic acid, L-ribose, L-arabinose, D-mannose and D-galacturonic acid, was prepared as stock solution with a concentration of 0.01 M of each sugar. Prior to derivatisation, the stock solution was diluted to 0.0025 M for each monosaccharide. 10 µL of this solution (0.0025 M of every monosaccharides) was then mixed with 8 µL of 95 mM APTS (in 25% of acetic acid) and 4 µL of 1 M sodium cyanoborohydride. After heating for 1 hour at 90 °C, the reaction mixture was diluted with water to 25 mL. The calibration series solutions were prepared by dilution of this concentrated stock solution.

4. The APTS derivative mixture of standard xylose, xylobiose, xylotriose, xylotetraose, xylopentaose was prepared for identification of xylan chains. The purity of these standards was not good enough for quantitative analysis.

5 µL of the mixture of standard xylanoligomers was taken into an Eppendorf vial, followed by addition of 8 µL of an APTS solution (0.095 M in 15% acetic acid solution) and 4 µL of sodium cyanoborohydride (1 M in THF). The mixture was heated at 90 °C for 1 hour and diluted with Milli-Q water prior to injection.

10.2.4 CE procedures

The experiments were carried out on a P/ACE system 2100 coupled with laser module 488 (Beckman, Fullerton, CA, USA). Detection was performed with laser induced fluorescence (LIF) at 488 nm excitation and 520 ± 20 nm emission. A

bare fused silica capillary was rinsed with 1.0 M sodium hydroxide solution for 20 minutes and water for 10 minutes. Between two runs, the capillary was conditioned with 1 M sodium hydroxide for 2 minutes and then with the run buffer for 4 minutes. The borate buffer was adjusted to the required pH using sodium hydroxide.

10.3 Results and discussion

10.3.1 Separation of native xylan

The APTS derivative of native xylan (from birchwood), i.e. the commercial xylan without chemical and enzymatic hydrolysis, was separated with CE based on borate complexation as shown in Figure 10.1.

The first mountain-like hump accompanied with non-separated peaks, results from the insufficient distinctions of apparent mobilities between high DP polymer chains. These early eluates with a relatively high MW constitute the major content of xylan although they give relatively low fluorescence absorption. Since every polymer chain is tagged by only one APTS molecule at the reducing terminals, the presence of high DP polymer chains can only contribute with trivial signals generated from one tagged fluorescence molecule.

The identification of the peaks was established by spiking with the standards of xylose (DP 0), xylobiose (DP 1), xylotriose (DP 2), xylotetraose (DP 3) and xylopentaose (DP 4). The peak height of xylobiose appeared to be relatively low in native xylan.

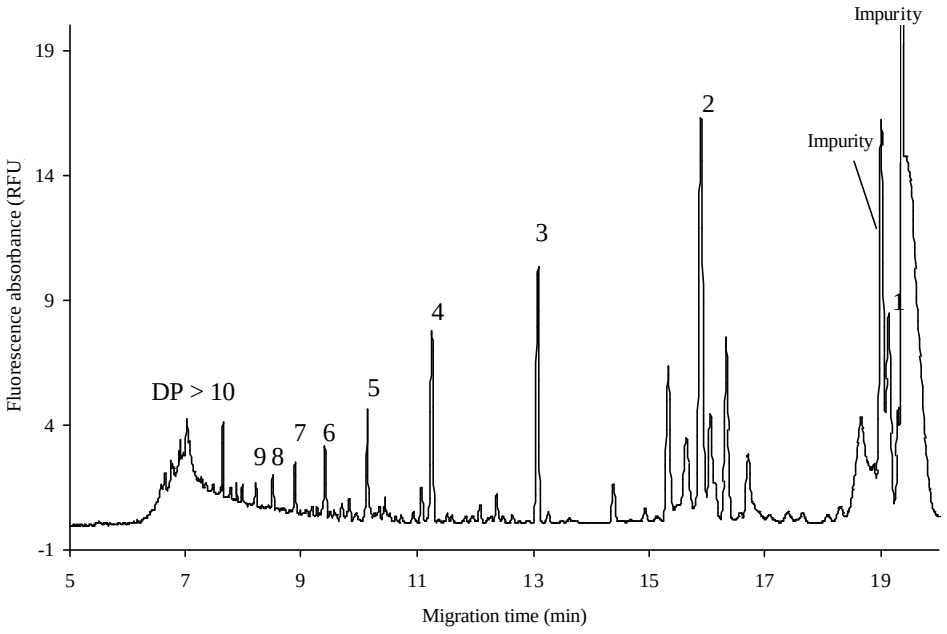

Figure 10.1 ***Electropherogram of native xylan from birchwood derivatised with APTS***

Peaks: 1 = xylobiose (DP 1), 2 = xylotriose (DP 2), 3 = xylotetraose (DP 3), 4 = xylopentaose (DP 4), etc.
CE conditions: bare fused silica capillary with 50 µm i.d. × 57 cm in length (50 cm to the detector window), voltage +20 kV, 10 s injection at 0.5 psi pressure, temperature 20°C, 100 mM borate buffer pH 10.2.
* The APTS reagent used for this application contained several impurities.

10.3.2 Separation of xylan treated with xylanase with varying incubation times

The enzymatic degradation profiles of xylan (from birchwood) obtained with different incubation times are illustrated in Figure 10.2. Xylanase from *Aureobasidium pullulans* was used for the depolymerisation.

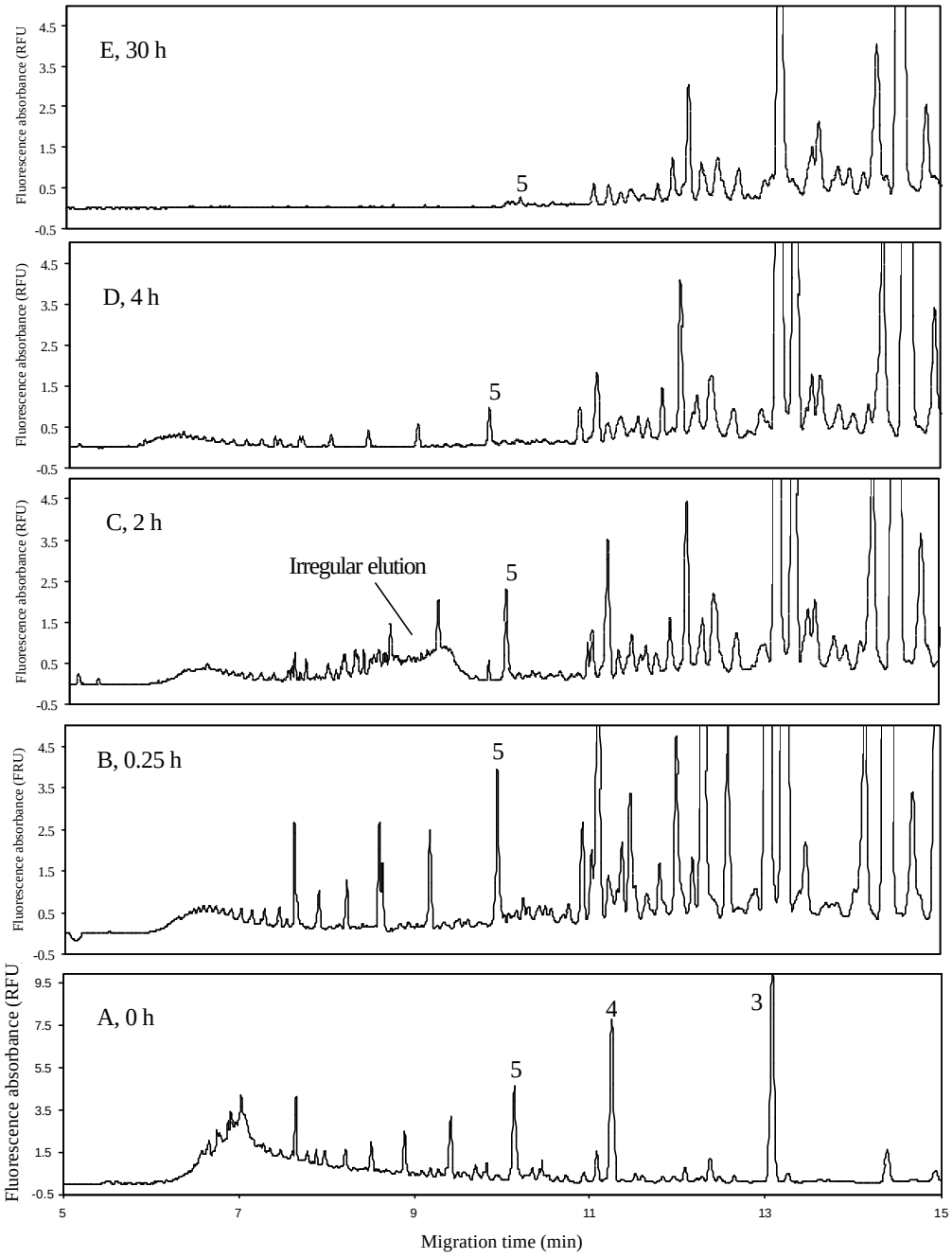

Figure 10.2 ***Analysis of xylan (from birchwood) submitted to enzymatic treatment for varying incubation times***

A 0 hour, B 0.25 hour, C 2 hours, D 4 hours, E 30 hours.
CE conditions as described in Figure 10.1.

As can been seen in Figure 10.2, the size of the mountain-like hump decreased with increasing incubation times. In the hydrolysate obtained after 30 hours of incubation (Figure 10.2 E), the mountain-like elution is no longer visible indicating that the high DP polymer chains are completely decomposed into low DP chains. This is also shown in Figure 10.3 B, where increased peak heights of xylose (DP 0) and xylobiose (DP 1) can bee seen for the enzymatically hydrolysed sample. Hence, a longer incubation time results in increased peak height for the lower DP chains. The peak height of xylopentaose (DP 4) almost remains the same after 15 minutes of incubation, and then also decreased with increasing incubation times (Figure 10.2 C, D, E).

In addition, between DP 1 and DP 3, except the recognised peaks, some unknown peaks appear irregularly as shown in Figure 10.2 B, C, D, E. The oligomers corresponding to these unknown peaks could not be completely broken down even after 30 hours of incubation (Figure 10.3 B). These unknown peaks could be the oligomers that were not linked by β-1,4-D-xylopyranosyl bonds and could therefore not be depolymerised by xylanase. In some cases, the regular elution was interrupted by an irregular migration, for example, as can be seen in Figure 10.2 C. This phenomenon seems to be associated with the polysaccharide behaviour in high electric fields. Sudor and Novotny [10] reported that the charged polysaccharides undergo molecular stretching, resisting the desired separation according to their molecular mass at constant potentials between 50 and 300 V/cm. However, it is not yet fully understood.

The differences between the native xylan and the degraded xylan after incubation for 30 hours are clearly shown in Figure 10.3. After xylan was incubated for 30

hours with xylanase and the high molecular weight polymers were depleted, large amounts of xylobiose (DP 1) and xylose (DP 0) are detected. The original contents of xylose and xylobiose were very low in the native xylan (Figure 10.3 A).

In conclusion, CE coupled with LIFD appears to be a valuable technique to monitor enzymatic degradation of polysaccharides.

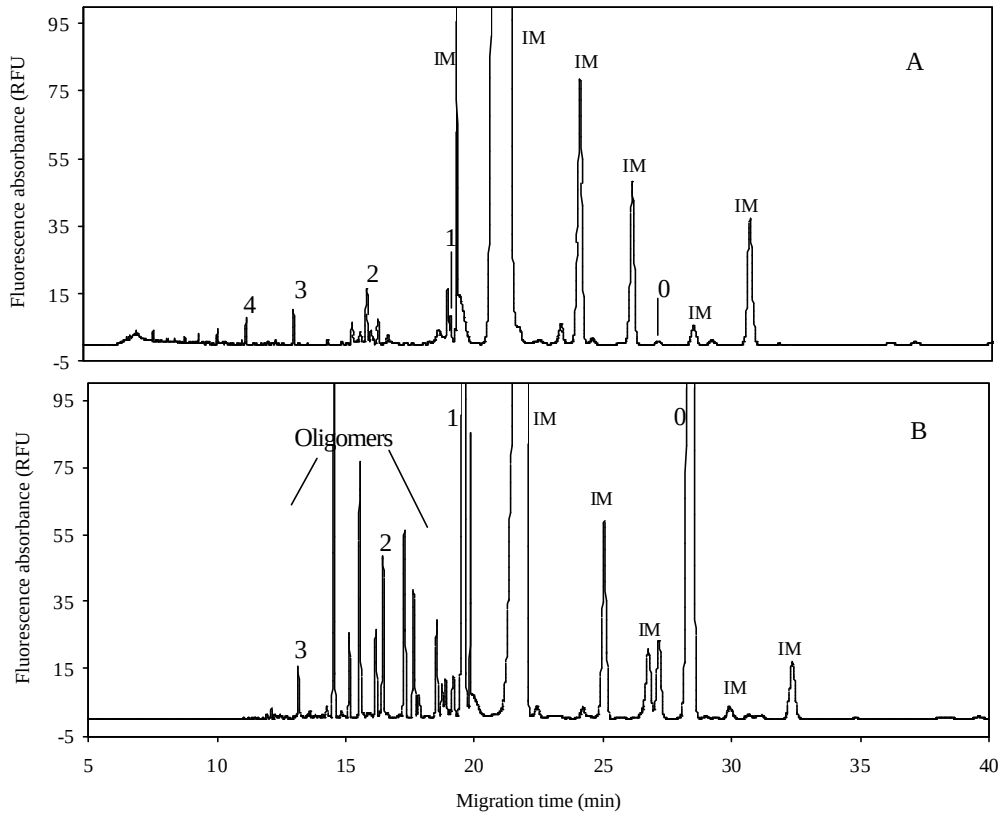

Figure 10.3 ***Comparison of the separation profiles of native xylan (A) and xylan after 30 hours of incubation (B)***

Peak: 0 = xylose (DP 0), 1 = xylobiose (DP 1), 2 = xylotriose (DP 2), 3 = xylotetraose (DP 3), 4 = xylopentaose (DP 4), IM = impurity
CE conditions as described in Figure 10.1.

10.3.3 Separation of the standard mixtures of xylan oligosaccharides and monosaccharides

Commercially available xylan oligosaccharides were separated as shown in Figure 10.4. This separation can also be completed in 13 minutes by using a shorter capillary (40 cm effective length).

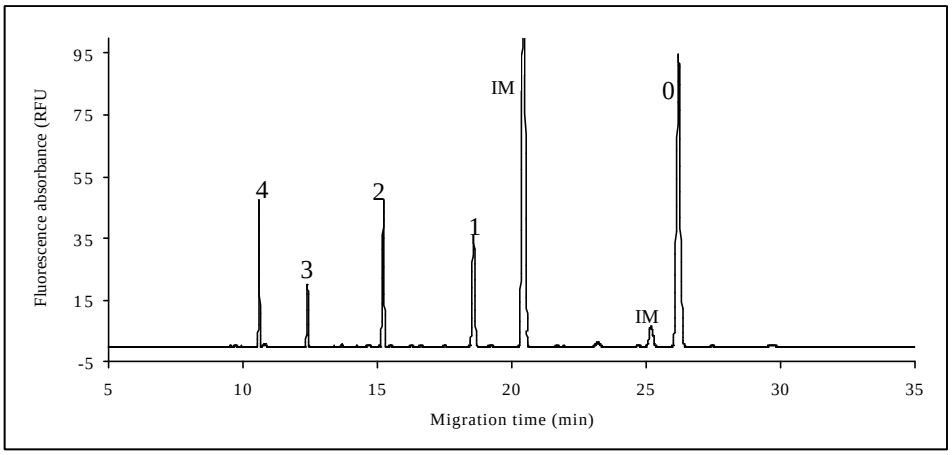

Figure 10.4 ***Separation of the standards of xylan oligomers***

Peaks: 0 = xylose (DP 0), 1 = xylobiose (DP 1), 2 = xylotriose (DP 2), 3 = xylotetraose (DP 3), 4 = xylopentaose (DP 4), IM = impurity.
CE conditions: bare fused silica capillary with 50 μm i.d. × 50 cm effective length; voltage +20 kV, 20°C, injection 4 s at 0.5 psi, 100 mM borate buffer pH 10.2.

Figure 10.5 depicts the separation of the standard mixture of neutral monosaccharides commonly found in hemicellulose. Ribose was used as internal standard. The differential complexation of borate with polyhydroxyl moieties of the monosaccharide derivatives is the primary mechanism of the separation of these monosaccharides (see Chapter 4, 4.3.1).

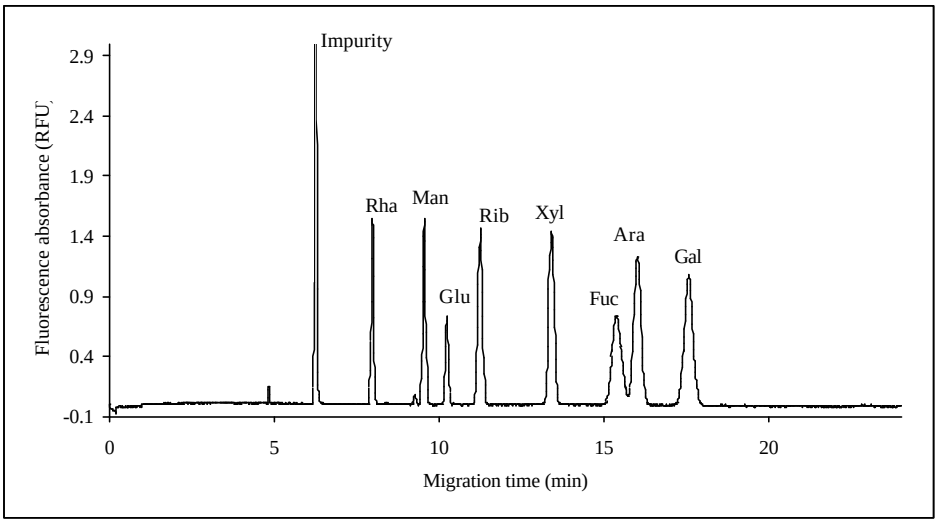

Figure 10.5 ***Separation of the standard mixture of neutral monosaccharides derivatised with APTS***

Peaks: Rha = rhamnose, Man = mannose, Glu = glucose, Rib = ribose, Xyl = xylose, Fuc = fucose, Ara = arabinose, Gal = galactose.
CE conditions: bare fused silica capillary with 20 μm i. d. × 27 cm in length (20 cm to the detector window), voltage +30 kV, injection 10 s at 0.5 psi, 20 °C, 222 mM borate buffer pH 9.6.

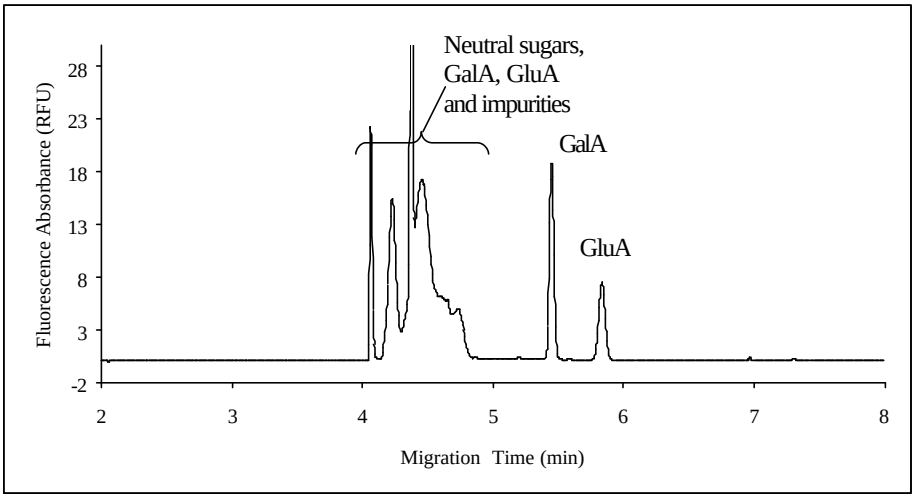

Figure 10.6 ***Separation of the mixture of neutral monosaccharides, galacturonic acid and glucuronic acid***

Peaks: GalA = galacturonic acid, GluA = glucuronic acid
CE Condition: bare fused silica capillary with 50 μm i.d. × 50 cm in effective length, voltage +30 kV, 20 °C, 4 s injection at 0.5 psi pressure, 20 mM borate buffer with pH 9.8

The two uronic acids could not elute under these separation conditions due to their high negative charge density. Using a low concentration (20 mM) of the borate buffer, galacturonic acid and glucuronic acid could be resolved as shown in Figure 10.6.

The multiple products of the uronic acid derivatives could be generated from the decarboxylation of uronic acids during the derivatisation. Wiedmer *et al.* [12] observed that decarboxylation occurred during the derivatisation of galacturonic acids with APTS. Therefore, the analysis of the two uronic acids derived from xylan was not further carried out in this work.

10.3.4 Investigation on monosaccharides derived from xylan

Two xylan samples, from birchwood and oat spelts, respectively, were first subjected to chemical hydrolysis and then enzymatic degradation, the hydrolysates were derivatised with APTS and analysed using CE-LIFD. The identification of the monosaccharides was performed by spiking the samples with the monosaccharide standards.

It was observed that xylan from oat spelts could not be completely digested through chemical hydrolysis either with trifluoroacetic acid or with sulphuric acid. Some solids still remained in the mixtures. The solution of enzymatic hydrolysate of xylan from oat spelts was not clear either, whereas the hydrolysates of xylan from birchwood were obtained as clear and homogeneous liquids after chemical and enzymatic hydrolysis. Figure 10.7 illustrates the separation of xylan (from birchwood) hydrolysates obtained after chemical and enzymatic hydrolysis.

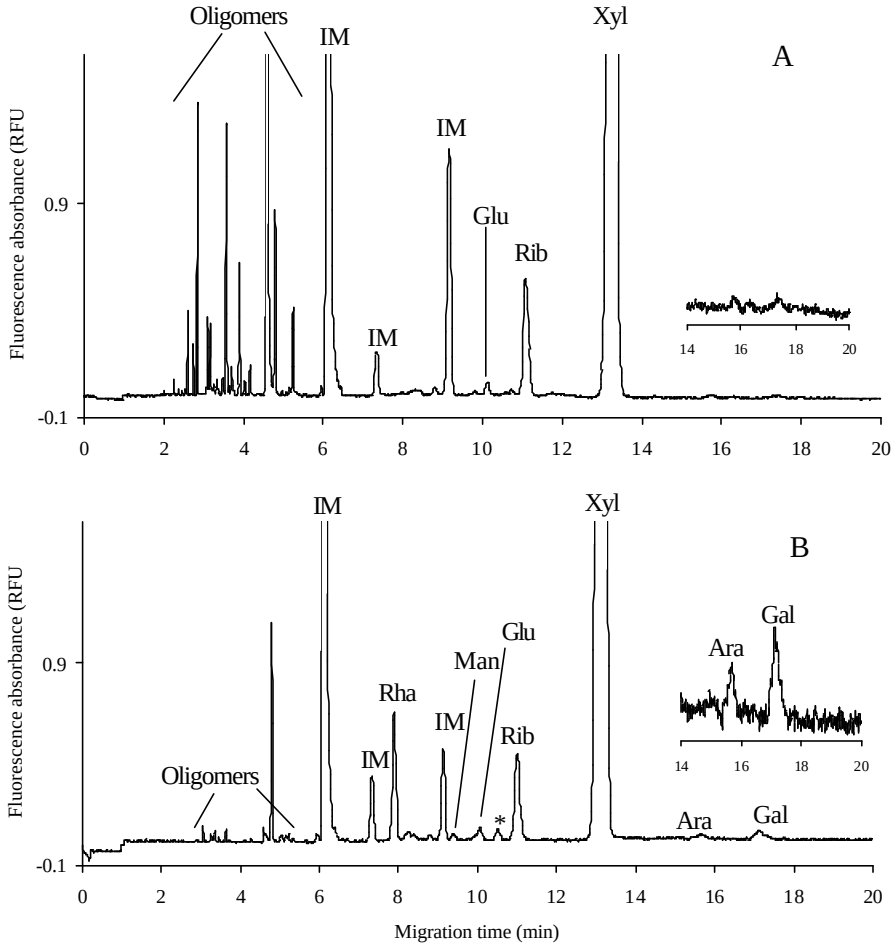

Figure 10.7 ***Analysis of neutral monosaccharides in xylan from birchwood after enzymatic hydrolysis (A) and chemical hydrolysis (B)***

Peaks: Rha = rhamnose, Man = mannose, Glu = glucose, Rib = ribose, Xyl = xylose, Fuc = fucose, Ara = arabinose, Gal = galactose, IM impurities. The asterisk indicates an unknown monosaccharide residue.
CE condition as described in Figure 10.5.

More monosaccharides were detected in the chemical hydrolysates due to the non-selective degradation, as can been seen in Figure 10.7 B. This is proven by detection of mannose, arabinose and galactose in the chemical hydrolysates but

not in the enzymatic hydrolysates (inserts in Figure 10.7 A and B). The electropherogram of the enzymatic hydrolysate shows some undegraded oligomer residues indicated as 'oligomers' in Figure 10.7 A. These oligomers could be the same compounds shown in Figure 10.3 B. The chemical hydrolysate could also contain a minor amount of these oligomers (Figure 10.7 B).

In addition, it was not known why rhamnose, having a relatively high content in the chemical hydrolysates of xylan both from birchwood (see Figure 10.7 B) and oat spelts, was not detected in the enzymatic hydrolysates of xylan from these two sources. Rhamnose was also not reported in the recent work of Dahlman and his colleagues, who even used a mixture of cellulase, xylanase and endoglucanase to hydrolyse the hemicellulose [9].

10.3.5 Quantitative determination of the neutral monosaccharides of xylan derived from chemical hydrolysis and enzymatic degradation

Calibration curves were constructed for the APTS derivatives of each neutral monosaccharide by plotting the peak area (y) as a function of the concentration of monosaccharides (x). The concentration range of each monosaccharide standard in the mixture was from 1×10^{-7} M to 1×10^{-6} M (1×10^{-7}, 3×10^{-7}, 5×10^{-7}, 7×10^{-7}, 9×10^{-7} and 1×10^{-6} M). The relative standard deviation (RSD) was calculated for the migration time of each run of the standard solution and they are good (0.99% - 2.50%). The linear regression coefficients (R^2) of the calibration curve are also satisfactory (Table 10.1).

Table 10.1 ***Relative standard deviation (RSD) of migration time, regression equation, slopes of the calibration curve and the corresponding correlation coefficients (R^2) of neutral monosaccharides***

Monosaccharide	RSD (%) (n > 8)	Regression equation (y peak area, x conc.)	Coefficient (R^2)
Rhamnose	0.99	$y = 3 \times 10^8 x$	0.9943
Mannose	1.20	$y = 4 \times 10^8 x$	0.9948
Glucose	1.30	$y = 2 \times 10^8 x$	0.9903
Ribose	1.50	$y = 5 \times 10^8 x$	0.9969
Xylose	1.90	$y = 6 \times 10^8 x$	0.9987
Fucose	2.10	$y = 5 \times 10^8 x$	0.9971
Arabinose	2.20	$y = 7 \times 10^8 x$	0.9986
Galactose	2.50	$y = 7 \times 10^8 x$	0.9955

Table 10.2 ***Relative yields of monosaccharides present in xylan after enzymatic and chemical hydrolysis in percent of initial weights of commercial xylan***

Contents of sugars in the dry mass (%)	Xylan from birchwood		Xylan from oat spelts	
	chemical	enzymatic	chemical	Enzymatic
Rhamnose	1.44	n. d.	0.62	n. d.
Mannose	d.	n. d.	n. d.	n. d.
Glucose	d.	d.	6.13	1.92
Xylose	40.53	17.21	52.54	16.05
Fucose	n. d.	n. d.	n. d.	n. d.
Arabinose	d.	n. d	6.78	4.28
Galactose	d.	n. d	1.07	d
Total sugars	41.97	17.21	67.14	22.25
Assumed yields	100	41	100	33

n. d. = not detectable, d. = detected: the component was detected, the contents, however, were lower than 0.36% in the dry mass and were not measured quantitatively because they were out of the concentration range of the calibration curve.

The recovery of ribose, the internal standard added in the hydrolysates, was 97.25% (RSD 7.6%, n = 8). However, the total yields of sugars obtained for both the chemical and the enzymatic hydrolysis were low (Table 10.2). Incomplete degradation could be a cause of this. If it is assumed that the total sugar yields for chemical hydrolysis is 100%, it can be seen that the total sugar yields of the enzymatic hydrolysates are 41% and 33% for xylan from birchwood and oat spelts, respectively (Table 10.2).

10.4 Conclusion

This is a preliminary study, far from complete. Nevertheless, it could be demonstrated that CE is a valuable technique for the study of both chemical and enzymatic hydrolysis of hemicellulose.

This part of the thesis was performed on request of the Department of Biochemistry, University of Stellenbosch, South Africa.

Further optimisation was not carried out for two reasons. Firstly the APTS reagent is very expensive and secondly LIFD is not an accessible for every one. The method is therefore translated into a CE-DAD method which is a cheap CE set-up and less expensive reagents can be used. This is actually evaluated and the experiment updated by the Department of Biochemistry, University of Stellenbosch, South Africa.

References

[1] R. L. Whistler and C. L. Smart, Polysaccharides chemistry", Academic Press, New York, **1953**

[2] K. C. B. Wilkje, *Adv. Carbohydr. Chem. Biochem.* 36, **1979**, 215

[3] E. Sjöström, Wood chemistry, Academic Press, New York, London, Toronto, Sydney San Francisco, **1981**

[4] J. S. Chen, J. L. Yu, Y. W. Shi, Z. W. Chang, G. X. Wu and R. Q. Yan, *Cellul. Chem. Technol.* 15, **1981**, 287

[5] D. A. Martens and W. T. Frankenberger, *Chromatographia* 29, **1990**, 7

[6] D. A. Martens and W. T. Frankenberger, *Chromatographia* 30, **1990**, 651

[7] C. Huber, E. Grill, P. Oefner and O. Bobleter, *Fresenius J. Anal. Chem*. 348, **1994**, 825

[8] A. Rydlund and O. Dahlman, *J. Chromatogr. A* 738, **1996**, 129

[9] O. Dahlman, A. Jacobs, A. Liljenberg and A. I. Olsson, *J. Chromatogr. A* 891, **2000**, 157

[10] J. Sudor and M. Novotny, *Proc. Natl. Acad. Sci.* (biochemistry) USA, 90, **1993**, 9451

[11] A. Bergholdt, J. Overgaard and A.Colding, *J. Chromatogr.* 644, **1993**, 412

[12] S. K. Wiedmer, A. Cassely, M. Hong, M. V. Novotny and M. –L. Riekkola, *Electrophoresis* 21, **2000**, 3212

Summary and Conclusion

Separation of saccharides was carried out by capillary electrophoresis (CE) coupled with laser induced fluorescence detection (LIFD), as well as with UV detection. 9-Aminopyrene-1,4,6-trisulfonate (APTS) is the most powerful fluorescence derivatising reagent. APTS not only introduces a fluorophore but also largely contributes to the electrophoretic properties of the derivatised sugars. Both bare fused silica capillaries and polyacrylamide (PAA) coated capillaries were applied. The technique of *in situ* capillary filling with a linear polyacrylamide gel was employed for the separation of neutral polysaccharides. Microcentrifuge filters were used to remove the excess reagent as well as to fractionate polysaccharides.

The separation principles of capillary electrophoresis (CE) are introduced in **Chapter 1** with emphasis on capillary zone electrophoresis (CZE) in combination with laser induced fluorescence detection (LIFD).

The structures of monosaccharides, oligosaccharides and polysaccharides, together with their characteristics and properties are presented in **Chapter 2**. Different polysaccharides including starches, cellulose, inulin, gums and hemicellulose are described.

The most important derivatising reagents and reaction schemes for the transformation of saccharides, as well as their applicability in CE-LIFD/UV analysis, are described in **Chapter 3**. The choice of the derivatising reagent for

saccharides is of utmost importance to obtain good electrophoretic properties. Pre-column derivatisation is by far the most universal and versatile method.

Separation of monosaccharides as their borate complexes in a bare fused silica capillary is demonstrated in **Chapter 4**. All aldehyde monosaccharides (aldoses) are giving high yields with APTS while fructose, a ketose, showed very low reactivity. The effects of tag selection on the separations are illustrated for different derivatising reagents useful in LIF and UV detection.

The separations of oligosaccharides obtained on a bare fused silica capillary with two CE conditions, namely in the positive polarity mode using an alkaline borate buffer and in the negative polarity mode using an acidic phosphate buffer, are presented in **Chapter 5**. The different separation mechanisms are discussed.

In **Chapter 6**, a quantitative investigation was performed for APTS-maltooligosaccharides with degrees of polymerisation (DP) from 0 to 6 using above mentioned two CE conditions. A linear range over 3 to 4 orders of magnitude was found. The quantitative aspect of the CE-LIFD analysis of saccharides should be further studied. Also the potential of CE-UV should be evaluated in this respect.

In **Chapter 7**, profiling of the high mass polysaccharide, amylose, was done by using a bare fused capillary and two CE conditions. Separation with DP numbers over 60 was achieved by using an acidic buffer in the negative polarity mode while migration of analytes was fast in an alkaline buffer in the positive polarity mode. These two separation conditions provide complementary information on the distribution of the polymer chains. The use of a linear polyacrylamide coated

capillary filled with linear polyacrylamide gel did not show an improvement in the resolving power of CE for neutral polysaccharides.

Chapter 8 discusses the separation of the non-reducing polysaccharide inulin. Fluorescein isothiocyanate (FITC) was used for the first time for the profiling of polysaccharides by CE. The separation of inulin chain lengths with high efficiency and speed was achieved in a polyacrylamide coated capillary. The derivatisation took place on more than one hydroxyl group of the sugars but this did not impair the characterisation of the different degrees of polymerisation (DP). Hence, elucidation of inulin hydrolysates was feasible.

Chapter 9 describes a simple, rapid CE method for the analysis of gums commonly used as food additives. The high molecular weight (MW) fractions of the polysaccharides were obtained by using microcentrifuge filters. The peaks for the gums are broad since they represent a very large distribution of different chain lengths. Using a PAA coated capillary, a wide range of pHs could be employed in the separation of gums. The effect of the buffer pH on the electrophoretic mobility and the peak shape was found to be significant.

A preliminary study on the analysis of hemicellulose by CE-LIFD is presented in **Chapter 10**. Separation profiles of hemicellulose by CE-LIFD after treatment with xylanase at different incubation times are shown. Chemical and enzymatic hydrolysis were applied to treat the samples and the identification and quantitative analysis of the monosaccharides present in hemicellulose are compared.

In conclusion, CE-LIFD is an advanced technique for qualitative analysis of saccharides, and especially useful for high DP separation of polysaccharides. Quantitative analysis, however, has to our knowledge not been sufficiently

studied. In depth study suffers from the high cost of the instrumentation, fluorescence reagents and the lack of standards. Further work should be performed here and the potential of CE-UV should be re-evaluated because this is a standard set-up and labelling reagents are much cheaper.

Samenvatting en Conclusie

Sacchariden werden gescheiden door middel van capillaire elektroforese (CE) gekoppeld met laser geïnduceerde fluorescentie detectie ('laser induced fluorescence detection', LIFD), alsook met UV-detectie. 9-Aminopyreen-1,4,6-trisulfonaat (APTS) is het meest geschikt derivatiseringsreagens voor dit doeleinde. Het is niet enkel verantwoordelijk voor de introductie van een fluorofoor maar draagt ook aanzienlijk bij in de elektroforetische eigenschappen van de gederivatiseerde suikers. Zowel 'fused silica' capillairen als capillairen waarvan de binnenwand bedekt is met polyacrylamide (PAA) werden gebruikt. Een techniek waarbij het capillair *in situ* wordt gevuld met een lineaire polyacrylamidegel werd toegepast om neutrale polysacchariden te scheiden. Er werd gebruik gemaakt van microcentrifuge filters om de overmaat reagens te verwijderen en om de polysacchariden te fractioneren.

De basisprincipes van CE worden uiteengedaan in **hoofdstuk 1**. Hierbij wordt de nadruk gelegd op capillaire zone elektroforese (CZE) in combinatie met LIFD.

De structuur van monosacchariden, oligosacchariden en polysacchariden, evenals hun karakteristieken en eigenschappen worden beschreven in **hoofdstuk 2**. Verscheidene polysacchariden waaronder zetmeel, cellulose, inuline, gommen en hemicellulose worden er besproken.

De belangrijkste derivatiseringsreagentia en reactieschema's voor de transformatie van sacchariden, alsook hun toepasbaarheid voor de analyse met behulp van CE-LIFD/UV zijn beschreven in **hoofdstuk 3**. De keuze van een geschikt reagens voor

derivatisatie van de suikers is van groot belang voor de elektroforetische eigenschappen van het reactieprodukt. Pre-kolom derivatisatie is veruit de meest universele en versatiele methode.

In **hoofdstuk 4** worden scheidingen gepresenteerd van monosacchariden als hun boraatcomplexen in 'fused silica' capillairen. Alle aldehyde monosacchariden (aldosen) hadden een hoog reactierendement met APTS. Dit in tegenstelling tot fructose, een ketose, dat weinig reactief was ten opzichte van APTS. Het effect van diverse 'tags' op de scheiding wordt geïllustreerd voor LIFD en UV-detectie.

De scheiding van oligosacchariden bekomen in een 'fused silica' capillair met twee verschillende CE-condities, namelijk positieve polariteit met een alkalische boraatbuffer en negatieve polariteit met een zure fosfaatbuffer, wordt getoond in **hoofdstuk 5**. De verschillende scheidingsmechanismen worden er besproken.

In **hoofdstuk 6** wordt aan de hand van de hierboven vermelde CE-condities een kwantitatief onderzoek uitgevoerd voor APTS-maltooligosacchariden met een polymerisatiegraad ('degree of polymerisation', DP) variërend van 0 tot 6. Lineariteit over drie tot vier grootte-ordes werd bekomen. Het kwantitatief aspect van de CE-LIFD analyse zou evenwel verder moeten bestudeerd worden. Ook het potentieel van CE-UV voor dergelijke analyses moet worden geëvalueerd.

De profilering van amylose, een polysaccharide met een hoog moleculair gewicht, werd uitgevoerd in een 'fused silica' capillair en wordt besproken in **hoofdstuk 7**. Scheiding van componenten met DP > 60 werd bekomen in de negatieve polariteit met een zuur buffersysteem. Het gebruik van een alkalische buffer en negatieve polariteit resulteerde in een snelle doch minder informatieve analyse. Deze twee

scheidingscondities leveren complementaire informatie op omtrent de distributie van de polymeerketens. Het gebruik van een capillair binnenin bedekt met lineair PAA en gevuld met een lineaire polyacrylamidegel gaf geen aanleiding tot een hoger resolverend vermogen van CE met betrekking tot neutrale polysacchariden.

Hoofdstuk 8 behandelt de scheiding van het niet-reducerend polysaccharide inuline. Fluoresceïne isothiocyanaat (FITC) werd voor de eerst maal gebruikt voor de CE-profilering van polysacchariden. De snelle en hoogefficiënte scheiding van de inulineketens werd bekomen in een met PAA bedekt capillair. Derivatisering vond plaats op meer dan één hydroxylgroep van de suikers. De karakterisering van de verschillende polymerisatiegraden werd echter niet verhinderd door dit fenomeen. Bijgevolg konden diverse inuline-hydrolysaten succesvol worden geanalyseerd.

Een eenvoudige en snelle CE-methode voor de analyse van gommen die vaak gebruikt worden als voedingsadditieven, wordt besproken in **hoofdstuk 9**. De polysaccharide- fracties met hoog moleculair gewicht werden bekomen door gebruik te maken van microcentrifugefilters. De resulterende pieken van de gommen zijn vrij breed als gevolg van de zeer brede distributie in hun ketenlengte in deze stalen. Door een met PAA bedekt capillair aan te wenden kon een wijde waaier aan pH-waarden worden uitgetest voor de scheiding van dergelijke gommen. Het effect van de zuurtegraad van de buffer op de elektroforetische mobiliteit en piekvorm bleek significant.

De resultaten van een inleidende studie over de analyse van hemicellulose met CE-LIFD worden gepresenteerd in **hoofdstuk 10**. De profielen van hemicellulose na behandeling met xylanase bij verscheidene incubatietijden worden getoond. Zowel

chemische als enzymatische hydrolyse werden toegepast en de identificatie en kwantitatieve analyse van de resulterende monosacchariden worden besproken.

Er kan besloten worden dat CE-LIFD een geschikte techniek is voor de kwalitatieve analyse van sacchariden. De techniek blijkt uitermate geschikt voor de scheiding van polysacchariden met hoog moleculair gewicht. De mogelijkheid tot kwantitatieve analyse daarentegen, werd tot op heden nog niet voldoende bestudeerd. Een diepgaand onderzoek wordt namelijk bemoeilijkt door de hoge kost van instrumentatie, fluorescentiereagentia en een gebrek aan standaarden. Hierop zou meer werk moeten worden verricht en het potentieel van CE-UV moet worden herzien omwille van de standaardinstrumentatie en de significant lagere kost van de derivatisatiereagentia.

概　述

这篇论文阐述了如何运用毛细管电泳(CE)分离方法连接激光(LIF)和紫外(UV)检测技术进行糖类分析。本研究采用高效荧光派生剂 9-aminopyrene-1，4，6-trisulfonate（APTS）。不仅赋予糖荧光性，而且很大程度地改善了糖的电泳性质。裸表面玻璃毛细管和涂附毛细管均被用于分离。电中性多糖的分离运用了直链聚丙烯酰胺（PAA）胶柱上（原位）填充毛细管技术。不同分子量的微量离心过滤器将多糖分成高分子量部分和低分子量部分并能除去过量的派生剂。

第一章描述了毛细管分离的基本原理并着重介绍了毛细管区间电泳和激光检测方法。第二章归纳了单糖，寡糖和多糖的结构和性质。对多糖类淀粉，纤维糖，半纤维糖，旋复花粉和各种多糖胶也作了描述。第三章列举出最重要的用于糖类分析的派生剂和反应模式以及它们在 CE LIF/UV 中的应用。派生剂的选择是使糖类获得良好电泳性质的关键。柱前派生是迄今为止最为普遍和通用的方法。第四章描述了单糖的分析。醛糖和 APTS 的反应获得高产率，但酮糖（果糖）和 APTS 的反应只有很低的活性。本章介绍了单糖分析的一般条件并讨论了不同派生剂对分离所产生的影响。第五章举例介绍了分析寡糖的两种条件并对分离机理进行了讨论。利用这两种分离条件，在第六章中讨论了利用激光检测寡糖的定量分析。获得了三到四个数量级线行范围的校正曲线。但各个寡糖的相对响应因素偏离 1。电中性的还原多糖即直链淀粉的分离展示在第七章。进一步的，对四种分离条件下得到的结果进行了比较并总结出获得分离多糖高聚合度的最佳条件。通过应用异硫氰酸酯荧光剂和涂附玻璃毛细管，第八章首次展示了非还原性多糖，旋复花粉及其酶降解产物在毛细管电泳上的分离。第九章描述了一种简便，快速的食用多糖胶质的毛细管电泳分析方法。缓冲剂的酸碱度明显地影响迁移时间和峰形。第十章探讨了利用毛细光电泳分离结合激光检测对半纤维糖的分析。利用此方法我们成功地得到了半纤维糖酶解产物的定性分析毛细管电泳分离图像。但酶解产物和化学水解产物中单糖的定量分析还需要进一步探讨。

综上所述，本研究成功地运用毛细管电泳分离和激光检测技术进行了单糖，寡糖和多糖的定性分析，尤其是多糖的高聚合度分离和大分子多糖的完整组份分离。但定量分析局限于昂贵的试剂和设备。样品的降解和派生过程也易带来分析误差。+

Abbreviations

2-AA	2-Aminoacridone
p-ABA	*p*-Aminobenzoic acid
ABEE	*p*-Aminobenzoic acid ethyl ester
p-ABN	*p*-Aminobenzonitrile
AEC	Anion exchange chromatography
AHNS	4-Amino-5-hydroxynaphthalene-2,7-disulfonic acid
3-ANDA	3-Aminonaphthalene-2,7-disulfonic acid
ANDSA	7-Aminonaphthalene-1,3-disulfonic acid
2,6-ANS	2-Anilinonaphthalene-6-sulfonic acid
2-ANSA	2-Aminonaphthalene-1-sulfonic acid
5-ANSA	5-Aminonaphthalene-2-sulfonic acid
ANTS	8-Aminonaphthalene-1,3,6-trisulfonate
2-AP	2-Aminopyridine
APTS	9-Aminopyrene-1,4,6-trisulfonate
6-AQ	6-Aminoquinoline
CBQCA	3-(4-Carboxybenzoyl)-2-quinolinecarboxyaldehyde
CDs	Cyclodextrins
CE	Capillary electrophoresis
CEC	Capillary electrochromatography
CGE	Capillary gel electrophoresis
CIEF	Capillary isoelectric focusing
CMC	Carboxylmethyl cellulose
CTAB	Cetyltrimethylammonium bromide
CZE	Capillary zone electrophoresis
DE	Degree of esterification
DNA	Deoxyribonucleic acid
DMSO	Dimethyl sulfoxide
DP	Degree of polymerisation
ECD	Electrochemical detection
EOF	Electroosmotic flow

FITC	Fluorescein isothiocyanate
GAG	Glycosaminoglycan
GC	Gas chromatography
GF	Sucrose
GFF	Kestotriose
GFF_2	1,1- Kestotetraose
GFF_3	1,1,1-Kestopentaose
GlcNAc	*N*-acetylglycosamine
GalNAc	*N*-acetylgalactosamine
HA	Hyaluronic acid
HOAc	Acetic acid
HPAEC	High performance anion exchange chromatography
HPLC	High performance liquid chromatography
ITP	Isotachophoresis
KDa	Kilo Dalton
LBG	Locust bean gum
LIF	Laser induced fluorescence
LIFD	Laser induced fluorescence detection
LMW	Low molecular weight
LOD	Limit of detection
LPAA	Linear polyacrylamide
MEKC	Micellar electrokinetic chromatography
MOPS	3-(*N*-Morpholino)propanesulfonic acid
MS	Mass spectrometry
MW	Molecular weight
N	Efficiency (theoretical plate number)
NMR	Nuclear Magnetic Resonance
PMP	1-Phenyl-3-methyl-5-pyrazolone
RNA	Ribonucleic acid
RPC	Reversed phase chromatography
R_s	Resolution
RSD	Relative standard deviation

PAA	Polyacrylamide
PAD	Pulsed amperometric detection
TEMED	N,N,N',N' - tetramethylethylenediamine
THF	Tetrahydrofuran
tris	Tris(hydroxymethyl)aminomethane
TRSE	5-Carboxytetramethylrhodamine succinimidyl ester
SA	Sulfanilic acid
SEC	Size exclusion chromatography
SDS	Sodium dodecyl sulfate
UV	Ultraviolet